The carbon, water and energy balances of two lodgepole pine stands recovering from mountain pine beetle attack in British Columbia

by

Mathew Brown

B.A., University of Victoria, 2000

M.Sc., Lincoln University, 2006

A THESIS SUBMITTED IN PARTIAL FULFILLMENT OF

THE REQUIREMENTS FOR THE DEGREE OF

DOCTOR OF PHILOSOPHY

in

THE FACULTY OF GRADUATE STUDIES

(Soil Science)

THE UNIVERSITY OF BRITISH COLUMBIA

(Vancouver)

April 2011

Abstract

Over the past decade British Columbia (BC) has experienced the largest mountain pine beetle (MPB) outbreak on record. This study used the eddy covariance (EC) technique to examine the impact of the MPB outbreak on the net ecosystem production (NEP) and evapotranspiration (*E*) of two lodgepole pine stands in the central interior of BC from 2007 to 2010. MPB-06, an 85-year-old stand, and MPB-03, a 110-year-old stand, were first attacked by the beetle in 2006 and 2003, respectively. EC measurements were also made in two harvested stands, one in 2005 and one in 1997 (CC-05 and CC-97, respectively) during the 2007 growing season.

Annual NEP increased from -81 to 64 g carbon (C) m^{-2} from 2007 to 2010 at MPB-06 due to an increase in gross ecosystem photosynthesis (P_g). At MPB-03, annual NEP also varied with P_g, ranging from -57 g C m^{-2} in 2007 to 6 g C m^{-2} in 2009. Annual ecosystem respiration (R_e) did not vary greatly over the four years at both sites. At MPB-03, P_g was reduced by drought in 2009 and 2010. The increase in P_g at both sites was due to an increase in the photosynthetic capacity of the surviving trees and vegetation, as shown by foliar net-assimilation measurements. Light response analysis indicated that daytime R_e values derived using nighttime NEP data were likely realistic estimates of the actual respiratory fluxes. NEP measurements at CC-97 and CC-05, showed that these stands are likely to remain C sources for as many as 10 years following harvesting. There was little interannual variation in *E* at both sites as the surviving trees and vegetation compensated for reductions in *E* due to the death of the overstory. Root-zone drainage was much greater at MPB-03 than at MPB-06, due to larger *P* at MPB-03. Growing season water deficit showed both stands to be water limited in spite of the high proportion of dead pine trees. Results from this study showed the importance of the remaining healthy trees and vegetation in the recovery of these stands from MPB attack.

Table of Contents

List of Tables

List of Figures

List of Symbols and Acronyms

Symbol / Acronym	Units	Definition
C		carbon
CCP		Canadian Carbon Program
CH_4		methane
CO_2		carbon dioxide
EC		eddy covariance
FCRN		Fluxnet Canada Research Network
GHG		greenhouse gas
IRGA		infrared gas analyzer
LAI	$m^2\ m^{-2}$	leaf area index
MPB		mountain pine beetle
NBP	g C m^{-2} time^{-1}§	net biome production (net ecosystem production including disturbance)
NEE	µmol $m^{-2}\ s^{-1}$	net ecosystem exchange
NEP	µmol $m^{-2}\ s^{-1}$ or g C m^{-2} time $^{-1}$	net ecosystem production
PAR	µmol $m^{-2}\ s^{-1}$	photosynthetically active radiation flux
SD		standard deviation
WD	mm	water deficit (E_{pot} - E)
WUE	g C kg^{-1} water	water use efficiency (P_g/E)
A_{max}	µmol $m^{-2}\ s^{-1}$	maximum assimilation rate , Chapter 2
A_{max}	µmol $m^{-2}\ s^{-1}$	leaf photosynthetic capacity, Chapter 4
A_n	µmol $m^{-2}\ s^{-1}$	foliar net assimilation
A_{Ta}	°C	amplitude of the diurnal course of T_a
D	kPa	vapour pressure deficit
D_r	mm	Drainage of water from the root zone
E	mm time^{-1}	evapotranspiration
E_{mod}	mm time^{-1}	modelled evapotranspiration
E_{pot}	mm time^{-1}	potential evapotranspiration
E_{eq}	mm time^{-1}	equilibrium evapotranspiration
F_c	µmol $m^{-2}\ s^{-1}$	CO_2 flux
G	W m^{-2}	soil surface heat flux
H	W m^{-2}	sensible heat flux
P	mm d^{-1}	precipitation
P_g	µmol $m^{-2}\ s^{-1}$ or g C m^{-2} time $^{-1}$	gross ecosystem photosynthesis
P_{gmax}	µmol $m^{-2}\ s^{-1}$	ecosystem photosynthetic capacity
P_{gmaxN}	µmol $m^{-2}\ s^{-1}$	ecosystem photosynthetic capacity, from P_g

Symbol / Acronym	Units	Definition
P_{gmaxP}	μmol m^{-2} s^{-1}	ecosystem photosynthetic capacity, from NEP
P_n	μmol m^{-2} s^{-1} or g C m^{-2} $time^{-1}$	net primary production
Q	μmol m^{-2} s^{-1}	downwelling photosynthetically active radiation
Q_{10}		relative increase in respiration per 10 °C increase in T_s
R_n	W m^{-2}	net radiation flux
R_a	W m^{-2}	available energy flux
- All units of respiration are in μmol m^{-2} s^{-1} or g C m^{-2} $time^{-1}$		
R_a		autotrophic respiration
R_d		daytime ecosystem respiration, Chapter 2
R_e		ecosystem respiration
R_{ed}		daytime ecosystem respiration, 3-day relationship, Chapter 4
R_{edN}		daytime ecosystem respiration
R_{eN}		measured ecosystem respiration / modelled ecosystem respiration
R_{e10}		ecosystem respiration at 10 °C
R_{ed10}		daytime ecosystem respiration (3-day relationship) at 10 °C
R_h		heterotrophic respiration
R_{ld}		leaf daytime respiration
R_s		soil respiration
S_b	W m^{-2}	heat storage in the tree boles
S_{br_fol}	W m^{-2}	heat storage in the branches and foliage
S_p	W m^{-2}	rate of energy consumption by photosynthesis
S_t	W m^{-2} (per unit ground area)	rate of change in energy storage in the air and biomass between the EC sensors and the ground surface
T_a	°C	air temperature at 26-m
T_b	°C	bole temperature
T_f	°C	foliage temperature
T_s	°C	soil temperature at 5 cm depth
W_w		water content on a wet mass basis
c_L	J kg^{-1} K^{-1}	leaf specific heat
c_p	J kg^{-1} K^{-1}	specific heat of air
e_a	kPa	vapour pressure
g_a	mm s^{-1}	aerodynamic conductance
g_c	mm s^{-1}	canopy conductance
g_{cmod}	mm s^{-1}	modelled values of canopy conductance
g_s	mmol m^{-2} s^{-1}	stomatal conductance
K	0.40	von Karman constant
S	kPa K^{-1}	change in the saturation vapour pressure with temperature

Symbol / Acronym	Units	Definition
T	hours	t is the time of day (PST)
U	m s^{-1}	horizontal velocity
u_*	m s^{-1}	friction velocity
u_{*th}	m s^{-1}	threshold friction velocity
V	m s^{-1}	lateral velocity
W	m s^{-1}	vertical velocity
z_m	m	measurement height
α	μmol C μmol photons	quantum yield, Chapter 2
α		Priestley-Taylor coefficient, Chapter 3
α_l	μmol C μmol photons	leaf quantum yield
α_N	μmol C μmol photons	quantum yield, from NEP
α_{max}		maximum Priestley–Taylor α
α_P		quantum yield from P_g
λE	W m^{-2}	latent heat flux
λE_{eq}	W m^{-2}	equilibrium latent heat flux
ρ_a	mol dry air m^{-3}	density of dry air
ϕ	°	phase angle of the diurnal course of T_a
θ	m^3 m^{-3}	soil fine fraction (soil particle size < 2 mm) volumetric water content
Ω		decoupling coefficient
γ	kPa K^{-1}	psychrometric constant
ψ_m		integral diabatic correction factor for momentum
ψ_h		integral diabatic correction factors for sensible heat transfer
ω	radians $hour^{-1}$	diurnal angular frequency
σ_L	g m^{-2}	specific leaf mass

[§] "time" indicates the use of seconds, hours, days and years.

Acknowledgements

First and foremost, thank you to my supervisor, Andy Black for his constant support over the past four plus years. Andy has been the ideal supervisor, spending countless hours guiding me and meticulously reviewing my work. I would also like to the thank Zoran Nesic, who gave so much of his time to my project and Dominic Lessard for his technical help in setting up and maintaining the sites. Biomet was a great place to work and I made several good friends who also contributed greatly to my project. These include, Nick (irie) Grant, Iain Hawthorne, Rick Ketler, Rachpaul (Paul) Jassal, Christian (C-Dawg) Brümmer, Andrew Hum (Mr. Hum), and Andrew Sauter. I would also like to thank my committee members Mike Novak, Rob Guy, Andreas Christen, Art Fredeen, Phil Burton for their support over the past 4 plus years.

I appreciate the financial support of grants from the Canadian Foundation for Climate and Atmospheric Science, the BC Forest Science Program, the BC Ministry of Forests and Range, and the Natural Science and Engineering Research Council of Canada. Special thanks to David Spittlehouse for his financial support in 2008. I would also like to thank the Faculty of Land and Food Systems and the Canadian Carbon Program for funding my participation at several national and international conferences.

I greatly appreciate the support my mom and John and my dad and Francine have provided over the last several years. Lastly, I would especially like to thank my special person Minh Ngo for her continuous support over the past year and for helping me blow off steam when I wasn't working.

1. Introduction

Anthropogenic emissions have increased atmospheric carbon dioxide (CO_2) concentrations from the pre-industrial level of 260 ppm to 387 ppm by the end of 2009 (Canadell *et al*. 2007, Friedlingstein *et al*. 2010). In 2009, total CO_2 emissions from fossil fuel burning and cement production were 8.40 Pg C, a decrease of 1.3 % from 2008 due to the global economic crises; however, with economic recovery, emissions are projected to increase by more than 3% in 2010 (Friedlingstein *et al*. 2010). Friedlingstein *et al*. (2010) also report that land-use change (LUC) accounts for additional emissions of ~0.90 Pg C. This is of major concern since modeling with and without greenhouse gas (GHG) forcing clearly indicates that the increase in the atmospheric concentration of CO_2 and other GHGs, such as methane and nitrous oxide, is very likely causing global climate warming (Grace 2004, IPCC 2007). Between 2000 and 2008, the terrestrial biosphere absorbed 29% of the annual anthropogenic CO_2 emissions resulting from fossil fuel burning, cement production and LUC, with the oceans absorbing a further 26%, although the year-to-year variability in the fraction absorbed was high (Le Quéré *et al.* 2009). Despite this uptake by the biosphere, the rate of increase in the atmospheric CO_2 concentration continues to rise, averaging 1.93 ppm $year^{-1}$ from 2000-2006 (Canadell *et al*. 2007), and the fraction of annual emissions remaining in the atmosphere increased 0.3% $year^{-1}$, from 1959 to 2008 (Le Quéré *et al.* 2009). Since GHGs affect the global climate, the uptake and release of these gases by the terrestrial biosphere has a direct influence on climate change (Heinmann and Reichstein 2008). The connection between the terrestrial carbon (C) cycle and climate change suggests that if a significant portion of the C stored in the terrestrial biosphere were to be released to the atmosphere, there would likely be a significant impact on climate (Heinmann and Reichstein 2008).

The exchange of CO_2 between terrestrial ecosystems and the atmosphere occurs through two main processes; ecosystem uptake of atmospheric CO_2 is the result of gross ecosystem photosynthesis (P_g), while ecosystem respiration (R_e) results in the release of CO_2 to the atmosphere. R_e is comprised of autotrophic respiration (R_a) from the foliage, stems, roots and mycorrhizae, and heterotrophic respiration (R_h) results from the microbial decomposition of above- and below-ground organic matter. The difference between the two (typically large) fluxes of R_e and P_g is the net ecosystem exchange (NEE), with a positive value indicating a gain of CO_2 by the atmosphere and a negative value indicating gain by the ecosystem. The eddy covariance (EC) technique has emerged as the preferred method for measuring NEE on land (Baldocchi 2003, 2008). The term net ecosystem production is defined by NEP = -NEE, with a positive value indicating a net CO_2 uptake by the ecosystem (C sink) over a period of time (e.g., a year), while a negative NEP indicates a net CO_2 release (C source) to the atmosphere (i.e., NEP = P_g - R_e).

Both within Canada and globally, networks, such as the Fluxnet Canada Research Network (FCRN), now known as Canadian Carbon Program (CCP), Ameriflux and CarboEurope, under the umbrella of FLUXNET, a global network of EC sites, have been established to monitor C balances in various ecological regions. FLUXNET includes more than 500 EC sites from many regional networks operating on a long-term basis (Fig. 1-1).

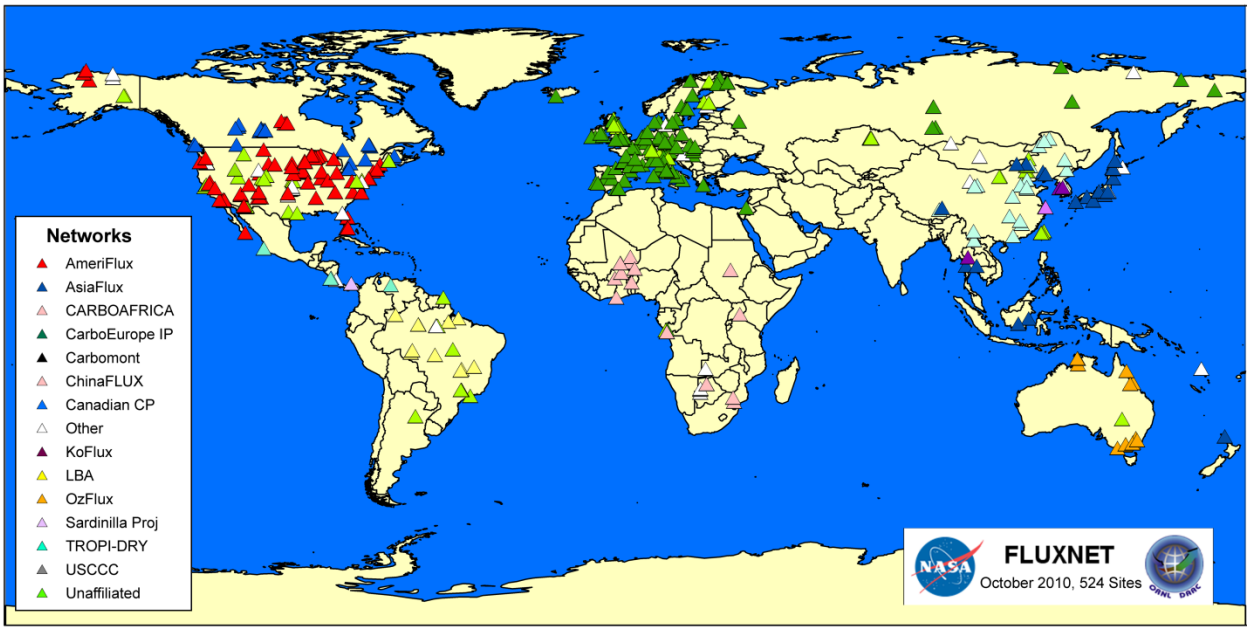

Figure 1.1. FLUXNET sites and list of regional networks. Source: http://www.fluxnet.ornl.gov.

In Canada, EC measurements made in the boreal forest have shown annual C balances of stands to vary widely, with stand composition, climate and disturbance all having an influence (e.g., Barr *et al.* 2007, Bergeron *et al*. 2007, Mkhabela *et al.* 2009). Disturbances, such as forest fires, insect attacks and harvesting, can result in some of the largest year-to-year variability in NEP and shift forests from acting as C sinks to sources (Amiro *et al.* 2010). Modelling studies have estimated that, primarily due to disturbance, Canada's forests recently switched from being a C sink, during the mid- to late-1990s, to being a C source during the last 10 years (Chen *et al*. 2000, Bond-Lamberty *et al*. 2007, Kurz *et al.* 2008). While the impact of forest fires and harvesting on NEP has received considerable attention in the past decade (Amiro *et al.* 2003, Humphreys *et al.* 2005, Amiro *et al.* 2006), insect attacks have only recently begun to be studied (Cook *et al.* 2008; Clark *et al*. 2010).

The current mountain pine beetle (MPB) (*Dendroctonus ponderosae*) outbreak in British Columbia (BC), which began in 2001-2002, is unprecedented in terms of tree mortality and area

affected. A 2009 aerial survey reported just under 9 million ha of forests showing beetle impact, down from the peak infestation of 10 million ha in 2007 (Westfall and Ebata 2009) (Fig. 1.2). The main host of the beetle is lodgepole pine (*Pinus contorta* var. *latifolia*), which is found throughout the interior of BC. The magnitude of the current outbreak is primarily due to the combination of an abundance of mature lodgepole pine and increasing wintertime minimum temperatures over the past several years (Safranyik and Wilson 2006). Although the beetles prefer mature lodgepole pine (~60-160 years old), they can inhabit virtually all *Pinus* spp. in western North America (Taylor *et al.* 2006). The beetles colonize through pheromone-mediated mass attacks which overwhelm the host's defences (Aukema *et al.* 2006). After eggs laid by the female beetles hatch under the bark, the larvae feed on the phloem, cutting off the tree's transport of photosynthate (Taylor *et al.* 2006). The beetles also introduce a blue-stain fungus into the tree which clogs the xylem, reducing the tree's capacity to transport water and nutrients from the soil (Gorte 2008). Generally, in the first year of MPB attack, the needles of attacked trees remain green (green attack stage). However, following the first winter of attack, the needles turn red on trees that have been killed (red attack stage) and one or two years later the needles fall, giving the trees a grey appearance (grey attack stage).

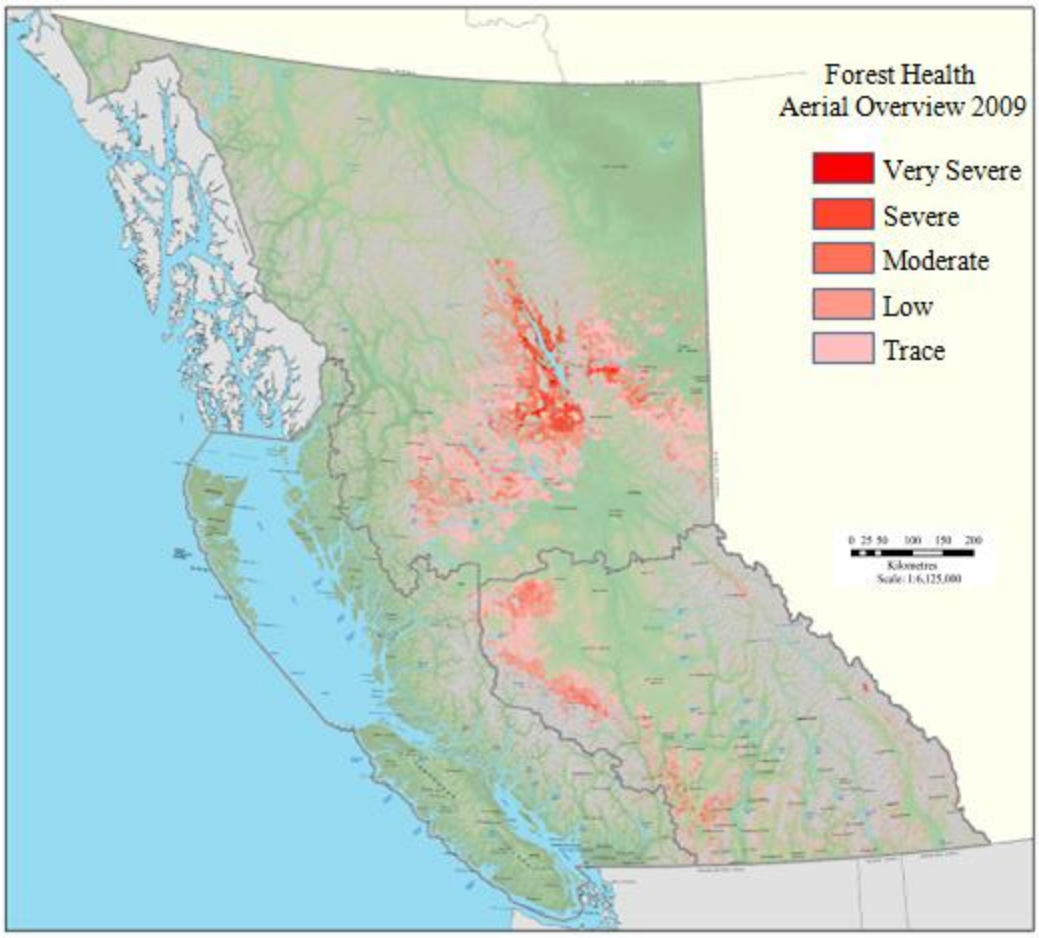

Figure 1.2. Mountain pine beetle infestation area recorded in British Columba in 2009. Source: Westfall and Ebata (2009). Polygons were classed based on percentage of trees attacked in polygons sketch-mapped during systematic aerial inspections (Very Severe = >50%, Severe = 30-49%, Moderate = 11-29%, Light 1-10% and Trace = <1%). A map of the cumulative area of attack can be found at: http://www.for.gov.bc.ca/hfp/mountain_pine_beetle/maps.htm.

The effects of MPB attacks on forest C cycling are not well understood. However, they have the potential to influence NEP, through their impact on P_g and R_e. Following MPB attack, the reduction in healthy leaf area associated with tree mortality would likely lead to a decline in P_g, while the increase in dead organic matter (needles, branches, stems and roots) would be expected to lead to an eventual increase in R_h. While no previous measurements of NEP have been made in MPB attacked stands, a study by Kurz *et al.* (2008), using the Carbon Budget

Model of the Canadian Forest Sector (CBM-CFS3), predicted the cumulative impact of the BC MPB outbreak from 2000-2020 to be a net loss 270 Tg C over 374,000 km^{-2} of forest, with the impact peaking in 2009 with a net biome production (NBP, defined as NEP plus the impacts of disturbance) of -53 g C m^{-2}. Coops and Wulder (2010) made MODIS-based estimates of P_g over the entire BC MPB infestation area, from 2002 to 2005, and reported a decreased of 10-20% from pre-outbreak levels, with more severely attacked stands having a greater reduction. While both of the preceding studies provide insight as to the impacts of the MPB attack on the C balance of these stands, the EC technique has the advantage of making continuous measurements of NEP at the stand level, with fluxes calculated every half-hour. This allows the C balance to be determined over a range of time scales, from half-hourly to annual. When these fluxes are combined with half-hourly climate measurements, empirical models of the response of NEP to climate variation can be developed (Barr *et al.* 2004). EC measurements are also essential for validating process models and remote sensing algorithms.

In addition to the potential impacts on the C balance, there is much concern over how the beetle outbreak will impact the hydrology of the affected stands, with predictions of an increase in water yield, peak flow and base flow (BC Ministry of Environment 2008; Rex and Dubé 2009). Higher water yield would likely lead to increases in the occurrence of flooding and changes in fish habitat and watershed nutrient status. A hydrological study by Potts (1984), on a watershed in Montana where 35% of the timber had been killed by the MPB, found a 15% increase in the annual water yield, a 10% increase in low flows and an increase in peak runoff in the first five years following attack. A change in water yield could partly occur through a decrease in canopy interception rates because after attack, forest canopies open up due to needle loss and eventual tree fall. Thus, beetle-attacked stands become similar to harvested stands,

which have greater winter snow accumulation and higher melt rates than unharvested stands (Winkler *et al.* 2010).

Evapotranspiration (*E*), which is comprised of evaporation from the soil surface and wet vegetation, and transpiration from vegetation, is likely to be affected by beetle attack too, but little is known about such impacts because existing water balance studies have tended to focus on water yields, rather than *E* specifically. A significant decrease in *E* due to a reduction in live leaf area associated with tree mortality can be expected to lead to higher water tables and water yields. The impact on *E* is likely to depend on the fraction of trees killed by the beetle, and the presence of secondary structure (living tree seedlings and saplings, sub-canopy and canopy trees that survive the attack), and the amount of shrub and herb vegetation. If only a small fraction of trees are killed, then *E* might not change greatly; however, if an entire stand without secondary structure is killed, then a large reduction in *E* can be expected to occur. As Hélie *et al.* (2005) note, the large variability in BC precipitation and temperature regimes and vegetation types make it difficult to predict whether post-outbreak changes in transpiration would be large or small.

In order to improve our understanding of the effects of insect attacks on forest C and water cycling, this thesis examines the impact of the MPB on the C, water and energy balances of two lodgepole pine stands in the northern interior of BC. The first stand is located at Kennedy Siding (MPB-06), about 35 km southeast of the town of Mackenzie (Fig.1.3). This approximately 80-year-old stand contained few non-lodgepole pine trees and was first attacked by the beetle during the summer of 2006, shortly before EC measurements began in late July. The second stand is located adjacent to Crooked River Provincial Park (MPB-03), about 70 km north of Prince George, and approximately 100 km south of MPB-06. MPB-03 is approximately 110 years old and was first attacked in 2003. When EC measurements began in March 2007, it

had > 95% pine canopy mortality. The overstory of MPB-03 was comprised of about 92% lodgepole pine and 8% subalpine fir (*Abies lasiocarpa*), and had a developed secondary structure consisting of lodgepole pine, subalpine fir and white hybrid spruce (*Picea glauca)* sub-canopy trees, saplings, and seedlings.

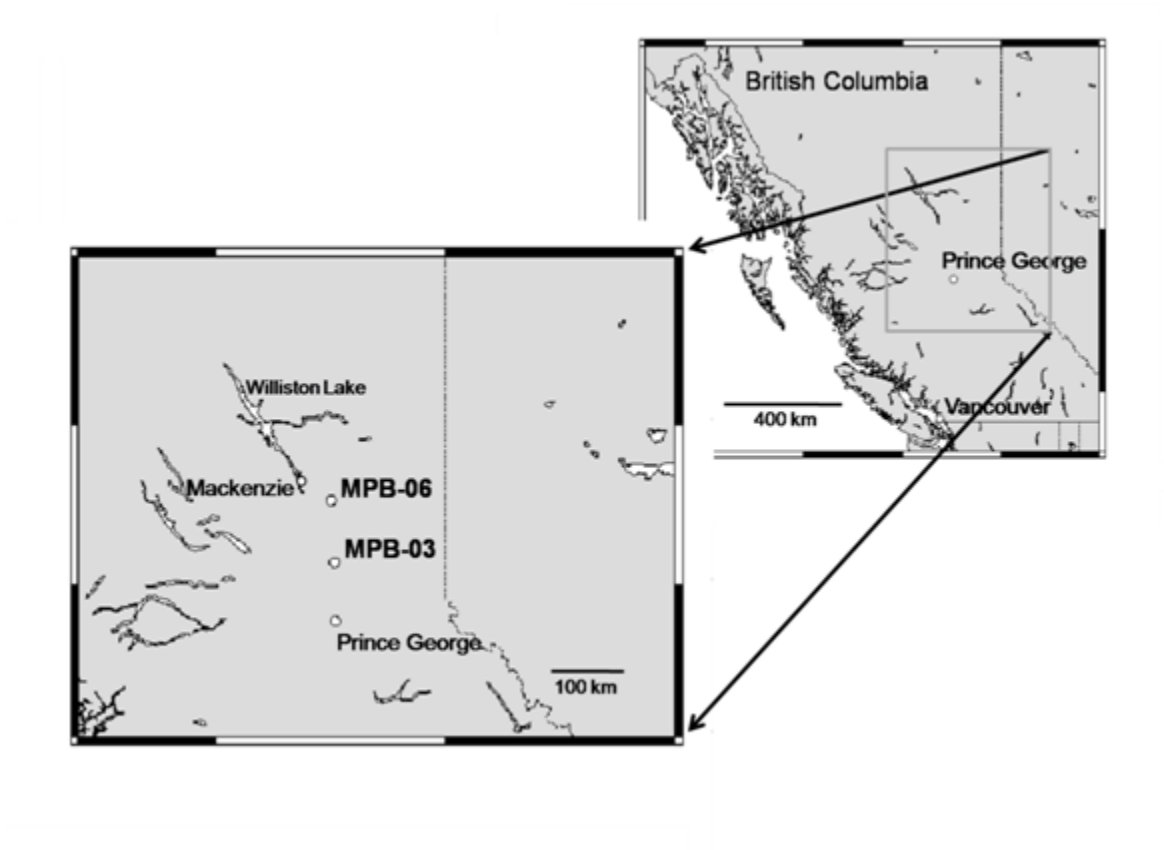

Figure 1.3. The locations of MPB-06 and MPB-03.

In Chapter 2, NEP from the first two years of measurements is examined. Chapter 2 has been published as: Brown M, Black TA, Nesic Z, Foord VN, Spittlehouse DL, Fredeen AL, Grant NJ, Burton PJ, and Trofymow JA. 2010. Impact of mountain pine beetle attack on the net ecosystem production of lodgepole pine stands in British Columbia. Agricultural and Forest Meteorology, 150: 254-264. 2007 and 2008 were the first and second year after the beetle attack at MPB-06, and were the fourth and fifth years after attack at MPB-03. Monthly diurnal NEP

over the two years is examined and annual totals of NEP, P_g and R_e are presented. A comparison of NEP measurements made in the two beetle-attacked stands and two harvested stands in the 2007 growing season provides insight into the contrasting management strategies of clearcut harvesting versus allowing stands to naturally regenerate.

Chapter 3 presents an analysis of E in MPB-06 and MPB-03 from 2007 to 2009. The canopy characteristics, consisting of canopy conductance (g_c), Priestley-Taylor α and the decoupling coefficient Ω are presented and E is modelled. The water deficit and drainage of water from the root zone of the two stands are compared and discussed in relation to the beetle attack.

Chapter 4 examines the C balance of both stands from 2007 to 2010, focusing on changes in P_g and R_e over a longer period than in Chapter 2. The response of R_e values derived from nighttime and daytime NEP data to T_s are compared, and a light response analysis of NEP and P_g provides insight into the recovery of the stands. Foliar CO_2 exchange measurements of various stand components are reported and compared to stand level P_g. Finally, the water use efficiency (WUE) of both sites is analysed.

Chapter 5 summarizes the major conclusions of this study, discusses how these findings relate to other research on the effects of MPB attack on forest C cycling and identifies areas for future research.

A number of appendices are also presented which include E data from MPB-06 in 2006 and from the two harvested sites in 2007, the flux footprints from the two sites and the design of the EC and climate measurement systems, photographs of the two canopies in each of the four years of the study, the EC data logger code, and the Matlab program used to calculate the CO_2 and water vapour fluxes.

2. Impact of mountain pine beetle on the net ecosystem production of lodgepole pine stands in British Columbia

2.1 Introduction

The current British Columbia (BC) outbreak of mountain pine beetle (*Dendroctonus ponderosae*) (MPB), which began in the late 1990's, had killed a total of 710 million m^3 of lodgepole pine (*Pinus contorta* var. *latifolia*) by the end of 2007, and is predicted to kill ~76% of the mature pine volume in the province by 2015 (Walton *et al.* 2008). Lodgepole pine accounts for almost 30% of the timber volume in the timber harvesting land base of BC and the pine-dominated stands located in the Sub-Boreal Spruce biogeoclimatic zone account for approximately 70% of BC's timber production (Meidinger and Pojar 1991). The current MPB outbreak is believed to have peaked in 2005 with a volume of ~141 million m^3 of merchantable pine killed that year on the timber harvesting land base (Walton *et al.* 2008). This compares with the average annual allowable cut of approximately 68 million m^3 (BC Ministry of Forests and Range 2006), between 1995 and 2005, from all provincial timber supply areas in BC. Although such epidemics have occurred in the past, none have been this large in areal extent or in duration. The size of the current epidemic is primarily due to the combination of an abundance of mature lodgepole pine and rising wintertime minimum temperatures for the past several years (Safranyik and Wilson 2006). Despite the fact that large areas have been affected by the epidemic and that the carbon (C) balance of Canadian forests is driven by disturbance (Kurz and Apps 1999; Amiro *et al.* 2006), there is a dearth of measurements examining the influence of insect attacks on C-

cycling in forests, and there are no known empirical studies examining net ecosystem CO_2 exchange measurements.

Net ecosystem production (NEP) is a direct measure of the degree to which an ecosystem is a source (NEP < 0) of, or a sink (NEP > 0) for atmospheric C over the time period of interest and is defined as the difference between gross ecosystem photosynthesis (P_g) (also known as gross primary production) and ecosystem respiration (R_e). A beetle epidemic could affect stand NEP in several different ways. First, P_g would be expected to be dramatically reduced with the increasing severity of attack due to the death of canopy trees. This would be accompanied by a corresponding decrease in autotrophic respiration (R_a), i.e., the release of CO_2 from the metabolic activity in roots, boles and leaves. The decline in P_g could be reduced by increased growth of secondary structure (consisting of tree seedlings and saplings, sub-canopy and canopy trees that survive a beetle attack (Coates *et al.* 2006)), if present, and shrubs and herbs. An increase in decomposable biomass, mainly in the form of fallen needles, dead roots, standing and fallen dead wood would be expected to lead to a large increase in heterotrophic respiration (R_h) or C released due to microbial decomposition. A study conducted in Oregon found that lodgepole pine killed by MPB began falling 3 and 5 years after death in thinned and unthinned stands, respectively (Mitchell and Preisler 1998) and that 50% of the attacked trees had fallen within 9 years in unthinned stands. A substantial increase in R_h would be expected once dead standing biomass begins to fall and decompose (Amiro *et al.* 2006).

The MPB is native to BC, and while epidemics are often associated with lodgepole pine, the beetles can inhabit virtually all *Pinus* spp. in western North America (Taylor *et al.* 2006). The beetles colonize via pheromone-mediated mass attacks which effectively overwhelm a tree's ability to defend itself (Aukema *et al.* 2006). When eggs laid by the female beetles under the

bark hatch, the larvae feed on the phloem, cutting off the tree's nutrient supply (Taylor *et al.* 2006). The beetles also introduce a blue-stain fungus into the tree which clogs the xylem, thereby reducing the tree's capacity to transport water (Gorte 2008).

There are three stages to a MPB attack. The green-attack stage describes the first year of attack, during which time a tree's foliage remains green. During the second year of attack, the red attack stage, the foliage senesces and turns red. Following the second year, the tree enters the grey attack stage and the needles turn brown and begin to fall.

Kurz *et al.* (2008) recently used the Canadian Forest Service C accounting model CBM-CFS3 to predict that the cumulative impact of the beetle outbreak in BC, between 2000 and 2020, will result in a net loss of 270 Mt C extending over an area of 374 000 km^2. This averaged to a net biome production (NBP) (defined as the NEP of stands in the region with the inclusion of the effects of disturbance) of -42 ± 21 g C m^{-2} yr^{-1} over the 20 year period. The same study predicted that the impact of the beetle (excluding the effect of additional harvesting in response to the attack) would peak in 2009 with an NBP of -53 g C m^{-2} yr^{-1}, with NBP slowly recovering thereafter. However, in 2020 the total area would still remain a net C source. The results presented here are the first measurements of NEP in MPB-attacked stands and thus will help determine ecophysiological responses at the stand level as well as provide empirical data for evaluating forest disturbance C models. To this end, this study had the following four objectives: 1) to measure the annual NEP in a stand without a well-developed secondary structure in the early to middle stages of attack, and in a stand with significant secondary structure in the middle to late stages of attack, 2) to determine the impact of beetle attack on P_g and R_e, 3) to determine the effects of the beetle on the photosynthetic characteristics of these stands, and 4) to evaluate the impact of salvage harvesting on the NEP of these stands.

2.2 Methods

2.2.1 Site locations

NEP measurements were made at two locations in the northern interior of BC (Fig. 2.1; Table 2-1). This region is located in the Sub-Boreal Spruce biogeoclimatic zone (Meidinger and Pojar 1991) and both stands were dominated by lodgepole pine (*Pinus contorta* Dougl. Ex Loud. var. *latifolia* Engelm.). The first stand is located approximately 35 km southeast of the town of Mackenzie at Kennedy Siding (MPB-06). This stand contained few non-pine trees, with the understory consisting mainly of pine seedlings, scattered shrubs and a ground cover of moss, lichen and dwarf shrub species. The second stand is located adjacent to Crooked River Provincial Park (MPB-03), approximately 70 km north of Prince George, BC and approximately 100 km south of MPB-06. In addition to overstory lodgepole pine and ground cover dominated by mosses, lichens and dwarf shrubs, MPB-03 had a developed secondary structure consisting of saplings of subalpine fir (*Abies lasiocarpa)* and white spruce (*Picea glauca)* and seedlings of all three tree species plus deciduous shrubs. Stand, understory, and soil characteristics were determined on three National Forest Inventory style ground plots (NFI 2004) at each site located 120^{o} apart and 50 m from each tower. The first major MPB attack at MPB-06 occurred during the summer of 2006. By May 2007 the majority of the canopy had been attacked (Table 2-2). MPB-03 was first attacked in 2003 and when NEP measurements began in 2007 the site was >95% in the red-attack and gray-attack stages. NEP measurements were also made in two harvested stands during the summer of 2007. They (CC-05 and CC-97) are located approximately 1 km E and 2 km SW, respectively, of the MPB-06 flux tower. CC-97 is a 10-year-old clearcut, which was left to naturally regenerate. The site is characterized by a large number of lodgepole pine seedlings (1200 stems ha^{-1}) with the soil surface covered by a mix of

lichens and moss (Seip and Jones 2007). CC-05 is a site that was salvage logged following MPB attack and planted in 2006 with a mixture of lodgepole pine and hybrid white spruce seedlings. The ground cover is similar to that of CC-97 except with a lower abundance of lichen (Seip and Jones 2007). Prior to harvest, both sites were dominated by lodgepole pine. All four sites are flat and on coarse textured gravelly soils of glacio-fluvial origin.

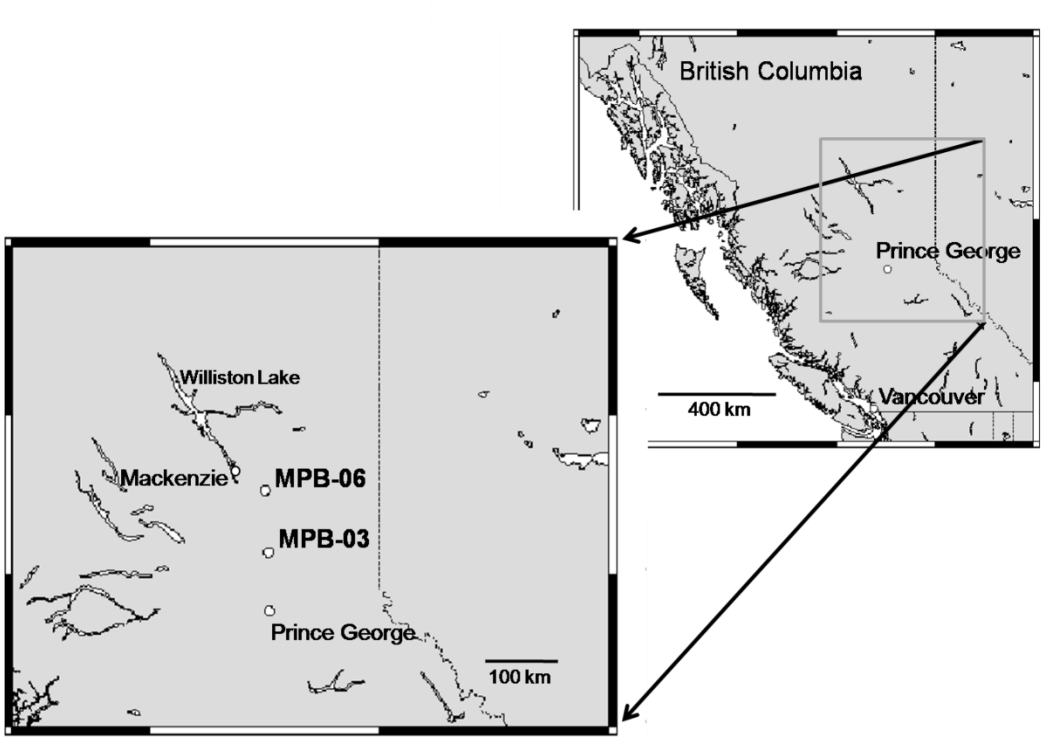

Figure 2.1. The locations of MPB-06 and MPB-03. CC-05 and CC-97 are located approximately 1 km E and 2 km SW, respectively, of the MPB-06 flux tower.

Table 2-1 Stand characteristics at MPB-06 and MPB-03.

	MPB-06	MPB-03
Stand age (yr)	~80	~110
Tower location	55°06'42.8''N 122°50'28.5''W	54° 28'24.8''N 122° 42'48.4''W
Elevation (m)	750	710
Canopy height (m)	~15	~17
Stand density (height > 10 m) (stems ha^{-1})	1275 (204[1])	558 (123)
Stand basal area m^2/ha (height >10m)	Live: 11.8 – 19.2 Dead: 0.2 – 0.9	Live: 0.7 – 3.2 Dead: 8.1 – 14.7
Seedling/sapling density (stems ha^{-1})	*Pinus contorta*: 7470 *Abies lasiocarpa*: 100 *Picea glauca*: 110	*Pinus contorta*: 2800 *Abies lasiocarpa*: 2300 *Picea glauca*: 190
Understory vegetation	*Alnus tenuifolia, Salix spp., Vaccinium spp.*	*Salix spp., Amelanchier alnifolia, Vaccinium spp., Arctostaphylos uva-ursi*
LAI (overstory) 2007 2008	 1.4 1.3	 0.9 0.8
% MPB attacked when tower established	<5	>90
Litter-fibric-humus C content (kg m^{-2})	1.10– 3.78	1.88 – 2.81
Mineral soil C content (0-55 cm) (kg m^{-2})	1.76 – 3.15	1.21 – 2.76
Fine soil bulk density (kg m^{-3})	1180 (220)	1160 (323)
Soil texture	Gravelly sandy loam	Gravelly sandy loam
Soil coarse fragments (% by volume > 2 mm)	34 (11)	70 (7)

[1] Standard deviation in brackets.

Table 2-2. Stand MPB attack status at MPB-06.

	August 2006	June 2007[1]	October 2007[1]	August 2008[2]
Non-attacked (%)	50	43	28	21
Green-attacked (%)	50	10	19	5
Red-/grey-attacked (%)	-	47	53	73

[1]Hilker *et al.* (2008)
[2]Means of values from this study and of Seip and Jones (2008).

2.2.2 Flux, climate and ecophysiological measurements

A thirty-two-meter-tall scaffold flux tower (~2.1 m long x ~1.5 m wide) was established at each of MPB-06 and MPB-03 in July 2006 and March 2007, respectively. Flux and climate measurements began on 18 July 2006 and 20 March 2007 at the respective sites. Both sites were generally located on horizontal ground with a homogeneous fetch greater than 1 km in all directions. NEP was measured directly using the eddy-covariance (EC) method, which has become the standard technique to measure net ecosystem CO_2 exchange (Baldocchi 2003). A 3-dimensional ultrasonic anemometer (model CSAT3, Campbell Scientific Inc. (CSI), Logan, Utah) was used to measure the three components of the wind vector, and turbulent fluctuations of CO_2 and H_2O were measured using an open-path infrared gas analyzer (IRGA) (model LI-7500, LI-COR, Inc, Lincoln, Nebraska,). Signals were measured with a data logger (CSI, model CR1000) with a synchronous-device-for-measurement (SDM) connection. High frequency (10 Hz) data were stored on a compact flash card that was replaced every 2-4 weeks. Half-hourly covariances and other statistics were calculated on the data logger and transmitted with climate data daily by cell phone to the laboratory. The system was powered using 3 100-W solar panels

(CTI-130, Carmanah Technologies Corp., Victoria, BC) with an 800-Ah battery unit consisting of 8 absorbent glass mat batteries (EX-1000, Carmanah Technologies Corp.). During the winter the sampling rate was reduced to 5 Hz to conserve power. At both sites, instrumentation was mounted at the height of 26 m, which was ~8 m and ~6 m above the top of the canopy at MPB-06 and MPB-03, respectively. These heights resulted in growing season upwind distances from the flux tower to the 80% cumulative flux contour being typically 400 m and 1500 m during the daytime and nighttime at both sites. Fluxes of CO_2 (F_c) were calculated as the covariance of the CO_2 mixing ratio (s_c) and vertical velocity (w), i.e., $F_c = \rho_a \overline{w's_c'}$, where ρ_a is the density of dry air, the overbar denotes half-hourly averaging and the primes indicate fluctuations from the average. High frequency signals were not detrended. Three coordinate rotations were applied to the high frequency wind data to make $\overline{v} = \overline{w} = 0$ (Tanner and Thurtell 1969). Net ecosystem exchange (NEE) was calculated as the sum of F_c and the rate of change of CO_2 storage in the air column beneath the EC instrumentation. The storage term was calculated from the difference between $\overline{s_c}$ measured at the 26-m height in the previous and following half hours applied to the air column beneath the EC sensors (see Morgenstern *et al.* 2004). NEP was calculated as NEP = -NEE.

Measurements of climate variables were also made continuously at both sites. These included: above-canopy upwelling and downwelling shortwave and longwave radiation (model CNR1, Kipp and Zonen B.V., Delft, The Netherlands) and above-canopy upwelling and downwelling, and below-canopy downwelling photosynthetically active radiation (PAR) (model LI-190AS, LI-COR Inc.), precipitation at canopy height (tipping bucket rain gauges, model TE525WS-L, CSI at MPB-03 and model 2501, Sierra Misco, Berkeley, CA at MPB-06), wind speed at the 25 m height (model 05103 R.M. Young Inc., Traverse City, MI), air temperature and

relative humidity at 6 m (model HMP45C, Vaisala Oyj, Helsinki, Finland), soil temperature (chromel-constantan 30 gauge thermocouple wire, Omega Engineering Stamford, Connecticut) at depths of 5, 10, 20 and 50 cm, soil heat flux (3 heat-flux plates model HP01, Hukseflux Delft, The Netherlands) at a depth of 5 cm and water content (model CS616, CSI) at 0-10 cm and 30-50 cm at MPB-06 and (model EC-5, Decagon Devices Inc, Pullman, Washington) at 10 cm, 20 cm and 50 cm at MPB-03. Meteorological measurements were made every second, and 30 min average values calculated. Measurements of diffuse PAR (model BF3, Delta-T Devices Inc., Cambridge, UK) were made at a weather station in the CC-97 clearcut located ~1.5 km east of the MPB-06 tower during the 2007 summer. Snow-pack depth was also measured at the clearcut weather station using an acoustic distance sensor (model SR50M, CSI) and precipitation calculated from these data and manual measurements of liquid water equivalent.

Leaf area index (LAI) was calculated for the canopies at both sites using a LI-COR Plant Canopy Analyzer (model LAI-2000, LI-COR Inc.) as well as a TRAC (Tracing Radiation and Architecture of Canopies) instrument (Third Wave Engineering, Nepean, Ontario, Canada) and hemispherical photography (Egginton *et al.* 2008).

To determine the influence the beetle had on the tree's ability to photosynthesize at an early stage of attack, foliar CO_2 exchange measurements were made on 24 pairs of green-attacked and non-attacked trees of similar size and age, located within 3 m of each other over three days at MPB-06. Shoots were clipped from the lower branches of the canopy at a height of approximately 6 m using a pruning pole and measured within 5 minutes of sampling. Measurements were made between 10:00 and 16:00h PST on August 21- 23 2006 in ambient light conditions. All three days were generally sunny with maximum downwelling PAR reaching 1800 μmol m^{-2} s^{-1}. Net assimilation (A_n) and stomatal conductance (g_s) measurements were made

using two portable photosynthesis measurement systems (model LI-6400, LI-COR Inc.), following the approach of Pypker and Fredeen (2002). One system used a clear acrylic conifer chamber (model 6400-05, LI-COR Inc.), while the other used a closed opaque chamber (model 6400-02B, LI-COR Inc.) with a red/blue LED light source. Shoots were placed in the conifer chamber under ambient light conditions, while 4 representative needles (intact to the branchlet) were placed in the LED light source chamber. In both systems a CO_2 concentration and air flow rate were maintained for 3 min at 400 ppmv and 500 μmol s^{-1} (300 mL min^{-1}), respectively. Air temperature, atmospheric water vapour pressure deficit and PAR were continuously recorded during each measurement along with A_n and g_s. Area-based estimates of A_n were calculated after determining half the total leaf area, using the volumetric displacement technique, for each branchlet or leaf sampled and leaf area to dry leaf biomass ratios (specific leaf area, SLA) were determined.

In order to assess the rate of advance of the beetle attack, tree health status inventories at MPB-06 were conducted in August 2006 and August 2008. The attack status of individual trees was determined along two 350 m long transects x 2 m wide. Green attack was identified by the presence of beetle core holes, while red attack was identified by foliage colour, and grey attack by the transition to brown colour. Inventories were also conducted in June and October 2007 by Hilker *et al.* (2008). In addition, independent tree health assessments were also made annually in August by biologists evaluating woodland caribou to partial retention logging of MPB attacked stands (Seip and Jones 2007).

2.2.3 Wintertime fluxes

Recently, the observation of wintertime CO_2 uptake has led researchers to question the reliability of the LI-7500 IRGA in cold air conditions (Grelle and Burba 2007; Burba *et al.* 2008). Comparisons using closed-path analysers suggest the problem is due to heat generated by the open-path analyser in cold conditions leading to a sensible heat flux inside the open-path array which affects the CO_2 density (Burba *et al.* 2008; Bonneville *et al.* 2008). To assess the reliability of our wintertime fluxes we first classified MPB-06 NEP as wintertime data when soil temperature at the 5 cm depth (T_s) was <1 °C and the air temperature at 26 m (T_a) was <5 °C. Of these data, in 2007, 32% showed negative NEE (CO_2 uptake) and were discarded. When separated into daytime and nighttime data, negative fluxes accounted 54% of the daytime data but only 19% of the nighttime data. This agrees with the findings of Lafleur and Humphreys (2008) who observed wintertime CO_2 uptake occurred 49% and 22% of the time during the daytime and nighttime, respectively. Burba *et al.* (2006) conducted experiments on the open-path wintertime CO_2 uptake phenomenon and reported that the problem is more serious during the daytime due to the absorption of solar radiation by the LI-7500, which further heats the instrument surface. They found that temperatures inside the open-path array were correlated with wind speed such that at higher wind speeds, heat produced by the instrument was more effectively removed from the open-path array so the difference between air temperature and surface temperature of the instrument was reduced. They found that for all air temperatures, winds exceeding 6-8 m s^{-1} reduced the surface temperature of the detector housing of the LI-7500 to less than 1 degree C above ambient. Thus we examined the effect of wind speed on our 2007 wintertime data at MPB-06 by plotting the fraction of negative NEE values against wind speed. The fraction of negative values decreased with increasing wind speed, with the largest

reduction (from 0.28 to 0.18) occurring as wind speed increased from 3 to 4 m s^{-1}. Consequently we discarded all daytime winter data when wind speed was <4 m s^{-1}, which removed a further 67% of these values, leaving 98 daytime winter values. During the nighttime, the fraction of negative values was relatively constant at ~0.12 regardless of wind speed, thus we did not discard any nighttime data based on wind speed. For the nighttime, there were 844 remaining acceptable wintertime values. In total, 56% of wintertime fluxes were accepted, leaving a total of 942 acceptable half-hour fluxes during the wintertime. The same screening procedure was applied to 2008 wintertime data.

At MPB-03, data collection did not begin until 22 March 2007, so we filled 1 January to 22 March 2007 with values modeled using the parameters from the 2008 empirical logistic relationship between NEE and T_s (see below for more details) and 2008 half hourly T_s data. It is not expected that the wintertime T_s would vary much between years. In fact, between January and March for 2008 and 2009, T_s was always within a 0.5 degree C range, slightly above 0 °C. At the Prince George airport, located ~80 km from MPB-03, wintertime snowfall was similar between years with an accumulation of 2.4 and 2.1 m in 2007 and 2008, respectively. Following the method of analysis of wintertime NEE data at MPB-06, we removed all negative NEE values and daytime data when the wind speed was < 4 m s^{-1} at MPB-03.

By removing only wintertime negative NEE measurements it is possible that a bias towards greater CO_2 loss was introduced because at these small rates of respiration instrumentation random noise could result in occasional small negative CO_2 fluxes. Alternatively, wintertime respiration might have been greater than the measurements suggest because heating in the open path array might have had the effect of lowering measured F_c from its actual value.

2.2.4 Flux quality control and data analysis

Flux quality control procedures included rejection of data when a 30-minute period had more than 30% of an individual trace with an instrument diagnostic warning flag that indicated a bad measurement, and setting minimum (300 µmol mol^{-1}) and maximum (1000 µmol mol^{-1}) bounds on CO_2 concentrations as measured by the open-path IRGA. Wind rose analysis showed that the predominant wind direction at MPB-03 was from the west to southwest but during the winter there was also strong flow from the north-east. At MPB-06 the predominant wind direction during the growing season was from the west to southwest. Fluxes were not rejected on the basis of wind direction since the fetch was greater than 1 km in all directions around the tower. Wind through the tower and sonic occurred seldomly and when it did there was no detectable effect.

EC measurements made during the night provide a direct measure of R_e (van Gorsel *et al.* 2008). At both sites, only nighttime EC data when friction velocity (u_*) was greater than the threshold u_* (u_{*th}) of 0.30 m s^{-1} were considered for analysis to ensure sufficient turbulent mixing (Baldocchi, 2003). Selection of u_{*th} was achieved by plotting half-hourly CO_2 flux (both annually, and for the growing season and the rest of the year) against u_* and determining the value for which a further increase in u_* no longer led to an increase in the flux (Massman and Lee 2002). Although u_{*th} was not clearly defined, which, unfortunately, is common-place in EC studies (Gu *et al.* 2005), the threshold was within ±0.05 m s^{-1} of 0.30 m s^{-1}. Daytime R_e was estimated using the standard algorithm established by the Fluxnet Canada Research Network (FCRN) of the Canadian Carbon Program (Barr *et al.* 2004) which assumes an empirical logistic relationship between nighttime R_e ($u_* > u_{*th}$) and T_s (the r^2 was 0.44 for MPB-06 in 2007 and 0.50 and 0.42 for MPB-06 and MPB-03 in 2008, respectively) and extrapolates to daytime (see Humphreys *et al.* 2005). P_g was calculated as daytime NEP + daytime R_e. Gaps in the daytime

NEP data were filled with the difference between modelled P_g and R_e. P_g was also modelled using the FCRN standard algorithm, which assumes a rectangular hyperbolic relationship between P_g and incident PAR (the r^2 for MPB-06 and MPB-03 was 0.18 and 0.13 for 2007, and 0.51 and 0.42 for 2008, respectively). The gap-filling procedure used was altered from that described in Barr *et al.* (2004) in that the moving window, which estimates the seasonal variation of the time-varying parameters from the empirical relationships described above, was not applied during the winter (when T_s was <1 °C). In the moving window approach, the parameter is calculated as the slope of the linear regression between estimates of R_e (and P_g) obtained from the annual relationships, and R_e (and P_g) from the measurements. The window is 100 data points wide and is moved in an increment of 20 points at a time. Ideally, each window would cover a period of a few days. However, during the winter at these sites, when NEE measurements were sparse due to the screening procedure, a single 100 point window was found to span weeks or 2-3 months. Over such time spans climatic variability, such as changes in T_a, could result in variations in R_e even though T_s varied little.

EC data were assessed for energy balance closure, although an energy balance correction was not applied. Half-hourly measurements of net radiation flux, surface soil heat flux, sensible and latent heat flux were used together with estimates of changes in air-column sensible and latent heat and biomass heat storage (Humphreys *et al.* 2003). Daytime energy balance closure during the 2007 growing season was 79% and 88% at MPB-06 and MPB-03, respectively.

To determine the photosynthetic and respiratory characteristics of the two ecosystems, the following Michaelis–Menten light response (rectangular hyperbolic relationship) was used

$$\mathrm{NEP} = \frac{\alpha Q A_{\max}}{\alpha Q + A_{\max}} - R_d \qquad (1)$$

where α is the quantum yield, A_{max} is ecosystem photosynthetic capacity, R_d is the daytime ecosystem respiration and Q is the incident PAR (Griffis *et al.* 2003). This analysis was done on a monthly basis using daytime data for $Q > 5$ μmol $m^{-2}s^{-1}$.

2.2.5 Uncertainty analysis

Uncertainties associated with annual totals of NEP, P_g and R_e were determined using the following two techniques. Random error was assessed using propagation of errors following Morgenstern *et al.* (2004), which assigned a 20% random error to each half-hourly value of NEP. The uncertainty due to the gap filling algorithms was estimated using Monte Carlo simulation following the procedure of Krishnan *et al.* (2006) which generated gaps in measured NEP (i.e., not gap-filled) ranging from a half-hour to 10 days using a uniformly distributed random number generator, 1000 times. For each time, the relationships between R_e and T_s, and P_g and Q were then determined using the algorithms described above. Modelled values were used to gap-fill the original dataset. The annual values of NEP, R_e and P_g were then sorted to determine the 95% confidence interval.

2.3 Results

2.3.1 Seasonal weather

Mean annual T_a at both sites was approximately 3.0 °C in 2007 and 2008. Growing season (May–September) T_a in the study region is typically cool with an average daily (24 h) T_a of 12 °C (1971-2000 normal from the Mackenzie Airport, Environment Canada). At MPB-06, the mean growing season T_a was 11.8 and 12.4 °C in 2007 and 2008, respectively. Growing

season rainfall was 246 mm in 2007 and 250 mm in 2008 (Fig. 2.2). Snowfall during the 2006-2007 winter at MPB-06 was estimated to be 354 mm (liquid water equivalent) and total annual precipitation (1 Nov 2006 to 31 Oct 2007 rain year) was approximately 732 mm. Snowfall during the 2007-2008 winter was estimated to be 339 mm and total annual precipitation was approximately 608 mm. Average soil fine-fraction (soil particles <2 mm) volumetric water content (θ) for the 0-10 cm depth, varied from 0.09 to 0.16 $m^3 m^{-3}$ at MPB-06 during the growing season of the two years. Field capacity (-0.1 MPa) and wilting point (-1.5 MPa) θ values for the soils at the two sites were estimated to be approximately 0.17 and 0.05 $m^3 m^{-3}$, respectively (Campbell and Norman 1998). At MPB-03, mean growing season T_a was 12.7 °C during both 2007 and 2008, while growing season rainfall was 576 mm in 2007 and 620 in 2008. The much higher precipitation total at MPB-03 compared to MPB-06 is likely due to a higher occurrence of convective showers and storms at MPB-03. Growing season θ (10 cm depth) at MPB-03 varied from 0.13 to 0.20 $m^3 m^{-3}$ over the two years. Wintertime T_s at both sites never dropped below -0.5°C, likely a result of the heavy snowfalls in late-October and November, which would have insulated the soil surface before the soil could freeze (Monson *et al.* 2006).

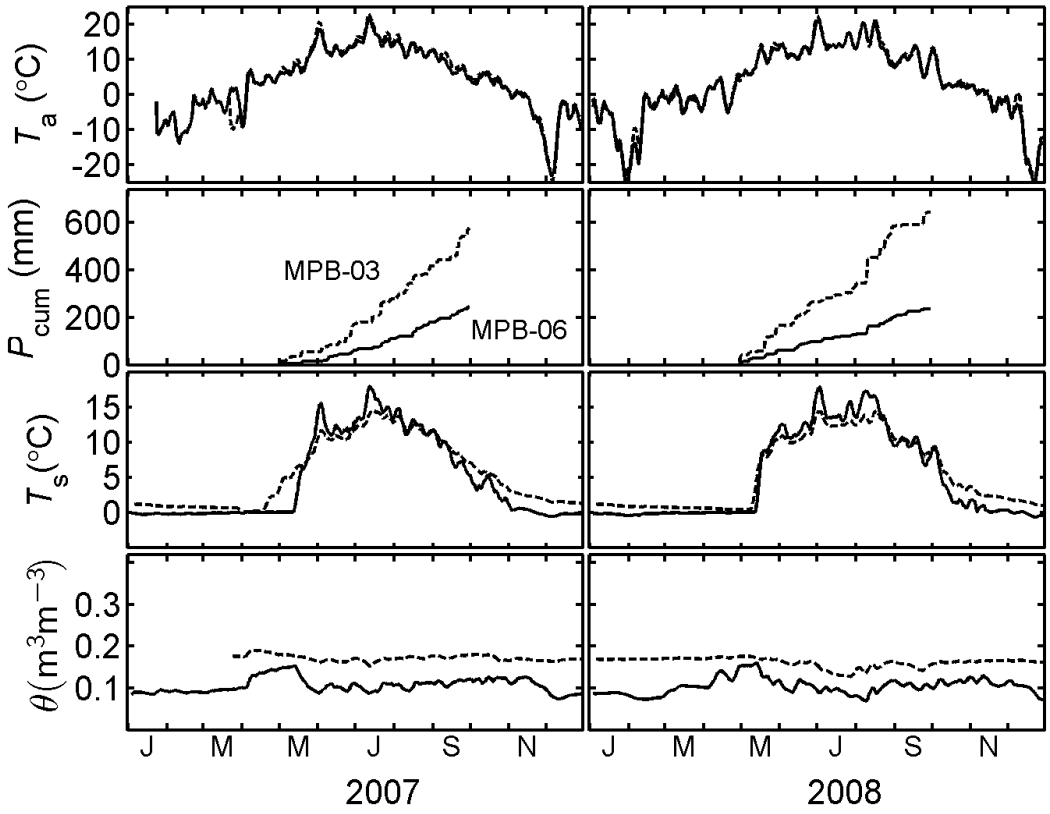

Figure 2.2. Air temperature (T_s), cumulative precipitation (P_{cum}), soil temperature (T_s), soil water content (θ), wind speed (u) and PAR (Q) at MPB-06 and MPB-03 for 2007 and 2008. For P_{cum} only the growing season (May to September) values are shown. At MPB-06 total annual precipitation was estimated to be 732 and 608 mm in 2007 and 2008, respectively.

2.3.2 Comparison of NEP in attacked and non-attacked trees and stands

Although MPB-06 was still green and appeared healthy during July and August 2006, ~50% of the trees had been attacked by late-July. The average bole diameter at 1.3 m above the ground of attacked lodgepole pine trees was 14.3 cm, while that of non-attacked trees was 8.0 cm, showing the preference of the beetle for larger trees. A_n and g_s measurements were made to determine the effect of the beetle attack on photosynthesis at this early stage of attack. A two-way analysis of variance showed that there was a slight but insignificant difference at the 95%

confidence level in A_n and g_s between pairs of green-attacked and non-attacked trees (Table 2-3) (A_n and g_s values were approximately 25 and 15 % higher respectively, for the LED light source measurements). As a result, we treated NEP measurements made between 29 July and 20 August 2006, as a healthy control period to compare with measurements made during the same interval in 2007, when approximately 50% of the trees had been killed. The climate during the comparison periods was similar, with average T_a, T_s and daytime PAR being 13.4°C, 12.7°C and 670 µmol m^{-2} s^{-1} in 2006 and 12.8 °C, 12.5 °C and 600 µmol m^{-2} s^{-1} in 2007. However, 2006 was a relatively dry summer and as a result average θ was only 0.06 m^3 m^{-3} compared to 0.10 m^3 m^{-3} in 2007.

Measured values of NEP over the comparison interval in both years were used to create an ensemble average diurnal course of NEP (Fig. 2.3a). All half-hourly nighttime measurements were averaged to a single nighttime value. For the 22-day comparison period, NEP was 18 g C m^{-2} in 2006 compared to 23 g C m^{-2} in 2007. Average nighttime NEP was less (more negative) in 2006 (-2.98 µmol m^{-2} s^{-1}) than 2007 (-1.95 µmol m^{-2} s^{-1}) and during the daytime (between 6:00 and 21:00h PST) average NEP was 2.36 and 1.90 µmol m^{-2} s^{-1} in 2006 and 2007, respectively. Light response analysis shows that A_{max}, α and R_d were all greater in 2006 than 2007 (Fig. 2.3b).

Table 2-3. Comparison of daily values of net assimilation (A_n) and stomatal conductance (g_s) of pairs of non-attacked (NA) and green-attacked (GA) trees at MPB-06.

Date 2006	n	A_n (µmol CO_2 m^{-2} s^{-1})				g_s (mmol H_2O m^{-2} s^{-1})			
		NA		GA		NA		GA	
		Ambient[2]	LED[3]	Ambient	LED	Ambient	LED	Ambient	LED
Aug 21	3	3.05 (1.08)[4]	2.48 (1.49)	3.17 (1.55)	2.55 (1.52)	0.019 (0.005)	0.008 (0.006)	0.011 (0.005)	0.011 (0.007)
Aug 22	11	4.01 (0.93)	5.02 (1.57)	2.85 (1.49)	4.23 (2.46)	0.016 (0.013)	0.022 (0.010)	0.012 (0.014)	0.020 (0.013)
Aug 23	10	3.58 (1.52)	3.94 (1.25)	2.88 (2.53)	2.72 (2.55)	0.016 (0.016)	0.016 (0.008)	0.012 (0.019)	0.012 (0.013)
All	24	3.21 (1.18)	4.49 (1.47)	2.97 (1.85)	3.39 (2.44)	0.016 (0.013)	0.018 (0.009)	0.011 (0.015)	0.015 (0.013)

[1] Daily averages of measurements made between 10:30 – 15:00h PST.
[2] Measurements were made using a conifer chamber under ambient light.
[3] Measurements were made using an LED light source chamber.
[4]Standard deviation.

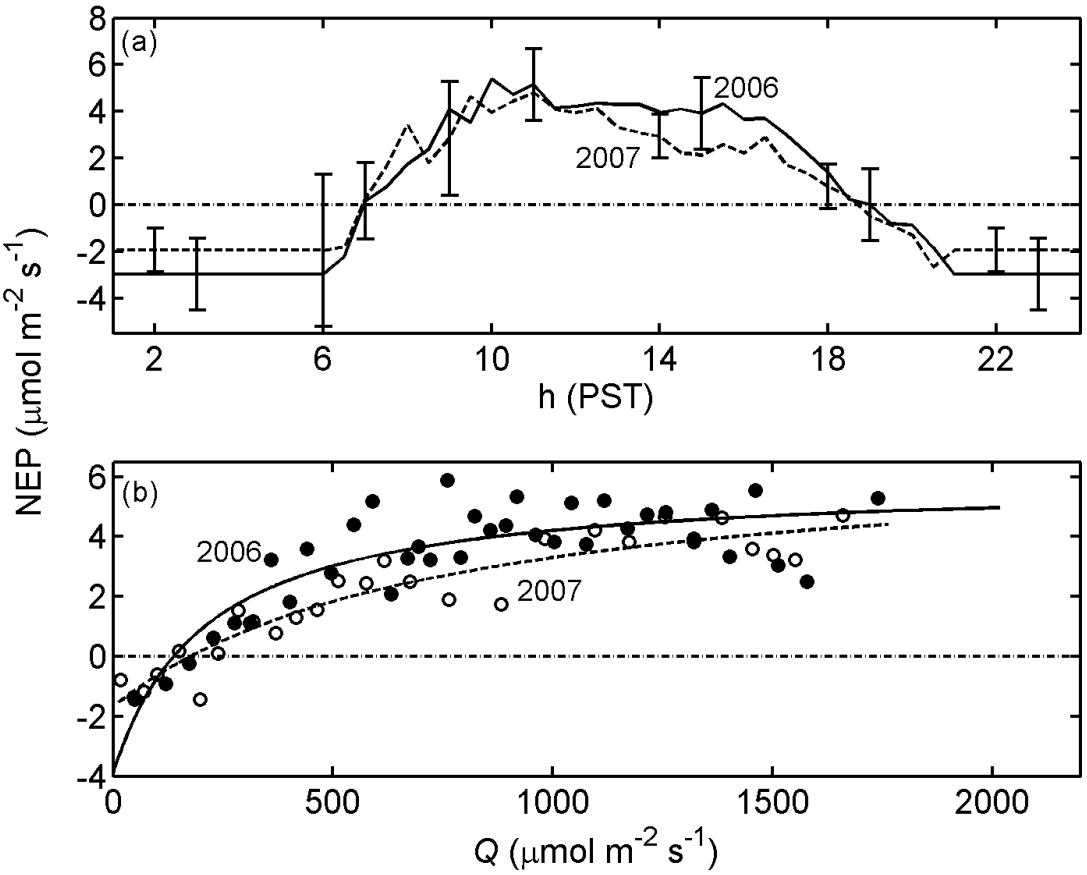

Figure 2.3. (a). Ensemble-average diurnal course of measured NEP measurements made between July 29 and August 20 2006 and 2007 at MPB-06. All half-hourly nighttime measurements were averaged to a single nighttime value for both years (see text). Vertical bars are standard deviations. (b). Light-response (Q) analysis for MPB-06 daytime NEP measurements made during the same period. Maximum assimilation rate (A_{max}), quantum yield (α) and daytime respiration (R_d), were 9.8 μmol m^{-2} s^{-1}, 0.05 and 3.93 μmol m^{-2} s^{-1} for 2006 and 8.6 μmol m^{-2} s^{-1}, 0.01 and 1.7 μmol m^{-2} s^{-1} for 2007.

2.3.3 Diurnal courses of monthly ensemble-averaged NEP in beetle-attacked stands

The diurnal courses of monthly ensemble-averaged half-hour values of NEP are compared in Fig. 2.4 for MPB-06 and Fig. 2.5 for MPB-03. For January to March and November to December, average NEP values for 2007 and 2008 were -0.52 and -0.42 μmol m^{-2} s^{-1} at MPB-06 and -0.41 and -0.35 μmol m^{-2} s^{-1} at MPB-03, respectively. These wintertime rates of C loss were similar to the value of ~0.45 μmol m^{-2} s^{-1} measured during February in a boreal aspen stand in

Saskatchewan, Canada (Black *et al.* 1996) where, like these sites, T_s remained at about -0.5 °C, despite the low values of T_a. Despite the widespread mortality caused by the beetle, total NEP during the growing season (May-September) was positive at both sites in both years (12 and 52 g C m^{-2} at MPB-06 and 17 and 68 g C m^{-2} at MPB-03 in 2007 and 2008, respectively). At MPB-06, daytime maximum half-hourly NEP values were significantly higher in June and July 2008, reaching 5 µmol m^{-2} s^{-1} in July. During the other growing season months, NEP was more similar between years. During the nighttime, C losses reached a maximum in July when half-hourly values of ~3 µmol m^{-2} s^{-1} were observed. At MPB-03, daytime half-hourly values of NEP were significantly higher in 2008, reaching a maximum of ~6 µmol m^{-2} s^{-1} in July, August and September. The highest nighttime half-hourly C losses were between 3 - 3.5 µmol m^{-2} s^{-1} in July and August 2007 and 2008.

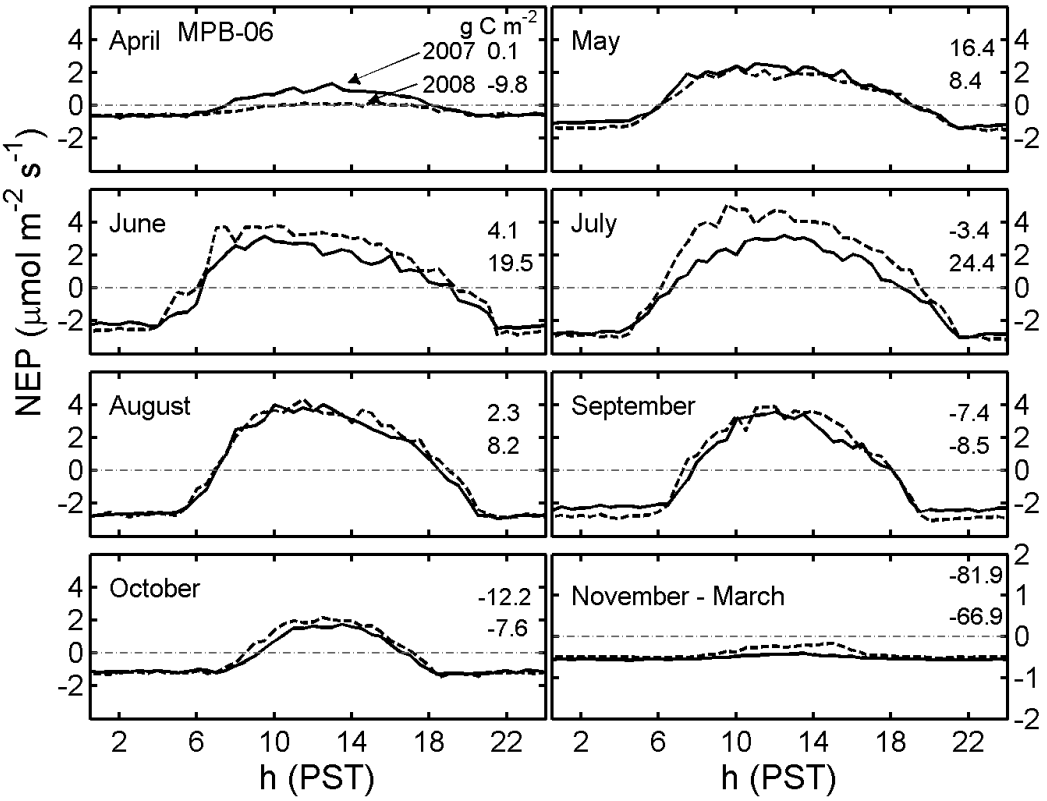

Figure 2.4. The diurnal patterns of monthly ensemble-averaged half-hour values of NEP for MPB-06 for 2007 and 2008. Values in panels are NEP in g C m^{-2} per month or for November to March.

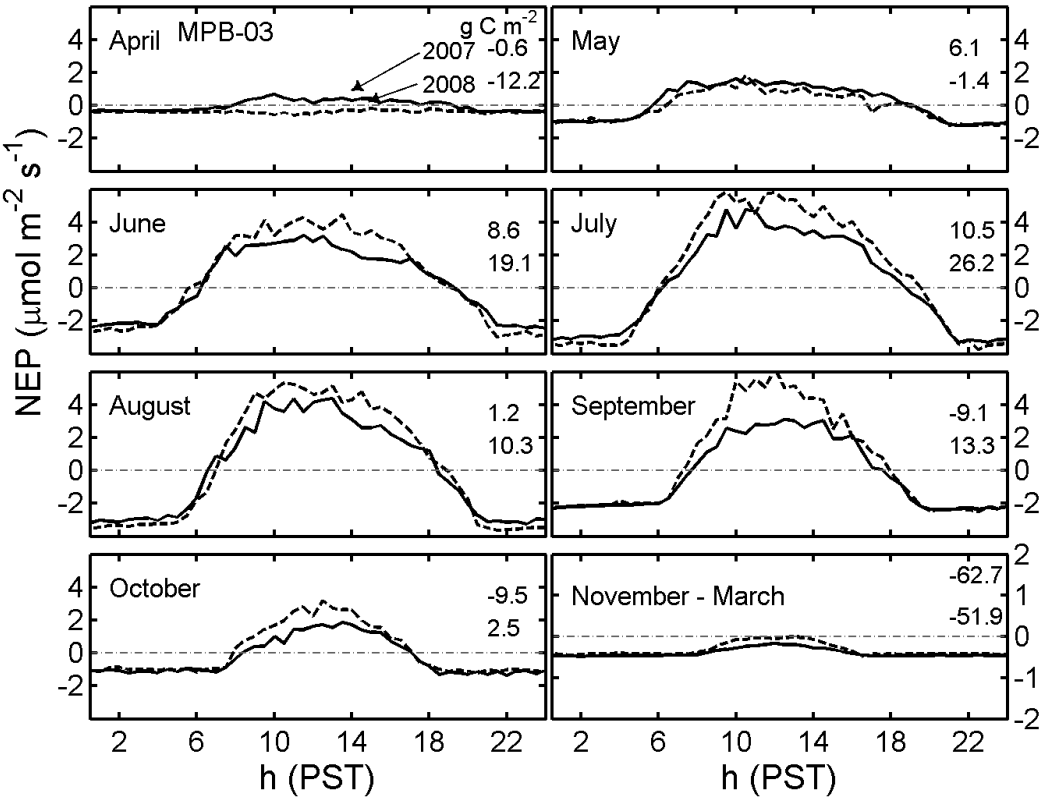

Figure 2.5. Same as Fig. 2.4, except for MPB-03.

Growing season monthly maximum values of A_{max}, α and R_d for MPB-06 and MPB-03 are shown in Figs. 2.6 and 2.7, respectively. At both sites values of all three parameters were generally higher in 2008. At MPB-06, A_{max} increased from 4 - 5 µmol m^{-2} s^{-1} in May to 9 - 10 µmol m^{-2} s^{-1} in September, while α and R_d tended to be highest in July and August. At MPB-03, A_{max} in 2007 reached its maximum value in July, while in 2008 the maximum was in September. In both years α and R_d were highest in June and July.

Using the Michaelis–Menten light response relationship, (equation 1) we found that Q explained between 26 and 48% of the variation in half-hourly NEP values at MPB-06, and

between 20 and 32% at MPB-03. During May 2007 and 2008 at MPB-03, *Q* only accounted for 11 and 3% of the variation in NEP.

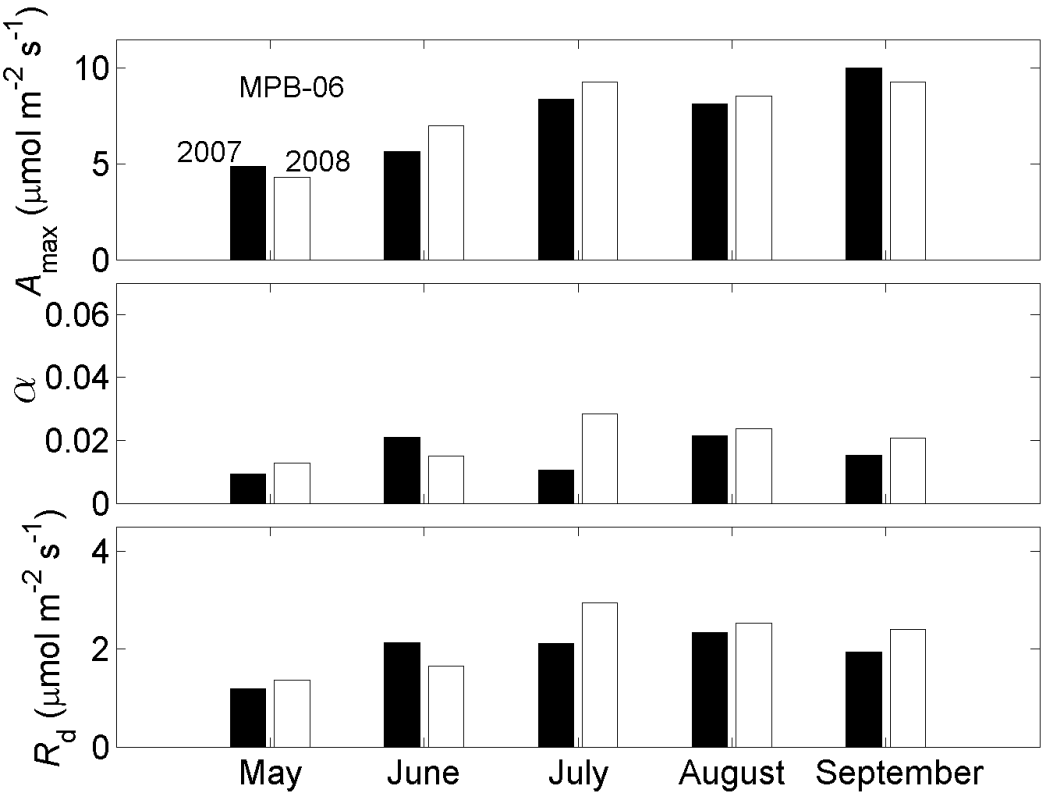

Figure 2.6. Maximum assimilation rate (A_{max}), quantum yield (α) and daytime respiration (R_d) for MPB-06 from May to September 2007 and 2008. From May to September 2007 and 2008, the r^2 of equation 1 was between 0.3 - 0.5.

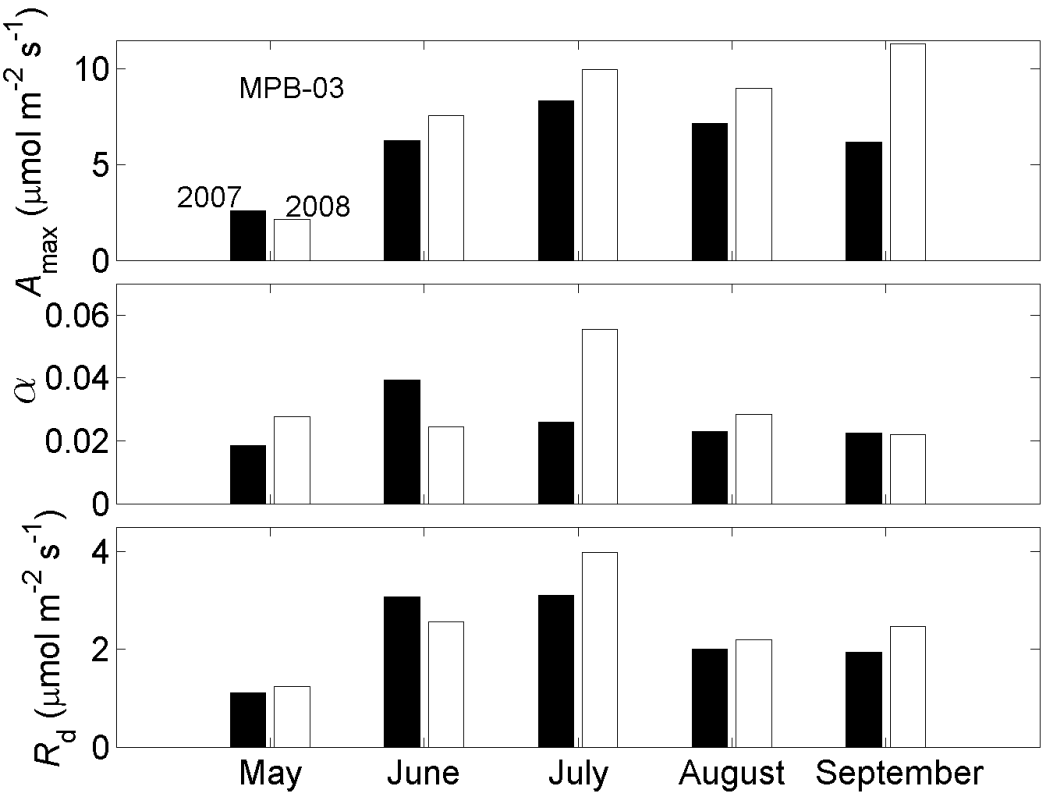

Figure 2.7. Same as Fig. 2.6, except for MPB-03. From May to September 2007 and 2008, the r^2 of equation 1 was between 0.1 - 0.3.

2.3.4 Comparison of cumulative half-hourly annual NEP, P_g and R_e

Cumulative NEP, P_g and R_e are shown in Figs. 2.8 and 2.9. Annual NEP was -82 and -33 g C m^{-2} at MPB-06 in 2007 and 2008 (Fig. 2.8). P_g increased from 440 g C m^{-2} in 2007 to 522 g C m^{-2} in 2008, indicating that the smaller fraction of healthy trees in 2008 was able to sequester more C than the larger fraction in 2007, although the growing season conditions (daytime T_a > 5°C) lasted a week longer in 2008. Annual R_e was significantly greater in 2008 (555 g C m^{-2}) than in 2007 (521 g C m^{-2}). At MPB-03, NEP increased from -56 g C m^{-2} in 2007 to 4 g C m^{-2} in 2008

(Fig. 2.9), while both P_g and R_e increased significantly from 432 and 469 g C m^{-2} in 2007 to 522 and 518 g C m^{-2} in 2008, respectively. Growing season conditions lasted 16 days longer at MPB-03 in 2008. Over both years at MPB-06 and MPB-03, the 20% random error assigned to each half-hour resulted in an annual NEP error of <3 g C m^{-2} $year^{-1}$. The uncertainties associated with the gap-filling relationships, which indicate that in all but one of the measurement years these sites were clear C sources, are shown in Table. 2-4.

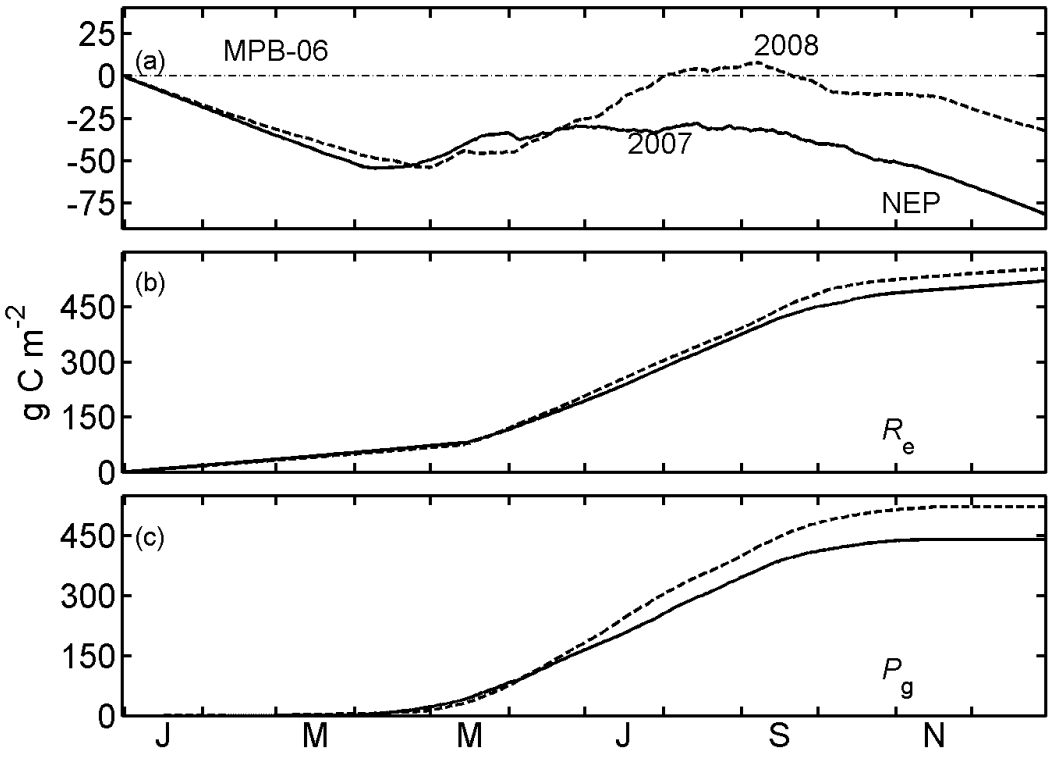

Figure 2.8. (a) Cumulative net ecosystem production (NEP), (b) ecosystem respiration (R_e) and (c) gross ecosystem photosynthesis (P_g) at MPB-06 for 2007 and 2008.

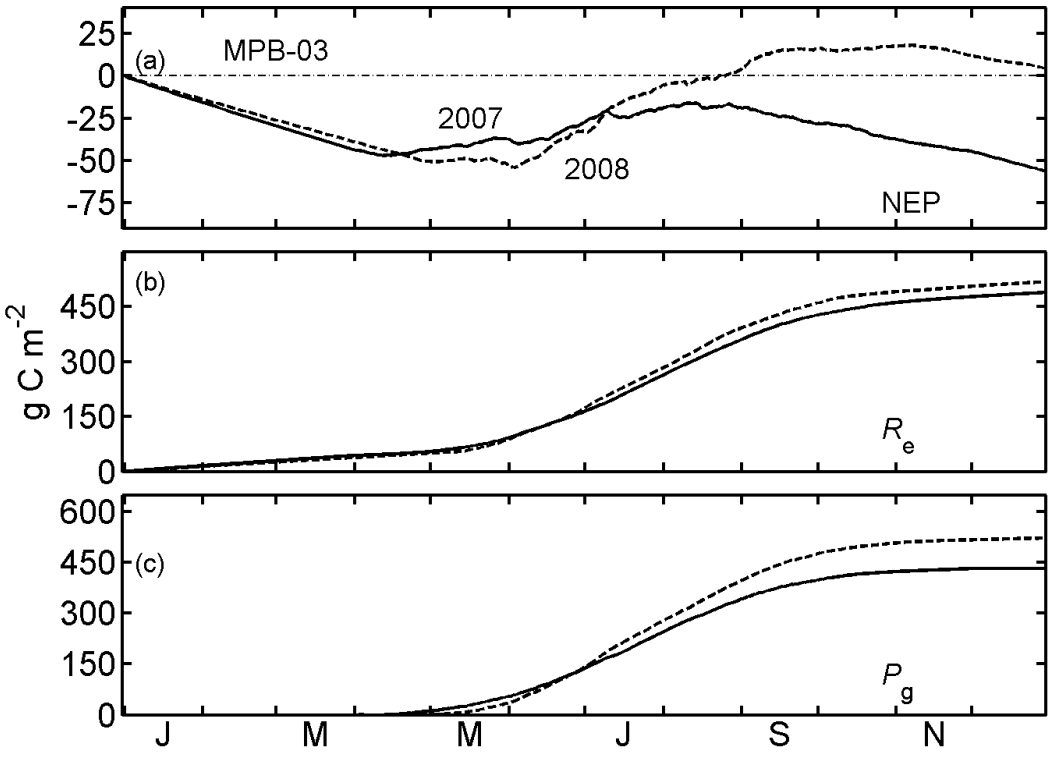

Figure 2.9. Same as Fig. 2.8, except for MPB-03.

Table 2-4. Annual totals and estimated uncertainties of net ecosystem production (NEP), ecosystem respiration (R_e) and gross ecosystem photosynthesis (P_g) (g C m^{-2}).

	MPB-06		MPB-03	
	2007	2008	2007	2008
NEP	-82 (-53, -93)[1]	-33 (-17, -61)	-56 (-6, -69)	4 (53,-15)
R_e	521 (552, 507)	555 (579, 532)	469 (514, 444)	518 (553, 492)
P_g	440 (480, 430)	522 (539,491)	432 (469, 419)	522 (567, 509)

[1]Upper and lower 95% confidence intervals. See Methods section for details. Confidence intervals at MPB-03 in 2007 were calculated using NEP measurements from the 2008 winter (soil temperature <1 °C).

2.3.5 NEP during the growing season at the harvested sites

During the daytime, half-hourly NEP reached a maximum of 1.7 μmol m^{-2} s^{-1} at CC-97, but was only briefly positive at CC-05 during mid-day hours (Fig. 2.10a). Average daily (24-h) NEP during the 29 June – 23 July 2007 measurement period at CC-97 was -0.37 ± 0.20 g C m^{-2}, while during this same period, MPB-06 had a near neutral daily NEP of -0.07 ± 0.35 g C m^{-2}. During the 24 July to 16 August 2007 measurement period at CC-05, average daily NEP was -0.87 ± 0.13 g C m^{-2}, while average daily NEP at MPB-06 was 0.40 ± 0.41 g C m^{-2} (Fig. 2.10b).

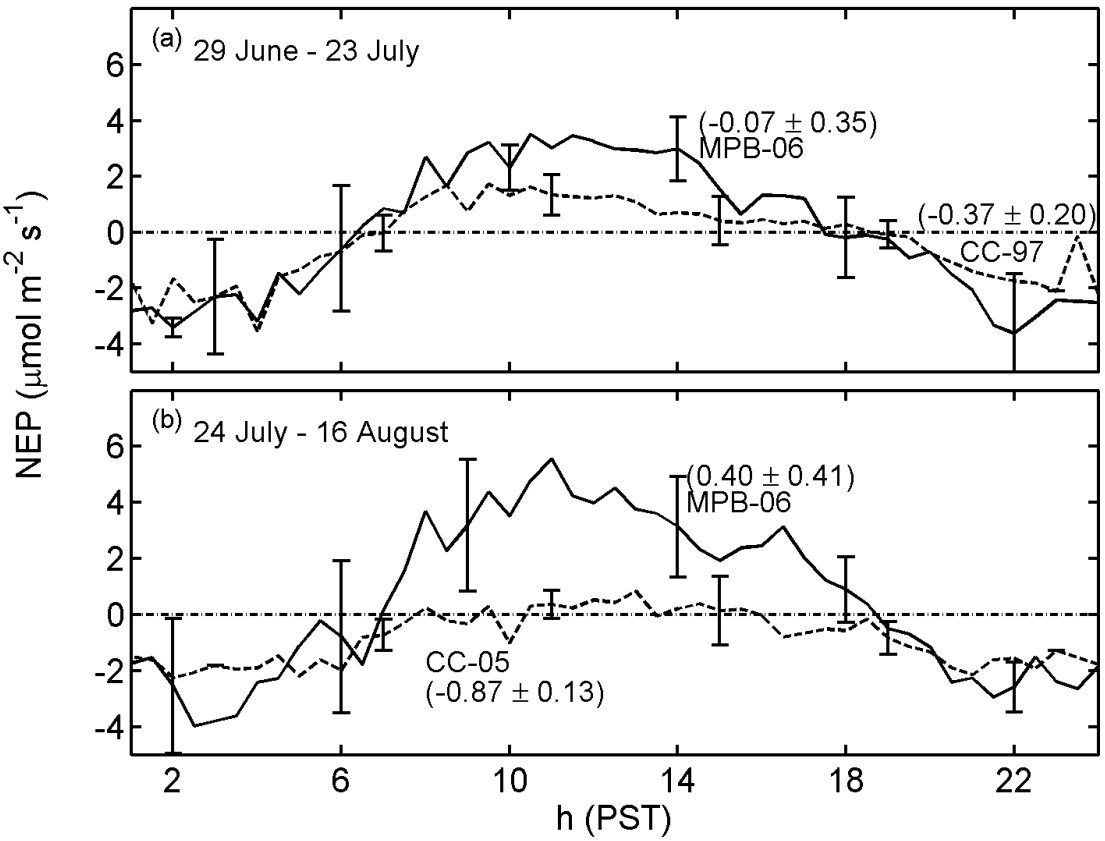

Figure 2.10. Ensemble-average diurnal course of measured NEP in 2007 at, (a) CC-97 and (b) CC-05, compared with measurements at MPB-06. Bars are standard deviations. Numbers in the brackets adjacent to the stand acronyms are average daily (24-h) NEP in g C m^{-2} for the measurement period. Average 24-h canopy downwelling photosynthetically active radiation and air temperature were 460 and 405 μmol m^{-2} s^{-1} and 16 and 14°C for 29 June – 23 July and 24 July – 16 August, respectively.

2.4 Discussion

2.4.1 CO_2 exchange in attacked and non-attacked trees

The non-significant difference in foliar CO_2 exchange rates between green-attacked and non-attacked trees suggests that during the first few weeks of attack, phloem and xylem flows had not yet been greatly affected. However, the coefficient of variation for LED and ambient light source

measurements was approximately twice as high for green-attacked trees compared to non-attacked trees, which in combination with reduced (though not significantly) stomatal conductances, is likely an indication of incipient effects of beetle attack. By the 2007 growing season, many of the attacked trees at MPB-06 had died, resulting in a reduced photosynthetic capacity compared to the comparison interval in 2006. However, total C sequestration was lower in 2006 than 2007 due to higher rates of respiration. The higher respiration in 2006 was likely due to the R_a from the higher fraction of healthy trees. In addition, in 2006, θ values were close to the estimated wilting point, which might have been sufficiently low to inhibit P_g (Lambers *et al.* 1998). Had θ values been more similar to those of 2007 it is likely P_g would have been greater.

2.4.2 NEP in MPB-attacked stands

While both MPB-06 and MPB-03 were close to C neutral in April 2007, April 2008 was a month of C loss, probably due to cooler air temperatures, which inhibited photosynthesis. In both years at MPB-06 the snow melted by mid-May. At MPB-03, the snow melted by late April in 2007 and by mid-May in 2008. May 2007 was a relatively productive month at both sites, as a combination of abundant soil water from melting snow and warm air temperatures led to favourable conditions for photosynthesis. During this time below-ground R_e was still limited by relatively cold soil conditions. Monson *et al.* (2005) reported that at a subalpine forest in Colorado, USA, the interannual variability in NEE (i.e., -NEP) over 5 years was mostly explained by variation in the length of the snowmelt period, having found that during the snowmelt period NEE was most negative in years when snowmelt occurred later in the spring. A later snowmelt can provide a constant supply of soil water when air temperatures are warmer than would have been the case if

snowmelt had occurred earlier (Monson *et al.* 2005). Some recent studies have shown that air temperature plays the dominant role in determining photosynthetic recovery in coniferous forests (Tanja *et al.* 2003; Ensminger *et al.* 2004, Krishnan *et al.* 2008). Although T_a was slightly higher at both sites in May 2008, there was a ~20% reduction in PAR, which likely partly accounts for the lower NEP observed for that month.

That MPB-06 was an annual C source shows that photosynthesis was greatly reduced due to the beetle epidemic. It was somewhat surprising that in 2008 MPB-06 was a greater growing season C sink than in 2007, despite a smaller percentage of healthy trees. The high productivity of the healthy 21% of trees in 2008 suggests those trees, along with shrubs and herbs, likely benefited from less competition for resources, such as soil water and nitrogen (Veblen *et al.* 1991). Berg *et al.* (2006) used dendrochronological techniques to conclude that in spruce-forests attacked by the spruce beetle (*Dendroctonus rufipennis*), non-attacked trees often rapidly increased their growth following attack, by similarly taking advantage of less competition for light, soil water and nutrients. The growing season C uptake at MPB-03 was likely a result of the high productivity of the secondary structure and shrubs and herbs, which remained healthy (and probably even experienced enhanced vigour) because the beetle attacks primarily mature lodgepole pine trees (Safranyik and Wilson 2006). The greater C accumulation in 2008 compared to 2007 at MPB-03 was likely due to an increase in below-canopy light levels from an opening of the stand due to needle fall, as shown by hemispherical photography (Egginton *et al.* 2008). Shrubs and herbs would also be expected to benefit from higher below-canopy light levels and are capable of sequestering C at relatively high rates (Pypker and Fredeen 2002).

In other studies, researchers have also observed an increase in the growth of surviving trees following beetle outbreaks, stand thinning and fire. For instance, Alfaro *et al.* (2004) used

dendrochronology to determine that following three historical large-scale MPB outbreaks in south-central BC, surviving trees experienced extended periods of increased growth, averaging 14 years. Heath and Alfaro (1990) estimated the growth releases to have begun between 2 to 6 years following the start of a severe outbreak in central BC. Waring *et al.* (1985) reported that following MPB attack in Oregon, the growth efficiency (the increment in stem biomass per square meter of foliage) of surviving trees increased 2 and 3 years following attack and concluded that the major impact of the attack was the reduction in canopy leaf area which increased the available light and improved photosynthesis for the remaining live trees. Like Berg *et al.* (2006), Veblen *et al.* (1991) used dendrochronological methods and found that a spruce beetle outbreak in the 1940s in Colorado accelerated the growth of shade tolerant tree species (not attacked by the beetle), rather than leading to new seedling establishment, which resulted in a shift in stand structure from spruce to fir dominated forests. Growth rates remained high for >40 years and were greater for smaller sub-canopy trees than larger canopy trees. Yang (1998) measured foliar and stand growth in a 40-year-old lodgepole pine stand in Alberta, Canada and found that needle length and mass increased significantly 3 and 4 years after thinning while tree height, DBH and basal area increased 5 and 10 years following thinning. Smirnova *et al.* (2008) observed a growth release of surviving trees in jack pine (*Pinus banksiana*) stands in Quebec, which had experienced medium intensity fires. These studies suggest that at MPB-03 there could be a shift from a pre-beetle-attack lodgepole pine canopy to a post-beetle-attack sub-alpine-fir dominated canopy as the latter comprises a significant portion of the secondary structure which is experiencing a rapid increase in growth following the attack.

The dissimilarity in response of stand level photosynthesis to *Q* between sites is probably attributable to the differences in species composition. While MPB-06 is a uniform lodgepole pine

canopy acclimated to full sunlight, which can be expected to respond to *Q* in a relatively uniform manner, MPB-03 is composed of a mix of shade acclimated sub-canopy conifers, all responding uniquely to *Q* (Lambers *et al.* 1998). Once the leaf out of the understory deciduous component occurred in June at MPB-03, a rapid increase in the photosynthetic response to *Q* was observed. The high A_{max} observed in September at both sites may be a result of the lower vapour pressure deficit than that observed during the mid-summer months when the trees limit water loss by lowering the stomatal conductance (Lambers *et al.* 1998).

There are few reported measurements of NEP in stands where insect attacks have occurred. In a Mediterranean forest in southern France, Allard *et al.* (2008) reported that a caterpillar attack decreased annual NEP compared to non-attack years. Similarly, Kirschbaum *et al.* (2007), in a modelling/EC study, reported that a psyllids (*Cardiaspina* spp.) attack in a *Eucalyptus delegatensis* forest, which led to a large unseasonable leaf-fall, had the effect of reducing P_g and increasing C loss through respiration by insects and decomposition.

For comparative purposes, it is useful to examine the results of studies of the effect of fire on forest C balance components. Amiro *et al.* (2006) found that a boreal mixed jack pine and black spruce (*Picea mariana*) stand that was severely burned in 1998 had an NEP of -87 and -132 g C m^{-2} yr^{-1} in 2001 and 2002, respectively. When these measurements were made, the stand consisted of aspen saplings and shorter jack pine and black spruce seedlings, as well as ~18-m tall standing dead trees. The burnt site that was the focus of the Amiro *et al.* study shares characteristics similar to those of MPB-06 and MPB-03 in that consisted of standing dead trees with decomposing dead roots below ground. Amiro *et al.* (2006) also measured an annual NEP of 68 g C m^{-2} in 2002 in a boreal forest stand burned in 1989, which consisted of balsam poplar (*Populus balsamifera*), jack pine, trembling aspen (*Populus tremuloides*) and birch (*Betula*

papyrifera), as well as dead snags of black spruce and jack pine. If left to naturally regenerate, it is possible that MPB attacked stands without secondary structure might follow a similar path to recovery as burnt stands, as in both cases the trees have been killed but remain standing. They differ in that while most of the needles are consumed during a fire, they fall to the ground over a number of years following a beetle attack. In addition, much of the understory and upper soil organic layer are also consumed during a fire (Amiro *et al.* 2006), whereas these components are not directly affected by a beetle attack. In terms of C losses, while burnt stands experience a rapid and large loss of C as a direct result of fire, both beetle-attacked and burnt forests likely experience a prolonged elevated R_h due to the decomposition of killed vegetation (Mkhabela *et al.* 2009). A significant difference is that while almost all trees are killed during severe crown fires, a portion of the trees survive a beetle attack, depending on the severity of attack and the stand composition. Thus, P_g would likely be much greater following a beetle attack, due to the accelerated growth of the surviving vegetation. Indeed, the jack pine and black spruce stand burned in 1998 (mentioned above), had a much lower P_g (271 and 319 g C m^{-2} yr^{-1} in 2004 and 2005) (Mkhabela *et al.* 2009), than that observed in this study.

2.4.3 NEP of harvested sites

CC-05 was a relatively large C source during the 2007 growing season, as expected, given the site had been harvested just two years prior. However, CC-97, which had been regenerating for 10 years, was also still a growing season C source, which is significant, given that the site is composed of an abundance of actively photosynthesizing lodgepole pine saplings and that coarse woody debris left following harvesting had a decade to decompose. Since there is no significant photosynthetic uptake of C during the rest of the year, these measurements indicate that both

these clearcut sites were annual C sources. There have been numerous other measurements of NEP made in early successional forests following clearcut harvesting (Zha *et al.* 2010; Kowalski *et al.* 2003; Pypker and Fredeen 2002, 2003; Rannik *et al.* 2002). Stands varying in age from 1 to 10 years following clearcut harvest, in a variety of biogeoclimatic zones, have been observed to be annual C sources (Humphreys *et al.* 2005). For example, Humphreys *et al.* (2005) reported a harvested and then replanted coastal Douglas-fir (*Pseudotsuga menziesii*) stand to be an annual C source of 620, 520 and 600 g C m^{-2} y^{-1} in the first, second and third years following harvesting. A sub-boreal clearcut planted with white spruce and lodgepole pine had an average daily growing season NEP of 0.3 g C m^{-2} day^{-1} 5 years after harvesting but became a C source during the sixth year with an average daily growing season NEP of -0.9 g C m^{-2} day^{-1} (Pypker and Fredeen 2002) illustrating the large interannual variation in NEP possible in recently harvested stands.

2.5 Conclusions

MPB-06 and MPB-03 were growing season C sinks and MPB-03 was a weak annual C sink in 2008, demonstrating the resiliency of sequestration in these stands to the beetle epidemic. The presence of secondary structure at MPB-03 likely accelerated the stand's return to C neutrality. In the MPB-06 stand, during the growing season the remaining live trees, along with shrubs, herbs and non-vascular plants provided a moderate level of C uptake, especially during the second year when below-canopy light and growth levels increased. Although needle fall and dead roots probably began to enhance heterotrophic respiration, we have yet to observe a large respiratory release from either site. Once a large portion of the dead trees fall, an increase in decomposition is likely, which could result in these sites becoming significantly larger C

sources. Conversely, an increase in C uptake due to the rapid growth of secondary structure would likely offset some or all of those C losses. Thus, NEP measurements made over longer time scales are required to determine how these forests will continue to evolve. Additionally, the rapid warming of northern interior of BC, which has enabled the current beetle epidemic to spread further north than during previous attacks (Safranyik and Wilson 2006), is projected to intensify, likely leading to an increase in the prevalence of forest fires (Lemmen *et al.* 2008) and insect and disease epidemics (Taylor *et al.* 2006). Growing season NEP measurements in harvested stands show they can remain significant C sources for at least 10 years, which, when compared to MPB-06 and MPB-03 which were growing-season C sinks, suggests that deferring the harvest of MPB attacked stands with significant levels of secondary structure could prevent areas from becoming C sources over extended periods.

3. Evapotranspiration and canopy characteristics of two lodgepole pine stands following mountain pine beetle attack in British Columbia

3.1 Introduction

In British Columbia (BC), the mountain pine beetle (MPB) (*Dendroctonus ponderosae*) had impacted an area just under 9 million ha in 2009 (Westfall and Ebata 2009). The beetle is native to BC forests and while there have been many outbreaks in the past, none has been as severe in duration or areal extent as the current one. The primary host for the MPB is lodgepole pine (*Pinus contorta* var. *latifolia*), which the beetles colonize via pheromone-mediated mass attacks (Aukema *et al.* 2006). Once eggs laid by the female beetles under the bark hatch, the larvae feed on the phloem, cutting off the tree's nutrient supply (Taylor *et al.* 2006). The beetles also introduce a blue-stain fungus into the tree which clogs the xylem, thereby reducing the tree's capacity to transport water (Gorte 2008). There are three stages to a MPB attack. The green attack stage occurs in the first several months after a tree has been attacked, during which time the needles remain green. The red attack stage follows the first winter after the initial attack when the tree has been killed and the needles turn red. Finally, the tree enters the grey attack stage one or two years later when the needles begin to fall.

There is currently much concern over how the outbreak will impact the hydrology of the affected stands, with many believing it will result in increased water yields, higher peak flows and higher base flows and that it could take 30 or more years before the hydrology returns to pre-attack levels (Rex and Dubé 2009; British Columbia Ministry of Environment 2008). Higher water yields would likely lead to increases in the occurrence of flooding as well as changes in

fish habitat and watershed nutrient status. Potts (1984) conducted a hydrological study on a watershed in Montana where 35% of the timber had been killed by the MPB, and found a 15% increase in the annual water yield, a 10% increase in low flows and an increase in peak runoff in the first five years following attack.

A change in water yields could occur through a decrease in canopy interception rates. Following attack, forests canopies open up because tree mortality leads to needle loss and then tree fall. Reduced interception allows more precipitation to reach the forest floor (Hélie *et al.* 2005). It is well documented that harvested stands have greater spring snow accumulation and higher melt rates than unharvested stands (Winkler *et al.* 2010). In the interior of BC, where snow accumulation and snow melt dominate the hydrology, this effect of reduced interception could be substantial.

Evapotranspiration (*E*) is likely to be affected by beetle attack, however little is known as existing water balance studies have tended to focus on water yields, rather than *E* specifically. A significant decrease in *E* due to tree mortality would lead to higher water tables and water yields. The impact on *E* is likely to depend on the fraction of trees killed by the beetle, and the presence of secondary structure (tree seedlings and saplings, sub-canopy and canopy trees that survive the attack). If a small fraction of trees are killed then *E* might not change greatly, however, if an entire stand without a secondary structure is killed then a large reduction in *E* could be expected. Hélie *et al.* (2005) note that in BC the large variability in precipitation regimes, vegetation types and temperatures make it difficult to predict whether changes in transpiration would be large or small.

Studies have found that trees that survive beetle attack can flourish in the following few years as a result of reduced competition for nutrients, water and light (Waring and Pitman 1985).

Similarly, if secondary structure is present, the death of the canopy can lead to a rapid increase in understory tree and vegetation growth. This could mitigate the expected reduction in *E* due to the death of attacked trees. In a thinning experiment in Alberta, Reid *et* a*l*. (2006) found that by the end of the first growing season of thinning, where the stand density was reduced by ~90%, there was a dramatic increase in total sap flow and transpiration per unit leaf area by lodgepole pine trees in thinned stands to rates more than double that of trees in un-thinned stands. Average daily sap flow over the growing season was 2.7 L for trees in stands thinned 5 years earlier, 1.9 L for trees in the stands thinned the same year (2002) and 1.3 L for the trees in the un-thinned stands.

This study used the eddy-covariance (EC) technique to measure water vapour exchange above two MPB attacked stands in central BC to determine how *E* has been affected by the beetle and how it and associated canopy characteristics changed during the first 5 years of recovery.

3.2 Methods

3.2.1 Site description

The measurements were made in two stands located in the northern interior of BC, in the Sub-Boreal Spruce biogeoclimatic zone (Meidinger and Pojar 1991). Both stands were dominated by lodgepole pine (*Pinus contorta* Dougl. Ex Loud. var. *latifolia* Engelm.). The first stand (MPB-06) is located at Kennedy Siding, approximately 35 km southeast of the town of Mackenzie. This stand was first attacked by the beetle late in the summer of 2006. The progression of the attack is shown in Table 3-1. This stand contained few non-pine trees, and the understory consisted mainly of pine seedlings, scattered shrubs and a ground cover of moss and lichen. The second stand (MPB-03) was located adjacent to Crooked River Provincial Park, approximately 70 km

north of Prince George, BC and approximately 100 km south of MPB-06. In addition to an overstory comprised of about 92% lodgepole pine and 8% subalpine fir (*Abies lasiocarpa*) and ground cover dominated by mosses, lichens and dwarf shrubs, MPB-03 had a developed secondary structure consisting of sub-canopy trees and saplings of lodgepole pine, subalpine fir and white spruce (*Picea glauca)* and seedlings of all three tree species plus deciduous shrubs. MPB-03 was first attacked in 2003 and when net ecosystem production (NEP) measurements began in 2007 the site was >95% in the red-attack and gray-attack stages. Both sites were flat and on coarse textured gravelly soils of glacio-fluvial origin. The fine soil bulk density measured approximately 1180 and 1160 kg m^{-3} and coarse fragment contents (volume >2mm) were 34 and 70 % at MPB-06 and MPB-03, respectively. In 2007, the stand density was ~1235 and ~560 and stand basal area is 12.0-20.1 m^2 ha^{-1} and 8.8-17.9 m^2 ha^{-1} (live and dead trees with height > 10 m) at MPB-06 and MPB-03, respectively. LAI decreased at both sites from 1.4 and 0.9 in 2007 to 1.3 and 0.6 in 2009 at MPB-06 and MPB-03, respectively. Live LAI at MPB-06, as determined by canopy photo analysis, was 0.42, 0.31, and 0.30 in 2007, 2008 and 2009, respectively.

Table 3-1. Stand mountain pine beetle attack status at MPB-06.

	August 2006	June 2007[1]	October 2007[1]	August 2008[2]	August 2009[3]	August 2010[4]
Non-attacked (%)	50	43	28	21	23	16
Green-attacked (%)	50	10	19	5	2	2
Red-/grey-attacked (%)	-	47	53	73	75	82

[1] Hilker *et al.* (2008)
[2] Means of values from this study and of Seip and Jones (2007).
[3] Means of values from this study and of Dale Seip (personal communication).A
[4] Means of values from photo analysis (Spittlehouse *et al.* 2010) and of Dale Seip (personal communication).

3.2.2 Flux, climate and ecophysiological measurements

A 32-m-tall scaffold flux tower (~2.1 m long x ~1.5 m wide) was established at each of MPB-06 and MPB-03 in July 2006 and March 2007, respectively. Flux and climate measurements began on 18 July 2006 and 20 March 2007 at the respective sites. Fluxes of CO_2 (F_c), sensible (H) and latent heat (λE) were measured directly using the EC technique. A 3-dimensional ultrasonic anemometer (model CSAT3, Campbell Scientific Inc. (CSI), Logan, Utah) was used to measure the three components of the wind vector, and turbulent fluctuations of CO_2 and H_2O concentration were measured using an open-path infrared gas analyzer (IRGA) (model LI-7500, LI-COR, Inc, Lincoln, Nebraska,). Signals were measured with a data logger (CSI, model CR1000) with a synchronous-device-for-measurement (SDM) connection. At both sites, EC sensors were mounted at the height of 26 m, which was ~8 m and ~6 m above the top of the canopy at MPB-06 and MPB-03, respectively. Following Webb *et al*. (1980), F_c and λE were calculated as the product of the dry air density and the covariance of the CO_2 and water vapour

mixing ratios, respectively, and vertical velocity measured at 10 Hz. Further details of the measurements system and the data processing procedure are provided in Chapter 2.

Climate variables measured included above-canopy (30-m height) upwelling and downwelling shortwave and longwave radiation (model CNR1, Kipp and Zonen B.V., Delft, The Netherlands) (at 30-m height) and above-canopy upwelling and downwelling, and below-canopy (3-m height) downwelling photosynthetically active radiation (PAR) (model LI-190AS, LI-COR Inc.), precipitation at canopy height (tipping bucket rain gauges, model TE525WS-L, CSI at MPB-03 and model 2501, Sierra Misco, Berkeley, CA at MPB-06), wind speed (model 05103 R.M. Young Inc., Traverse City, MI), air temperature and relative humidity (model HMP45C, Vaisala Oyj, Helsinki, Finland) at the 25-m height, soil temperature (chromel-constantan 30 gauge thermocouple wire, Omega Engineering Stamford, Connecticut) at depths of 5, 10, 20 and 50 cm, soil heat flux (3 heat-flux plates model HP01, Hukseflux Delft, The Netherlands) at a depth of 5 cm and water content (model CS616, CSI) at the 0-10 cm and 30-50 cm depths at MPB-06 and (model EC-5, Decagon Devices Inc, Pullman, Washington) at the 10-cm, 20-cm and 50-cm depths at MPB-03. Meteorological measurements were made every second, and 30-min average values were calculated. Snow-pack depth was also measured at a clearcut weather station located ~1 km from MPB-06, using an acoustic distance sensor (model SR50M, CSI) and precipitation calculated from these data and manual measurements of liquid water equivalent. Leaf area index (LAI) was calculated for the canopies at both sites using a LI-COR Plant Canopy Analyzer (model LAI-2000, LI-COR Inc.) as well as a TRAC (Tracing Radiation and Architecture of Canopies) instrument (Third Wave Engineering, Nepean, Ontario, Canada) and hemispherical photography (Egginton *et al.* 2008). Live LAI at MPB-06 was determined by canopy photo analysis. Photographs of the forest canopy were taken each year in 8 directions

from the tower. The images were adjusted to ensure the same area of the canopy was analysed each year and the fraction of green leaf area was determined by overlaying a 240-point grid on each image and counting the number of grid points on green forest canopy. Each year, live LAI was determined as the LAI measured in 2006 adjusted by the fraction of green canopy from the photographic analysis.

Tree health status inventories at MPB-06 were conducted in August 2006 and August 2008. The attack status of individual trees was determined along two 350 m long x 2 m wide transects. Green attack was identified by the presence of beetle entry holes in the bark, while red attack was identified by foliage colour and grey attack by the predominant loss of foliage. Inventories were also conducted in June and October 2007 by Hilker *et al.* (2008). In addition, independent tree health assessments were also made annually in August by biologists evaluating woodland caribou response to partial retention logging of MPB attacked stands (Seip and Jones 2007).

3.2.3 Flux quality control and data analysis

A 32-m-tall scaffold flux tower (~2.1 m long x ~1.5 m wide) was established at each of MPB-06 and MPB-03 in July 2006 and March 2007, respectively. Flux and climate measurements began on 18 July 2006 and 20 March 2007 at the respective sites. Fluxes of CO_2 (F_c), sensible (H) and latent heat (λE) were measured directly using the EC technique. A 3-dimensional ultrasonic anemometer (model CSAT3, Campbell Scientific Inc. (CSI), Logan, Utah) was used to measure the three components of the wind vector, and turbulent fluctuations of CO_2 and H_2O concentration were measured using an open-path infrared gas analyzer (IRGA) (model LI-7500, LI-COR, Inc, Lincoln, Nebraska,). Signals were measured with a data logger (CSI, model

CR1000) with a synchronous-device-for-measurement (SDM) connection. At both sites, EC sensors were mounted at the height of 26 m, which was ~8 m and ~6 m above the top of the canopy at MPB-06 and MPB-03, respectively. Following Webb *et al*. (1980), F_c and λE were calculated as the product of the dry air density and the covariance of the CO_2 and water vapour mixing ratios, respectively, measured at 10 Hz. Further details of the measurements system and the data processing procedure are provided in Chapter 2.

Climate variables measured included above-canopy (30-m height) upwelling and downwelling shortwave and longwave radiation (model CNR1, Kipp and Zonen B.V., Delft, The Netherlands) (at 30-m height) and above-canopy upwelling and downwelling, and below-canopy (3-m height) downwelling photosynthetically active radiation (PAR) (model LI-190AS, LI-COR Inc.), precipitation at canopy height (tipping bucket rain gauges, model TE525WS-L, CSI at MPB-03 and model 2501, Sierra Misco, Berkeley, CA at MPB-06), wind speed (model 05103 R.M. Young Inc., Traverse City, MI), air temperature and relative humidity (model HMP45C, Vaisala Oyj, Helsinki, Finland) at the 25-m height, soil temperature (chromel-constantan 30 gauge thermocouple wire, Omega Engineering Stamford, Connecticut) at depths of 5, 10, 20 and 50 cm, soil heat flux (3 heat-flux plates model HP01, Hukseflux Delft, The Netherlands) at a depth of 5 cm and water content (model CS616, CSI) at the 0-10 cm and 30-50 cm depths at MPB-06 and (model EC-5, Decagon Devices Inc, Pullman, Washington) at the 10-cm, 20-cm and 50-cm depths at MPB-03. Meteorological measurements were made every second, and 30-min average values were calculated. Snow-pack depth was also measured at a clearcut weather station located ~1 km from MPB-06, using an acoustic distance sensor (model SR50M, CSI) and precipitation calculated from these data and manual measurements of liquid water equivalent. Leaf area index (LAI) was calculated for the canopies at both sites using a LI-COR Plant Canopy

Analyzer (model LAI-2000, LI-COR Inc.) as well as a TRAC (Tracing Radiation and Architecture of Canopies) instrument (Third Wave Engineering, Nepean, Ontario, Canada) and hemispherical photography (Egginton *et al.* 2008). Live LAI at MPB-06 was determined by canopy photo analysis. Photographs of the forest canopy were taken each year in 8 directions from the tower. The images were adjusted to ensure the same area of the canopy was analysed each year and the fraction of green leaf area was determined by overlaying a 240-point grid on each image and counting the number of grid points on green forest canopy. Each year, live LAI was determined as the LAI measured in 2006 adjusted by the fraction of green canopy from the photographic analysis.

Tree health status inventories at MPB-06 were conducted in August 2006 and August 2008. The attack status of individual trees was determined along two 350 m long x 2 m wide transects. Green attack was identified by the presence of beetle entry holes in the bark, while red attack was identified by foliage colour and grey attack by the predominant loss of foliage. Inventories were also conducted in June and October 2007 by Hilker *et al.* (2008). In addition, independent tree health assessments were also made annually in August by biologists evaluating woodland caribou response to partial retention logging of MPB attacked stands (Seip and Jones 2007).

3.2.4 Canopy characteristics

In order to investigate the processes controlling E, we calculated canopy conductance (g_c), the Priestley-Taylor α (Priestley-Taylor 1972) and decoupling coefficient (Ω) (McNaughton and Jarvis 1983). The combination of the stomatal conductance and leaf area of the trees and

understory vegetation (including the moss layer), collectively referred to here as g_c, was calculated by rearranging the Penman-Monteith equation (Monteith and Unsworth 2008) as

$$\frac{1}{g_c} = \frac{\rho c_p D}{\gamma \lambda E} + \frac{1}{g_a}[\frac{s}{\gamma}(\frac{R_a}{\lambda E} - 1) - 1] \quad (1)$$

where s is the change in saturation vapour pressure with temperature (kPa K^{-1}); R_a is the available energy flux, $R_n - G - S_t$, in which R_n is the net radiation, G (W m^{-2}) is soil (surface) heat flux (W m^{-2}), and S_t is the rate of change in energy storage (per unit ground area) in the air and biomass between the EC sensors and the ground surface (W m^{-2}) (calculation of S_t is described below); ρ is the air density (kg m^{-3}); c_p is the specific heat of air (J kg^{-1} K^{-1}); γ is the psychrometric constant (kPa K^{-1}); D the vapour pressure deficit (kPa) and g_a is the aerodynamic conductance (mm s^{-1}) for heat and mass transfer as described in Jassal *et al.* (2009):

$$g_a = u_* \left(\frac{u}{u_*} + \frac{2}{k} + \frac{(\psi_m - \psi_h)}{k} \right)^{-1} \quad (2)$$

where k is the von Karman constant (0.40) and ψ_m and ψ_h are the integral diabatic correction factors for momentum and sensible heat transfer, respectively (Jassal *et al.* 2009). The coefficient 2 is recommended for all vegetated surfaces by Garratt (1978). Using 1 as the coefficient resulted in g_a values generally 2-3 times greater than when using 2; however, there was not a significant change in g_c. Typically, the second term on the right hand side of Eq. 1 accounted for < 20% of the calculated value of g_c.

The Priestley–Taylor α was calculated as $\alpha = \lambda E / \lambda E_{eq}$, where λE_{eq} is the equilibrium latent heat flux, calculated as $\lambda E_{eq} = s / (s + \gamma) R_a$. The decoupling coefficient Ω is effective for describing how well D at the leaf surface is coupled to D of the atmosphere (Jarvis and McNaughton 1986):

$$\Omega = \frac{s/\gamma + 1}{s/\gamma + 1 + g_a/g_c} \quad (3)$$

in which Ω approaches 0 when the canopy is well-coupled to the atmosphere as g_a/g_c increases (E driven by D), and approaches 1 when the canopy is decoupled from the atmosphere as g_a / g_c decreases, in which case E is controlled by R_a.

In order to determine the physiological controls of E, only values of g_c, α and Ω were used for analysis when the foliage was dry. Thus data measured 3 hours before or after a rainfall event were discarded.

To estimate potential evapotranspiration (E_{pot}), the Priestley-Taylor (1972) equation was used:

$$E_{pot} = \alpha_{max} E_{eq} \quad (4)$$

where E_{eq} is the equilibrium evapotranspiration rate. α_{max} was calculated as

$$\alpha_{max} = 1/(a + bD) \quad (5)$$

This parameterization of α_{max} was used because maximum values of E/E_{eq} were found to increase as D decreased (see Results).

3.2.5 Energy balance closure

Eddy covariance data were assessed for energy balance closure (i.e., confirmation that $R_a = \lambda E + H$). Half-hourly measurements of R_n, G, H and λE were used together with estimates of S_t. The rate of change in energy storage (S_t) is comprised of changes in sensible (S_H) and latent heat storage ($S_{\lambda E}$) in the air column, and heat storage in the tree boles (S_b), branches and foliage (S_{br_fol}), and the rate of energy consumption by photosynthesis (S_p). Heat storage in the tree boles was calculated following Lee and Black (1993) as, $S_b = 2.5\, A_{Ta} \cos(\omega t - \varphi + \frac{\pi}{4})$. The

coefficient 2.5, was selected because the bole volume of the stand is 0.70 that of the Douglas-fir stand studied by Lee and Black (1993) for which a coefficient of 3.57 was used, A_{Ta} (°C) and φ are the amplitude and phase angle of the diurnal course of T_a, ω is the diurnal angular frequency (radians hour^{-1}) and t is the time of day (PST). The rate of energy consumption by photosynthesis was calculated as $S_p = - F_c C$, where F_c is (μmol m^{-2} s^{-1}) positive upward and C is the photosynthetic energy conversion factor (0.469 J μmol^{-1}). Heat storage in branches and foliage was calculated as $S_{br\_fol} = \text{LAI}\ \sigma_L c_L(\Delta T_L / \Delta t)/(1 - W_w)$, where σ_L is the specific leaf weight (mass of dry leaves per metre square of leaf), W_w is the water content on a wet mass basis (~0.40), c_L is the leaf specific heat (calculated using this wet mass fraction), and $\Delta T_L / \Delta t$ is the average rate of leaf temperature change (°C s^{-1}) over a half-hour. Sensible heat and latent heat storage were calculated as $S_H = \rho\, c_p\, z_m\, \Delta T_L / \Delta t$, and $S_{\lambda E} = (\rho\, c_p / \gamma)\, z_m\, \Delta e_a / \Delta t$, where $\Delta e_a / \Delta t$ is the average rate of change in vapour pressure over a half-hour and z_m is the measurement height. The calculations of S_H and $S_{\lambda E}$ assume the changes in leaf temperature and vapour pressure are similar at all heights up to 26 m, where air temperature and humidity were measured which might cause a slight overestimation in these terms. However, these stands are quite open so the overestimation should be minimal.

The relationships between half-hourly values of $H + \lambda E$ and R_a are shown in Fig. 3.1 and Table 3-2. The slopes for both sites were always >0.89 on an annual basis, and >0.92 for the growing season data. The coefficient of determination, r^2 was higher at MPB-03, with the lowest r^2 occurring in 2009 at MPB-06. When R_a was > 500 W m^{-2}, $\lambda E + H$ tended to underestimate R_a. This was more so the case at MPB-06, especially in 2009 where $\lambda E + H$ underestimated R_a by up to 40% at these high values of R_a.

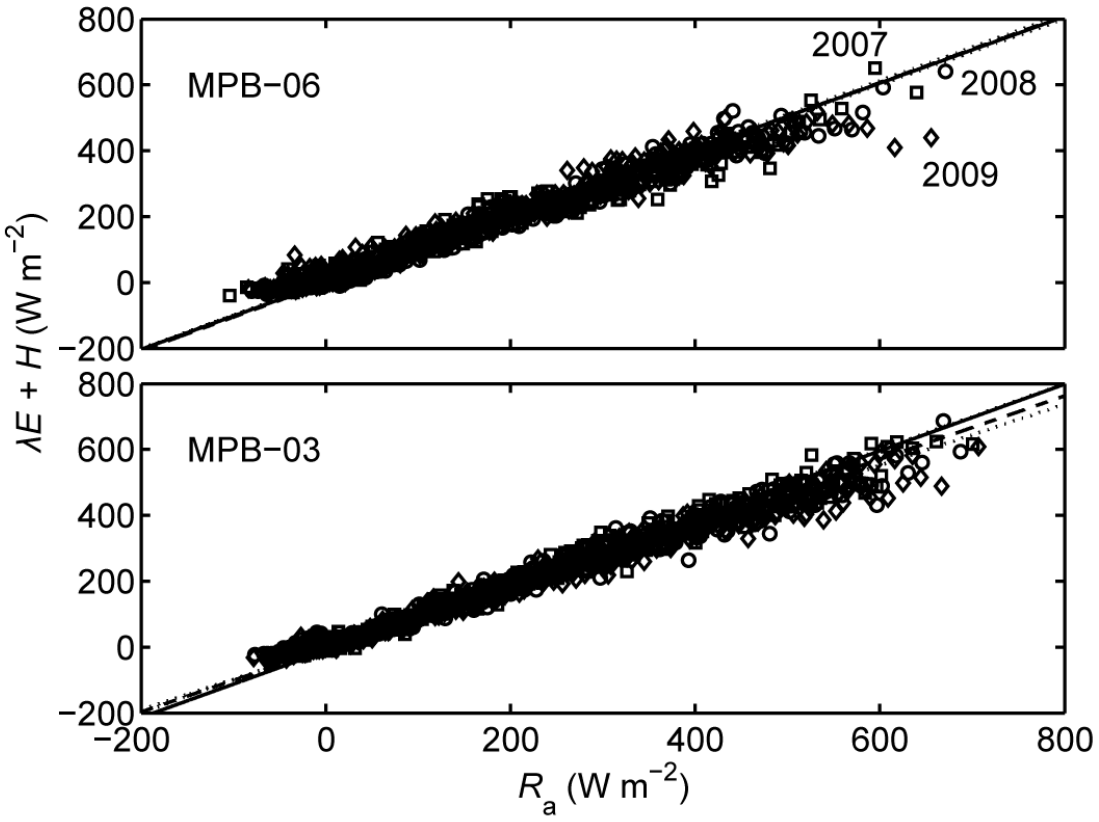

Figure 3.1. Energy balance closure at the two sites as shown by the relationships between half-hourly values of latent and sensible heat ($\lambda E + H$) and available radiation (R_a) for the 2007, 2008 and 2009 growing seasons. Data points are bin averages of 10 values starting from the smallest value. Individual linear orthogonal regression lines are shown for the three years. Statistics for the linear regression are shown in Table 3-2.

Table 3-2. Linear orthogonal regression parameters between half-hourly latent and sensible heat ($\lambda E + H$) and available energy (R_a).

	MPB-06			MPB-03		
	2007	2008	2009	2007	2008	2009
Annual						
Slope	0.90	0.92	0.92	1.00	0.96	0.95
Intercept	-3.89	-2.52	2.86	-14.53	-7.01	-9.88
r^2	0.75	0.79	0.73	0.81	0.83	0.83
Growing Season (1 May-30 September)						
Slope	0.97	0.95	0.97	1.03	0.98	0.97
Intercept	-3.33	-1.33	3.75	-11.27	-4.29	-4.68
r^2	0.74	0.79	0.75	0.84	0.83	0.84

Wilson *et al.* (2002) evaluated energy balance closure at 22 eddy-covariance sites, ranging from Mediterranean to arctic ecosystems, and found an average lack of closure of about 20%. A lack of closure can stem from errors associated with either or both the EC and the available energy flux. Wilson *et al.* (2002) concluded that although it was not possible to evaluate all possible sources of error, there seemed to be a connection between the lack of closure and fluxes of CO_2. At boreal aspen (*Populus tremuloides*), black spruce (*Picea mariana*) and jack pine (*Pinus banksiana*) stands in Saskatchewan, Canada, Barr *et al.* (2006) reported $H + \lambda E$ to underestimate R_a by 11, 15 and 14%, respectively, resulting in closure values slightly greater than those reported here. The very flat terrain on which these stands are located is likely a major contributing factor to the relatively good closure determined for these sites as such terrain minimizes the likelihood of horizontal advective loss of scalars. As well, the homogeneity of these stands increases the likelihood that the net radiometer and soil heat flux plates are

measuring a flux representative of the larger footprint measured by the EC system (Wilson *et al.* 2002).

3.3 Results

3.3.1 Climate

5-day averages of climate variables from 2007 – 2009 are shown in Fig. 3.2, and average growing season (1 May – 30 September) climate values are presented in Table 3-3. 2009 was the warmest, driest and sunniest of the three years. The low growing season rainfall in 2009 resulted in the lowest volumetric water content of the soil fine fraction (soil particles < 2 mm) (θ) (0 – 10 cm depth at MPB-06 and 10 cm depth at MPB-03) values observed. At MPB-06, total annual snowfall liquid water equivalent was 330, 305 and 384 mm and total annual precipitation was 730, 589 and 681 mm in 2007, 2008 and 2009, respectively. At MPB-06, snowmelt was completed (as indicated by abrupt increases in soil temperature and heat flux) on 15 May in 2007 and 2008 and on 7 May in 2009; at MPB-03 snowmelt was completed on 20 April in 2007, 15 May in 2008 and 7 May in 2009. During 2009 there was a hot and dry period which began on 17 July and lasted until 10 August. During this time MPB-06 received only 6 mm of rainfall and MPB-03 received none. Conditions were especially warm from 21 July to 2 August with maximum daily T_a always being > 25 °C and D consistently reaching values > 2.5 kPa, peaking at 3.65 kPa on 27 July. At MPB-06, θ dropped steadily from mid-July 2009, reached a low of 0.04 $m^3\ m^{-3}$ in early August and did not recover until early September. At MPB-03, θ reached a low of 0.12 $m^3\ m^{-3}$ on 9 August and fluctuated with rainfall thereafter until reaching more seasonably normal values in early September. Further details of the mean annual climate are provided in Chapter 2.

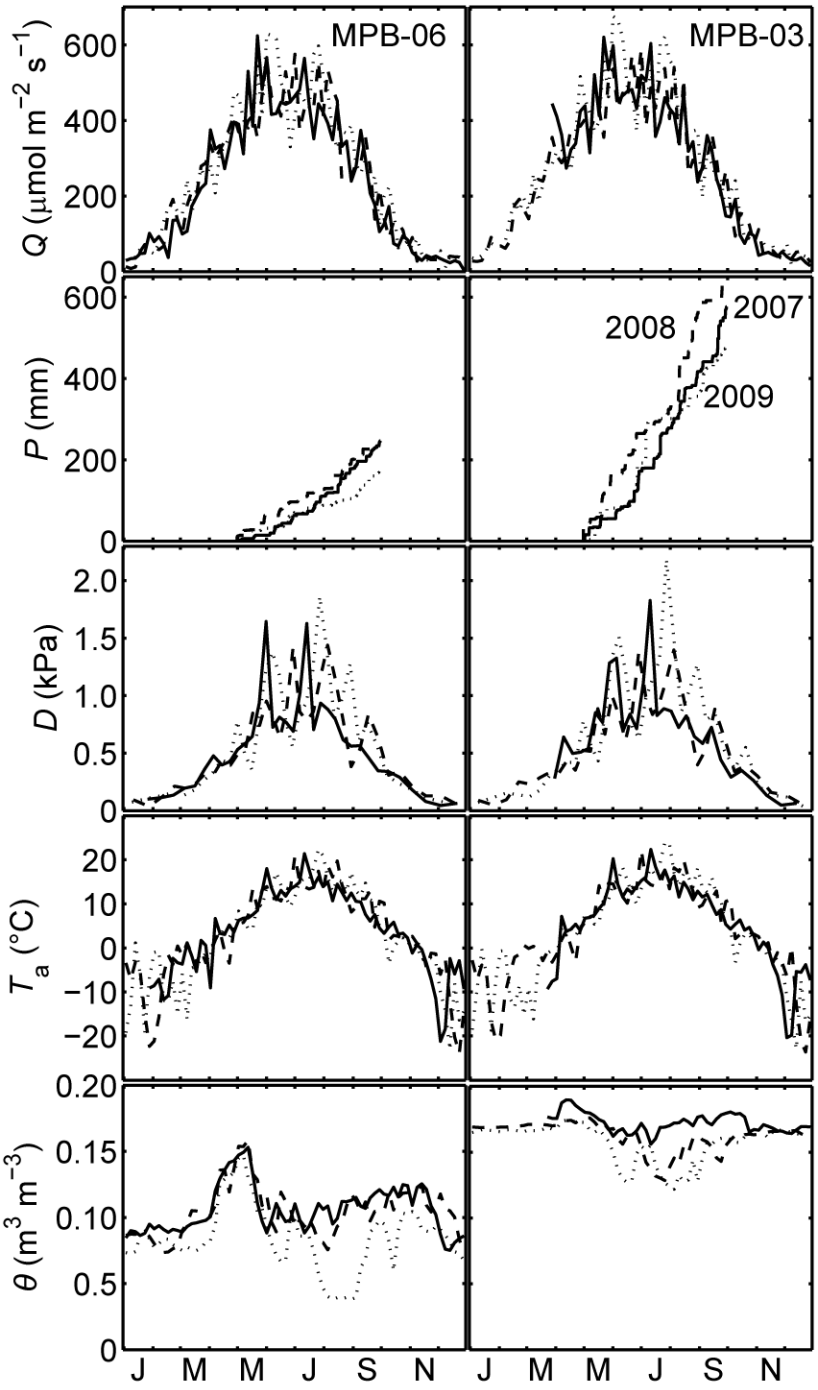
MPB-06
MPB-03
Q (μmol m−2 s−1)
P (mm)
2007
2008
2009
D (kPa)
Ta (°C)
θ (m3 m−3)
J M M J S N J M M J S N

Figure 3.2. 5-day average values of photosynthetically active radiation (Q), precipitation (P), vapour pressure deficit (D), air temperature (T_a) and soil fine fraction volumetric water content (θ). Values of D are calculated from daytime values ($Q > 0$) and values of P are only for the growing season.

Table 3-3. Average values of climate variables for the growing season (1 May – 30 September).

	MPB-06			MPB-03		
	2007	2008	2009	2007	2008	2009
Air temperature (26 m height) (° C)	11.8	12.4	12.9	12.7	12.7	14.0
Soil temperature (5-cm depth) (° C)	10.4	11.1	11.9	10.3	10.3	10.8
Rainfall (mm)	246	250	177	576	620	477
θ (m^3 m^{-3}) (0-30-cm depth)	0.11	0.11	0.08	0.17	0.16	0.15
Q (μmol m^{-2} s^{-1})	396	396	418	413	410	442
D[1] (kPa)	0.80	0.83	0.94	0.86	0.84	1.04
GSL[2] (days)	136	141	134	147	160	155
R_n[3] (GJ m^{-2})	1.49	1.57	1.57	1.70	1.63	1.72

[1] Daytime average values.
[2] Growing season length (half-hourly values of air temperature and soil temperature were > 0 and 1°C, respectively).
[3] Growing season total.

3.3.2 Diurnal energy balance

The ensemble-averaged diurnal energy balance for July, the month R_n tends to peak, is shown in Fig. 3.3 for 2008. For this month, the slope of the relationship between $H + \lambda E$ and R_a was 1.01 and 0.97 with intercepts of 2.0 and -12.5 W m^{-2} for MPB-06 and MPB-03, respectively. During July, the Bowen ratio (β) was approximately 2.0 at MPB-06 and 1.7 at MPB-03. Sensible heat was virtually the same at both sites, reaching a mid-day high of 270 to 280 W m^{-2} while maximum daytime λE was 130 and 145 W m^{-2} at MPB-06 and MPB-03, respectively. During the nighttime, mean R_n was -53 and -58 W m^{-2}, H was -12 and -9 W m^{-2} and λE was 7 and 4 W m^{-2} at MPB-06 and MPB-03, respectively. The sum of $G + S_t$ reached a high of 75 and 35 W m^{-2} and a low of -40 and -25 W m^{-2}, at MPB-06 and MPB-03, respectively.

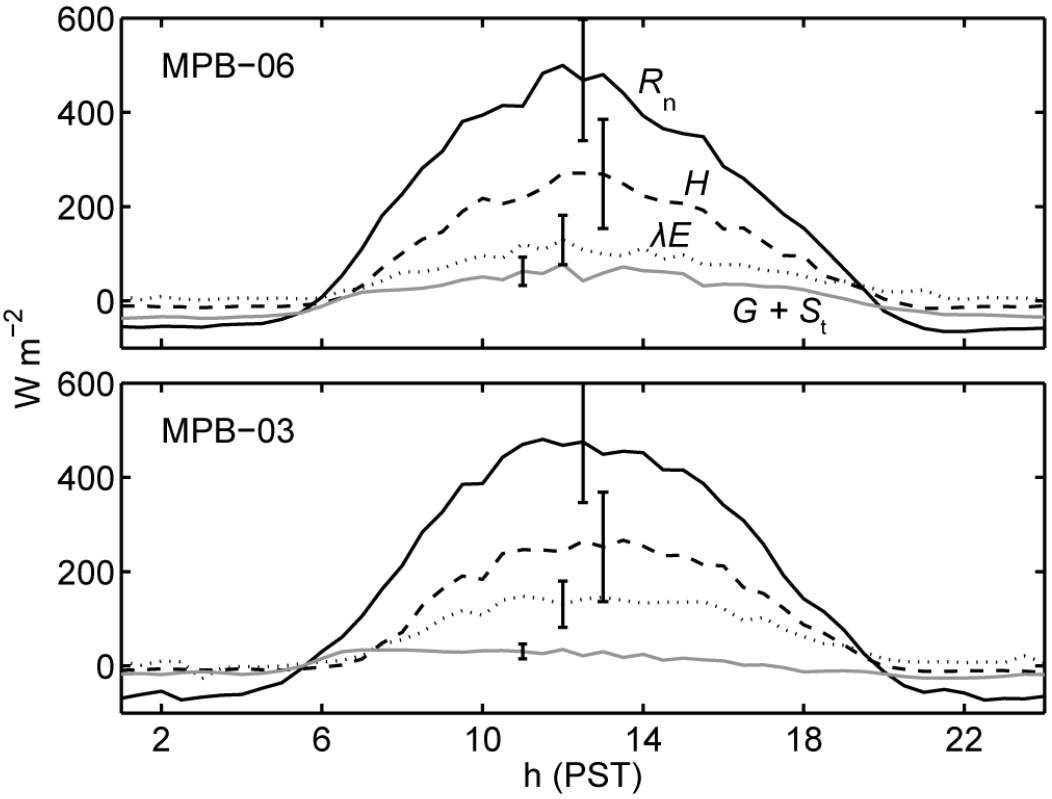

Figure 3.3. Ensemble averaged net radiation (R_n), sensible (H) and latent (λE) heat fluxes, and ground heat flux (G) + total energy storage change (S_t) for July 2008 for MPB-06 and MPB-03. Bars are standard deviations.

3.3.3 Seasonal energy balance

At MPB-06, daily (24-h) averages of R_n varied from a maximum of ~150 W m^{-2} during the growing season to a low of ~-20 W m^{-2} during the winter (Fig. 3.4). Daily averages of H peaked between May and June at 84, 92 and 94 W m^{-2} in 2007, 2008 and 2009, and λE in July at ~45 W m^{-2} in all three years. At MPB-03, which is more southerly, values were greater, with R_n peaking between June and July at 160-190 W m^{-2}. Maximum daily averages of H increased during the three years from 93 W m^{-2} in 2007, to 100 W m^{-2} in 2009, and λE reached a maximum of ~55 W m^{-2} in July of all three years. During the winter, H and λE averaged ~-5 and ~7 W m^{-2}

respectively, at both sites. Monthly values of H followed R_n very closely, increasing rapidly between March and May as the days became longer, during which time λE remained low. Although these stands are technically classified as sub-boreal forests, the relatively low λE values during the spring are typical of boreal coniferous systems as T_a is still cool, D is low and cold soils limit water uptake by the trees (Arain *et al*. 2003). Latent heat, was slightly positive during the winter due to sublimation and at times λE was greater (~10 W m^{-2}) when T_a warmed up for short periods. At MPB-06, over the three years monthly β ranged from a winter low of ~-1.5 to a high of 5 – 7 in April. As λE increased, β gradually declined throughout the growing season from ~2.5 in June to just over 1.0 in September. At MPB-03, average β in winter was ~0.6 and it declined from 4.4 – 5.0 in April to 1.7 – 2.1 in June and ~1.5 in September. Throughout the year 24-h $G + S_t$ was small, as is common for coniferous forests (Baldocchi *et al.* 1997; Arain *et al.* 2003). Maximum and minimum monthly $G + S_t$ values occurred in May and September/October and were ~10 and ~-10 W m^{-2} at MPB-06 and ~6 and ~-4 W m^{-2} at MPB-03, respectively. Minimum G (i.e., greatest loss of soil heat) occurred in the fall because the soils were still warm at depth and there was not yet a snow layer to insulate the soil surface. During the winter, when the snow was deep, there was a small heat loss from the ground of ~-1 and ~-3 W m^{-2} at MPB-06 and MPB-03, respectively.

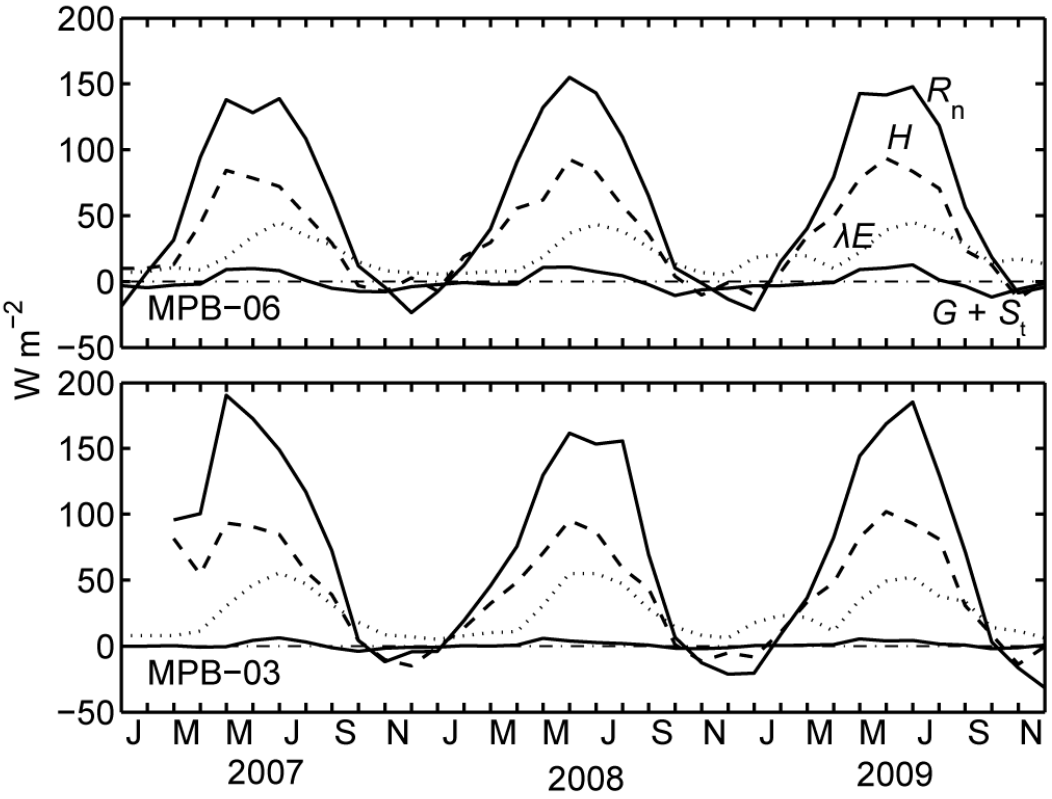

Figure 3.4. Monthly average net radiation (R_n), sensible (H) and latent (λE) heat flux, and ground heat flux (G) + total energy storage change (S_t) (2007 to 2009) at MPB-06 and MPB-03.

3.3.4 Evapotranspiration

5-day average values and annual totals of E are shown in Fig. 3.5. There was little annual variation at either site, with E varying by less than 10 mm y^{-1} at MPB-06 and by just over 20 mm y^{-1} at MPB-03 over the three years. Growing season averages of E at MPB-06 and MPB-03 were, respectively, 1.12 and 1.48 mm day^{-1} in 2007, 1.14 and 1.54 mm day^{-1} in 2008, and 1.21 and 1.46 mm day^{-1} in 2009. Maximum daily values of E, which occurred in late July, were ~2.5 and ~3.0 mm day^{-1} at MPB-06 and MPB-03, respectively. The highest values tended to occur in the hours and days following rainfall. During the winter, E was approximately 0.2 mm day^{-1} at both sites

and increased rapidly following snow melt in May. These wintertime values of *E* are similar to the values of 0.1 – 0.25 mm day^{-1} from a black spruce stand reported by Arain *et al.* (2003).

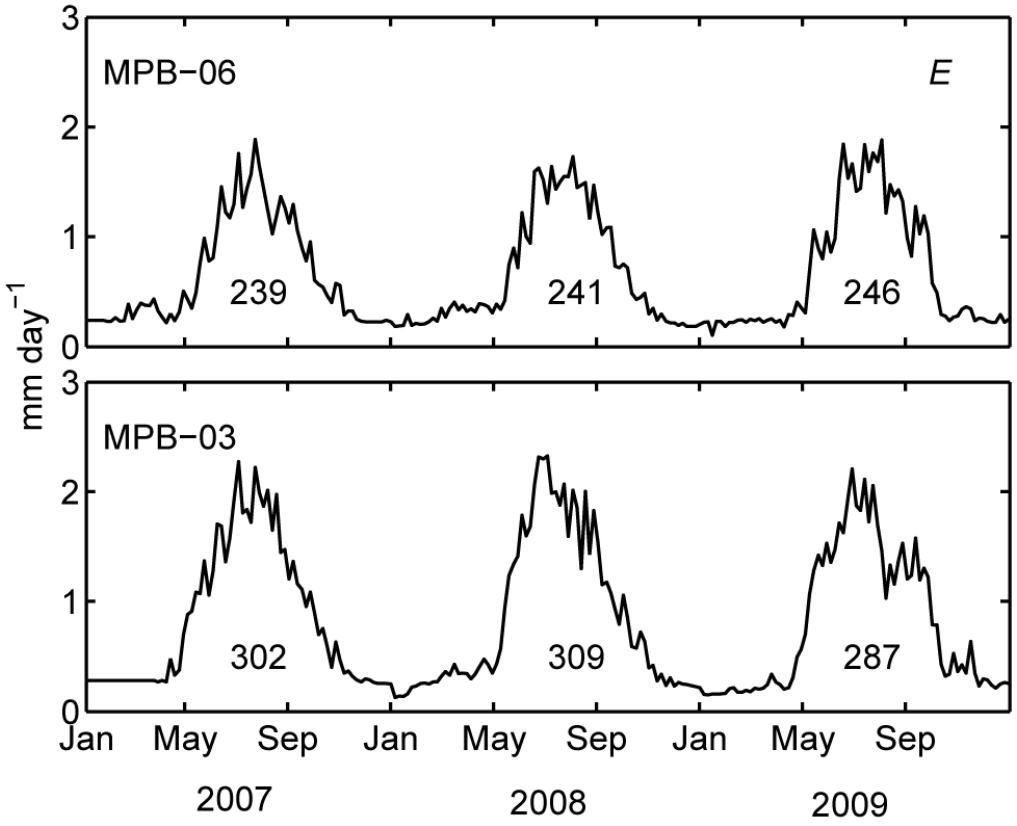

Figure 3.5. 5-day averages of evapotranspiration (*E*) from 2007 to 2009. Values are annual totals of *E* (mm).

3.3.5 Canopy conductance, Priestley-Taylor α and Ω

The annual means of daytime g_c under dry foliage conditions (T_a > 0 °C) were 3.25, 3.35 and 2.89 mm s^{-1} at MPB-06 and 3.92, 4.24 and 3.38 mm s^{-1} at MPB-03 in 2007, 2008 and 2009, respectively. The lowest values occurred in 2009, the driest of the three years, and the highest occurred in 2008, the wettest year. Monthly mean values of daytime g_c varied from 1 to 6 mm s^{-1} and 2 to 6 mm s^{-1} (Fig. 3.6) with daytime means being as high as 6.5 and 7.4 mm s^{-1} at MPB-06

and MPB-03, respectively. Values of g_c were relatively low in April and May, when snow was still on the ground for much of the time, and rose steadily until reaching maximum values in September and October when D and R_n were in rapid decline due to shorter day lengths and lower solar elevation. At MPB-03, there was more variation in growing season g_c than at MPB-06, especially in 2008 when June g_c was quite high, and in 2009 when there was a sharp reduction in August. At MPB-06, monthly g_c values were highest during the latter half of the growing season in 2007. Monthly g_a values were between 100 and 150 mm s^{-1} at MPB-06 and between 110 and 160 mm s^{-1} at MPB-03. Values were highest in April and May and reached a minimum in September.

Over the three growing seasons, α averaged 0.53 and 0.51 at MPB-06 and MPB-03, respectively, showing these sites to be water stressed, since α is much less than unity (when $\lambda E = \lambda E_{eq}$). Like g_c, α increased steadily throughout the growing season, until reaching a maximum in September and October (Fig. 3.6). At MPB-03, there was a significant drop in α in August 2009 during the dry period. There was very little change in monthly values of Ω over the three years, with the exception of August 2008 when there was an abrupt drop. Monthly Ω increased from April to September and ranged from 0.04 to 0.2 at both sites, although values were slightly higher at MPB-03. These low Ω indicate that both these stands are strongly coupled to the atmosphere.

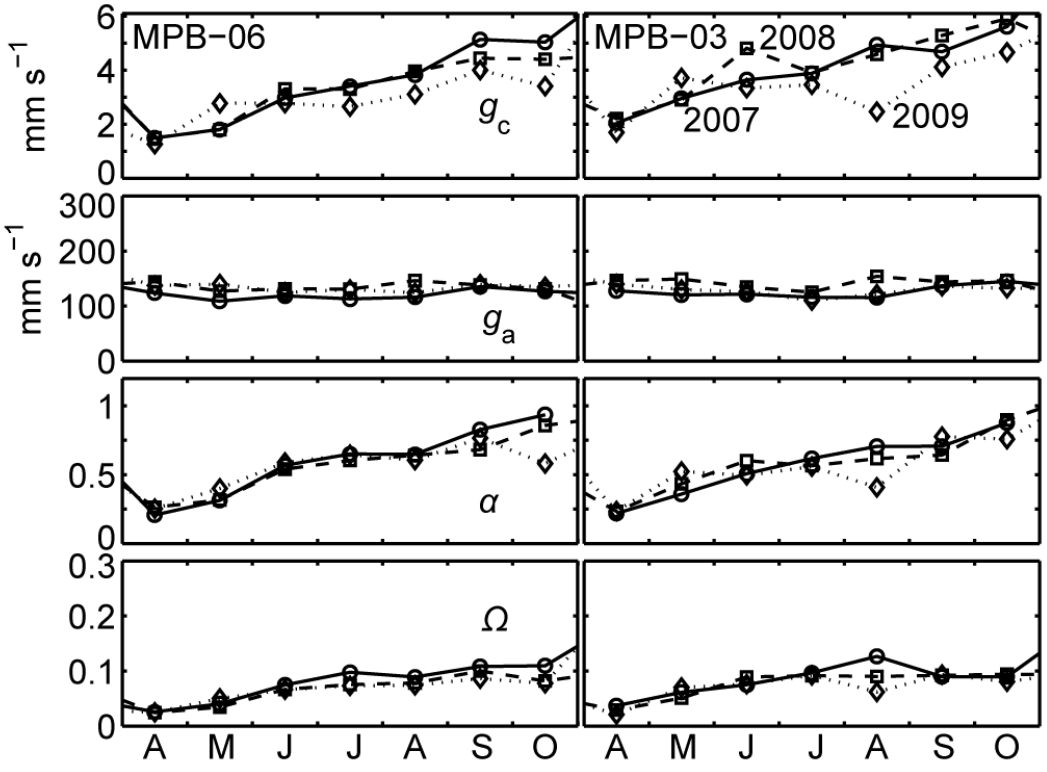

Figure 3.6. Monthly growing season averages of daytime dry foliage canopy conductance (g_c), aerodynamic conductance (g_a), Priestly-Taylor α and decoupling coefficient Ω.

Diurnal ensemble average g_c for July over the three years is shown in Fig. 3.7. Following sunrise, g_c rose quickly to reach the highest levels of the day by mid-morning, during which time D was still low, allowing the stomata to open and maximize photosynthetic uptake while minimizing water loss through transpiration. In the morning the vegetation also tends to be less water stressed due to overnight xylem recharge (Lambers *et al.* 1998). Following the morning maxima, g_c gradually declined during the afternoon as D increased. In the late-afternoon downwelling PAR (Q) decreased quickly, resulting in low g_c. Although the diurnal pattern was

similar in all years, July g_c was lowest in 2009, probably due to the drier conditions at both sites that year.

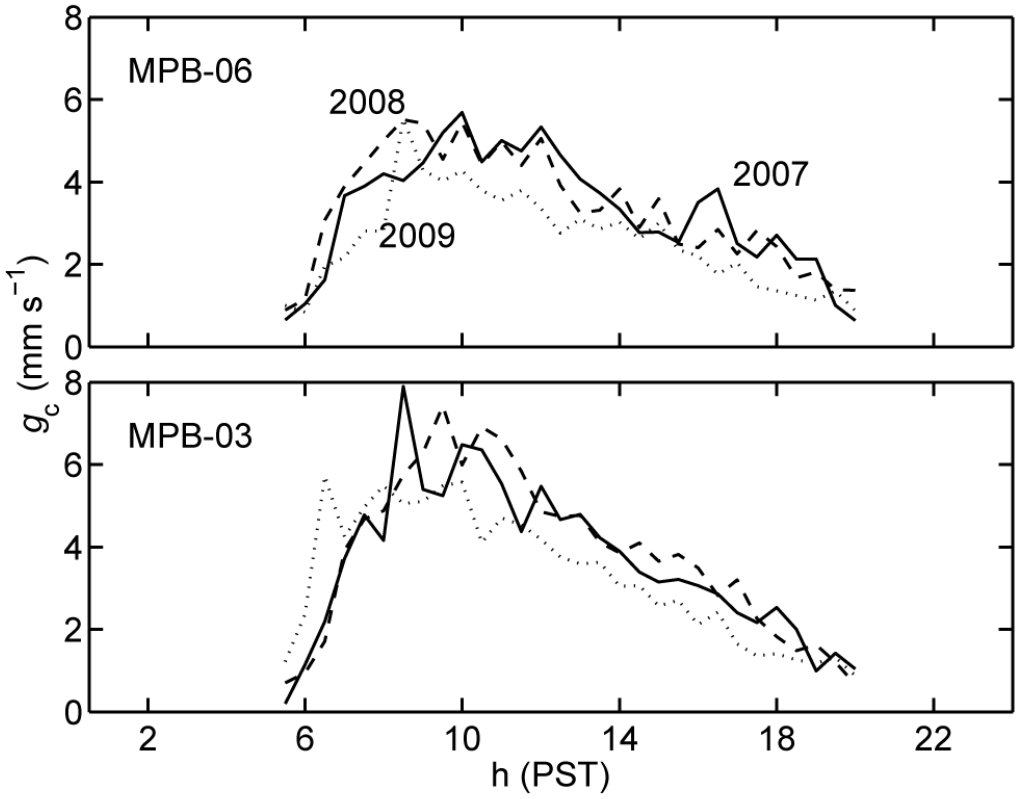

Figure 3.7. Diurnal ensemble average canopy conductance (g_c) for July.

3.3.6 Climatic controls on g_c

Since g_c is known to strongly respond to *D*, we attempted to model half hourly g_c for the period of 15 May to 30 September using the following equation.

$$g_{c\,\mathrm{mod}} = 1/(c + dD) \tag{6}$$

where *c* and *d* are empirically determined parameters. The first half of May was excluded from the analysis because snow was still present on the ground, causing *E* to be significantly lower than after the snow had melted. When g_c was calculated from (Eq. 6), modelled g_c ($g_{c\mathrm{mod}}$)

consistently underestimated g_c, especially during the middle hours of the day when D was high. When plotted against D at low, medium and high Q levels the response of g_c to D was found to vary, with a higher g_c for a given D at higher Q levels (Fig. 3.8). Thus a Q function was added so that:

$$g_{c\,\mathrm{mod}} = [1/(c + dD)](e + fQ) \qquad (7)$$

This resulted in g_{cmod} accounting for approximately 47 and 49% of the variation in g_c at MPB-06 and MPB-03, respectively (Fig. 3.9; Table 3-4), with g_{cmod} underestimating g_c at higher values.

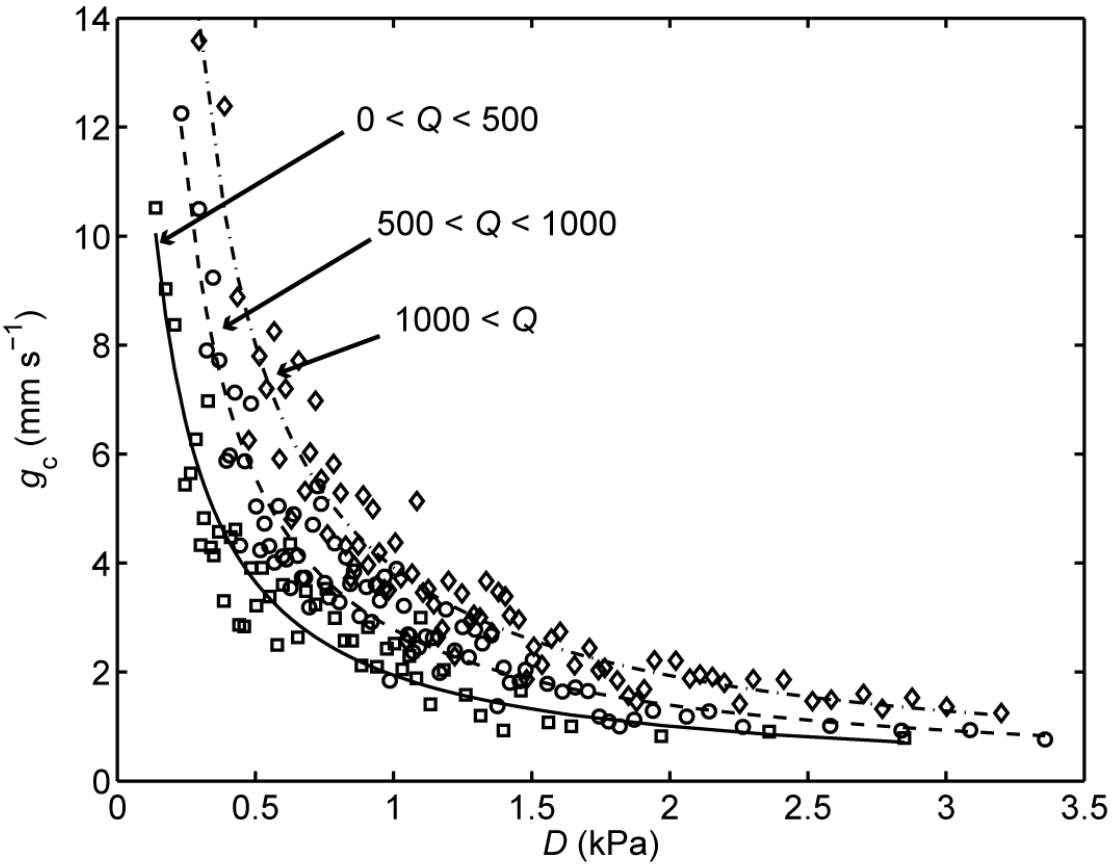

Figure 3.8. The response of dry foliage canopy conductance (g_c), to vapour pressure deficit (D) at different levels of photosynthetically active radiation (Q) at MPB-06 in July 2008. Data points are the averages of bins of 10 values of g_c starting at the smallest values of D. Curves are fits to Eq. (6) with the following values of c and d: 0.032 and 0.483 for $Q < 500$ μmol m^{-2} s^{-1}, 0.0003 and 0.358 for $500 < Q < 1000$ μmol m^{-2} s^{-1} and -0.006 and 0.261 for $Q > 1000$ μmol m^{-2} s^{-1}.

Table 3-4. Parameters in Eq. 7 and cumulative totals of evapotranspiration (E) and E modelled (E_{mod}) for daytime only for 15 May and 30 September.

	MPB-06			MPB-03		
	2007	2008	2009	2007	2008	2009
c	0. 0090	0. 0013	0. 0127	0. 0162	0. 006	0. 0067
d	0. 1212	0. 1023	0. 1084	0. 096	0. 0516	0. 0551
e	0. 2373	0. 1112	0. 1873	0. 1615	0. 0538	0. 0806
f	1.981×10^{-4}	2.356×10^{-4}	2.264×10^{-4}	3.488×10^{-4}	2.330×10^{-4}	1.813×10^{-4}
r^2	0.44	0.51	0.45	0.46	0.57	0.45
E (mm)[1]	164	169	180	213	226	210
E_{mod} (mm)[1]	165	157	167	201	211	203

[1] Total of daytime values only.

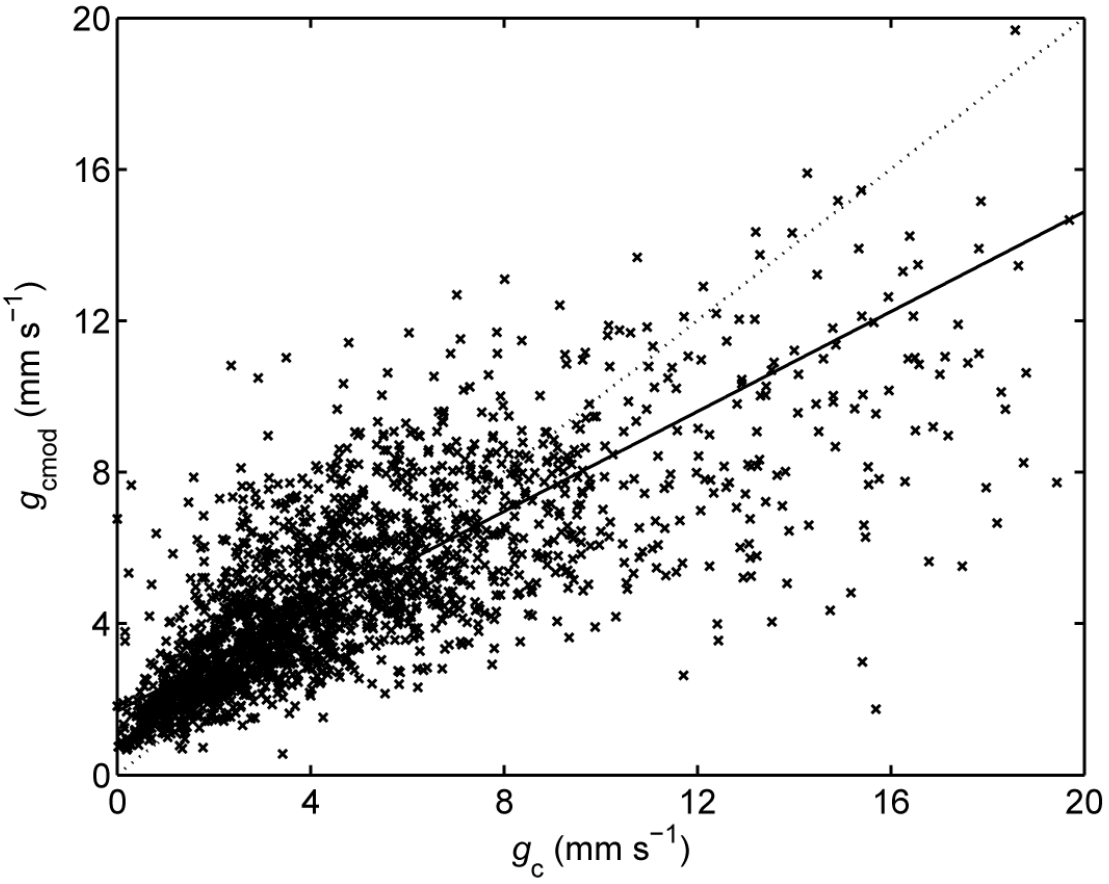

Figure 3.9. Relationship between canopy conductance (g_c) calculated from measurements (Eq. 1) and that modelled (g_{cmod}) (Eq. 7) at MPB-03 between 1 June and 30 September 2008. The solid line represents the regression: g_{cmod} = 1.50 g_c -2.47. *Q*. r^2 = 0.44, RMSE = 2.46. The dotted line is the 1:1 line.

Daytime means of dry foliage g_c also responded to daily mean θ. At both sites the relationship was strongest in 2007 when θ was slightly higher than the other two years (Fig. 3.10). We added a θ function to Eq.7 to see if the coefficient of variation between g_{cmod} and g_c would improve, but since the improvement was < 2% the function was not included in the model.

We then used the Penman-Monteith equation with g_{cmod} (Eq. 7) and g_a (Eq. 2) to obtain modelled E (E_{mod}). Cumulative totals of half-hourly 15 May – 30 September E and E_{mod} agreed with each other to within 10% (Table 3-4).

To examine the diurnal variation in g_c and E, as well as to assess the accuracy of g_{cmod}, half-hourly values of R_n, D, g_c, g_{cmod}, E and E_{mod} are shown in Fig. 3.10, for the period between 21 and 25 July 2008. During this period, R_n peaked at ~650 W m^{-2} around midday and fell to ~-100 W m^{-2} at night. At both sites, D increased steadily over the five days from a daytime maximum of 1.2 kPa on 21 July to 2.9 kPa on 25 July. The diurnal variation in D lagged that of R_n by 2-3 h, with values being relatively low in the morning and highest in the late afternoon when R_n had already begun to decline. Canopy conductance was much higher at the beginning of the period when D was low, especially during the morning hours. There was a pronounced decrease in g_c over the five days as D steadily rose, but the diurnal trend remained the same. Modelled canopy conductance followed g_c quite closely during most of the measurement period, with the exception of 21 and 22 July, 2008, at MPB-06 when g_c was quite erratic and g_{cmod} did not reach the maximum levels. During the same 5 days at MPB-03, g_{cmod} was often higher than g_c, with the exception of 21 July when there was good agreement. Evapotranspiration increased rapidly in the morning, reached maximum values around mid-day and decreased in the afternoon when D was high. During the early morning when g_c was high, E was still low due to low Q and D but during the afternoon E closely followed g_c. Not surprisingly, like g_{cmod}, E_{mod} followed E more closely at MPB-06, than at MPB-03 where E_{mod} overestimated E.

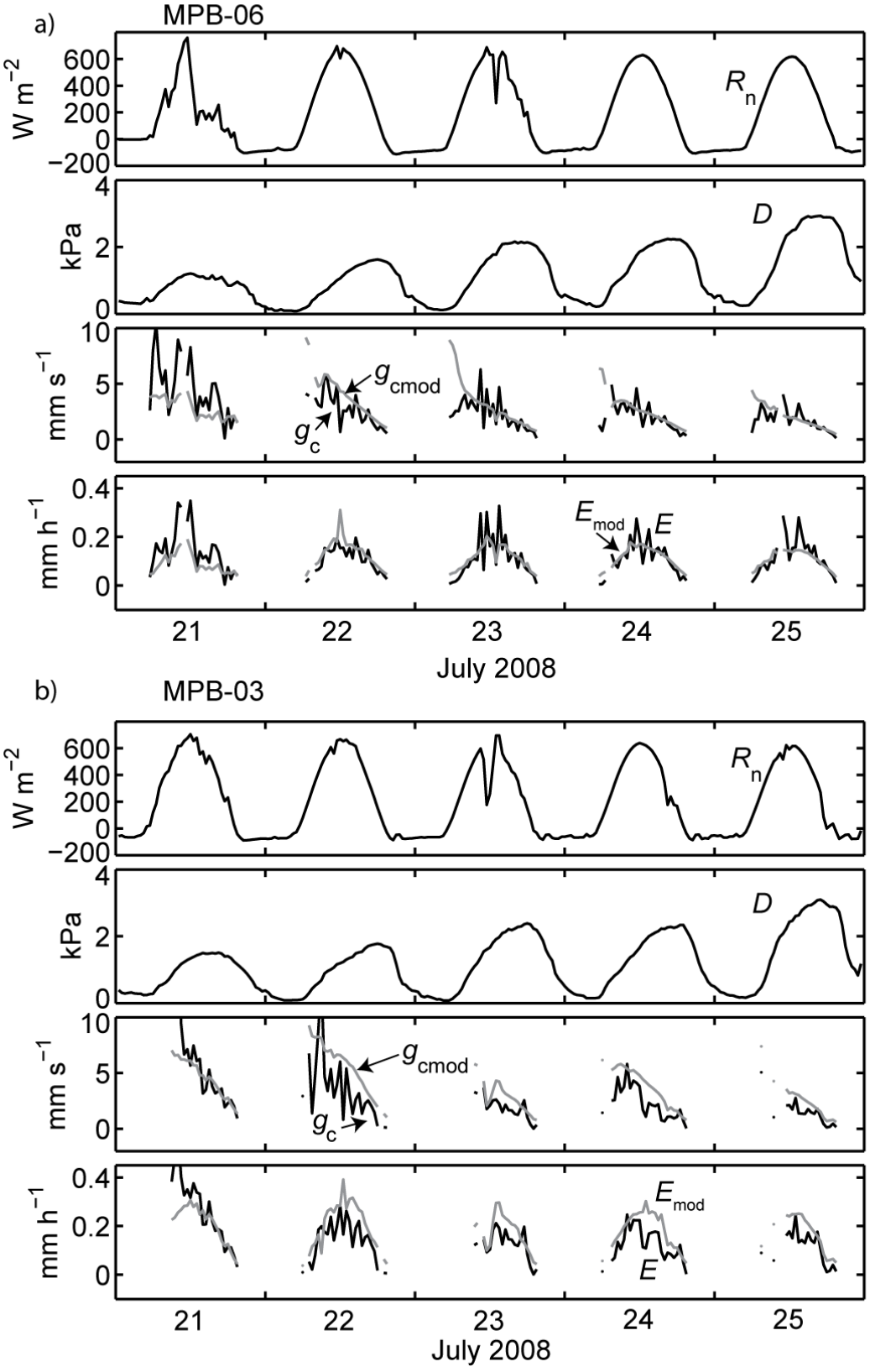
a)
MPB-06
W m^{-2}
600
400
200
0
−200
R_n
kPa
4
2
0
D
mm s^{-1}
10
5
0
g_{cmod}
g_c
mm h^{-1}
0.4
0.2
0
E_{mod}
E
21
22
23
24
25
July 2008
b)
MPB-03
W m^{-2}
600
400
200
0
−200
R_n
kPa
4
2
0
D
mm s^{-1}
10
5
0
g_{cmod}
g_c
mm h^{-1}
0.4
0.2
0
E_{mod}
E
21
22
23
24
25
July 2008

Figure 3.10. Net radiation (R_n), water vapour deficit (D), measured and modelled canopy conductance (g_c and g_{cmod}) and measured and modelled evapotranspiration (E and E_{mod}) at a) MPB-06 and b) MPB-03. Grey lines are modelled values.

3.3.7 Water balance and deficit

The daily change in root zone soil water storage (ΔS) and daily $P - E$ are compared in Fig. 3.11 and Table 3-5. The analysis period was from 1 June, following snow melt and drainage, to 30 September. In 2007 and 2008 at MPB-06, P exceeded E by < 100 mm, generating a small water surplus, whereas in 2009 E was greater than P during much of the growing season. At MPB-03 the water surplus was much larger, as P exceeded E by over 200 mm in every year. Cumulative ΔS was calculated as the sum of the daily changes in soil water storage (S) (i.e., $\Sigma\Delta S$) to the soil depth of 60 cm since 1 June. At both sites during much of the growing season there was a general decline in S with recharge occurring in August and September. The decline in S was greater at MPB-06 than MPB-03, due to the lower P. At MPB-03, there was a small increase in S throughout the 2007 growing season due to a more even rainfall distribution in that year. At both sites, the greatest decline in S occurred in 2009, with a maximum decrease of 46 mm reached at MPB-06; however, both sites recovered by October. Cumulative root zone drainage (D_r) from the 60-cm soil depth was calculated as $\Sigma(P - E - \Delta S)$. Drainage totals were much greater at MPB-03 (200-300 mm) than at MPB-06, where growing season D_r was never greater than ~60 mm.

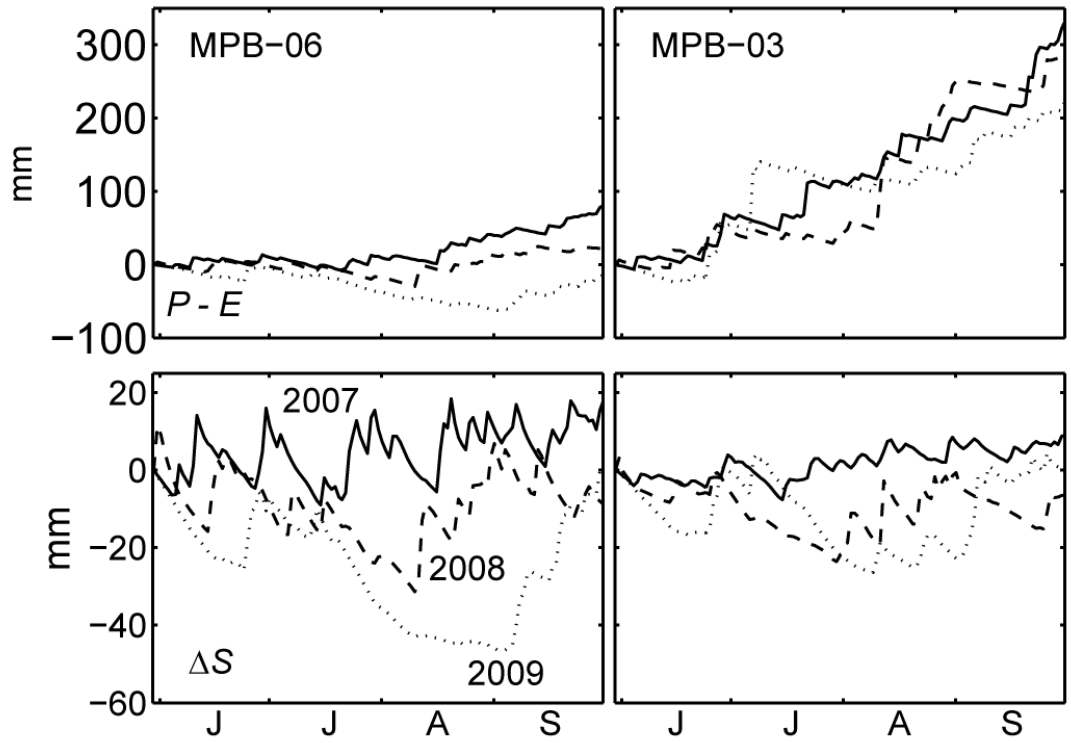

Figure 3.11. Water balance. Precipitation (*P*) - evapotranspiration (*E*) (upper panels) and daily change in root zone soil water storage (Δ*S*) (lower panels) from 1 June to 30 September.

Table 3-5. Cumulative daily totals of precipitation (*P*), evapotranspiration (*E*), daily change in root zone soil water storage (Δ*S*) and root zone drainage (D_r) from 1 June to 30 September. D_r was calculated as $D_r = P – E - \Delta S$.

	MPB-06			MPB-03		
	2007	2008	2009	2007	2008	2009
P	234	192	149	529	514	413
E	154	159	164	198	209	189
ΔS	18	21	-14	18	-9	1
D_r	62	12	-1	313	314	223

When modelling daily values of α_{max} (Eq. 5) to calculate E_{pot}, only growing season data following snowmelt, from 15 May to 30 September, when θ was high ($\theta_{theshhold}$) (> 0.11 and > 0.16 m^3 m^{-3} at MPB-06 and MPB-03, respectively) were included for analysis for individual years. At both sites, the field capacity and wilting point θ values for the soil fine fraction (soil particles <2 mm) were estimated to be 0.17 and 0.05 m^3 m^{-3}. The use of a different threshold at the sites is likely a result of the large difference in precipitation between them. At MPB-06 in 2009, the threshold value was lowered to 0.10 m^3 m^{-3} to include more data. Because θ was usually less than these thresholds, with the exception of 2007 when steady rainfall throughout the growing season kept the soils relatively moist, data from all three years were also combined to establish the relationships in Eq. 5. Although year to year changes in the physiology of the stand were likely occurring as the recovery progressed, the small variance of E over the three years suggested there would be little yearly variation in the response of α_{max} to D. The annual values of the parameters were similar to those obtained using the combined data (Table 3-6). The parameters derived from the model were then used to calculate daily α_{max} values for each year.

Table 3-6. Evapotranspiration (E), equilibrium E (E_{eq}) and potential E (E_{pot}) for 15 May – 30 September at MPB-06 and MPB-03. Also shown are the parameters and coefficients of variation for Eq. 5 and water deficit (WD) totals.

	MPB-06	MPB-03

	2007	2008	2009	2007	2008	2009
a	0.62	0.75	1.24	0.52	0.70	0.74
b	1.25	1.32	0.65	1.38	1.05	0.83
r^2	0.21	0.35	0.04	0.29	0.42	0.18
E_{eq} (mm)	328	340	349	404	420	436
E_{pot} (mm)	216	202	208	255	273	275
E (mm)	166	172	183	214	227	212
WD (mm)	50	31	25	41	45	63
WD (mm)[1]	41	41	33	42	39	36

[1]Water deficit (WD) using α_{max} calculated for all the years combined. For the combined method a = 0.78, b = 1.15 and r^2 = 0.20 for MPB-06 and a = 0.65, b = 1.18 and r^2 = 0.28 for MPB-03.

Over the course of the growing season, α_{max} calculated for each of the years (Eq. 5) ranged from a high of 1.0 and 1.1 to a low of 0.31 and 0.25 at MPB-06 and MPB-03, respectively (Fig. 3.12). Although D explained only a small proportion of the variation in α_{max} (Table 3-6), generally high α_{max} occurred when D was low (Fig. 3.13). The ratios of E_{pot} to E_{eq} for 15 May – 30 September, for both sites were very similar (0.60-0.66 for MPB-06, and 0.63-0.65 for MPB-03). At MPB-06, the interannual variability in E_{pot} was relatively small, with it being greatest in 2007 and smallest in 2008 (Table. 3-6). At MPB-03, the trend was different with E_{pot} being highest in 2009 and lowest in 2007. The daily water deficit (WD = daily E_{pot} – daily E) (Fig. 3.14) tended to be high at both sites in late May to early June as a result of E_{pot} being elevated due to high R_n and low D, and low E due to cool air temperatures. Maximum daily WD was 1.5 mm at MPB-06 and 2.0 at MPB-03. At MPB-06, the cumulative WD was largest in 2007, while at MPB-03 it was largest in 2009 (Fig. 3.15; Table. 3-6). Using the value of α_{max} calculated by combining data from all three years resulted in similar values of WD for all years at both sites except for 2009 at MPB-03 when it was 40% lower.

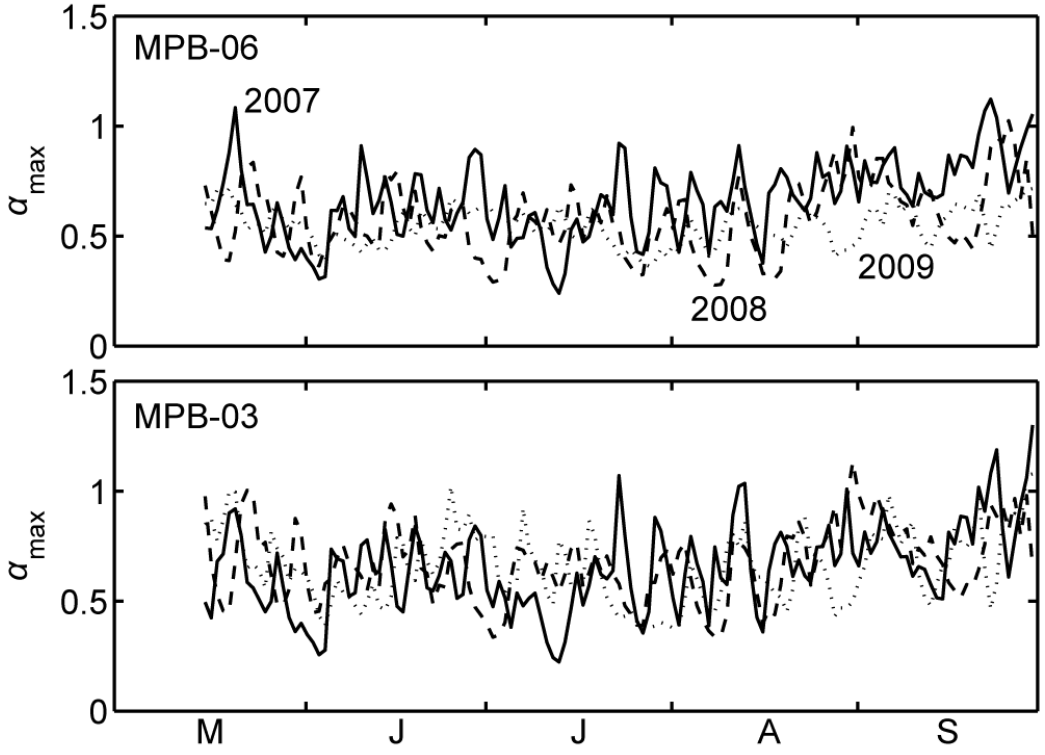

Figure 3.12. Calculated daily values of maximum Priestley-Taylor α (α_{max}) using Eq (5) from 15 May to 30 September at MPB-06 and MPB-03.

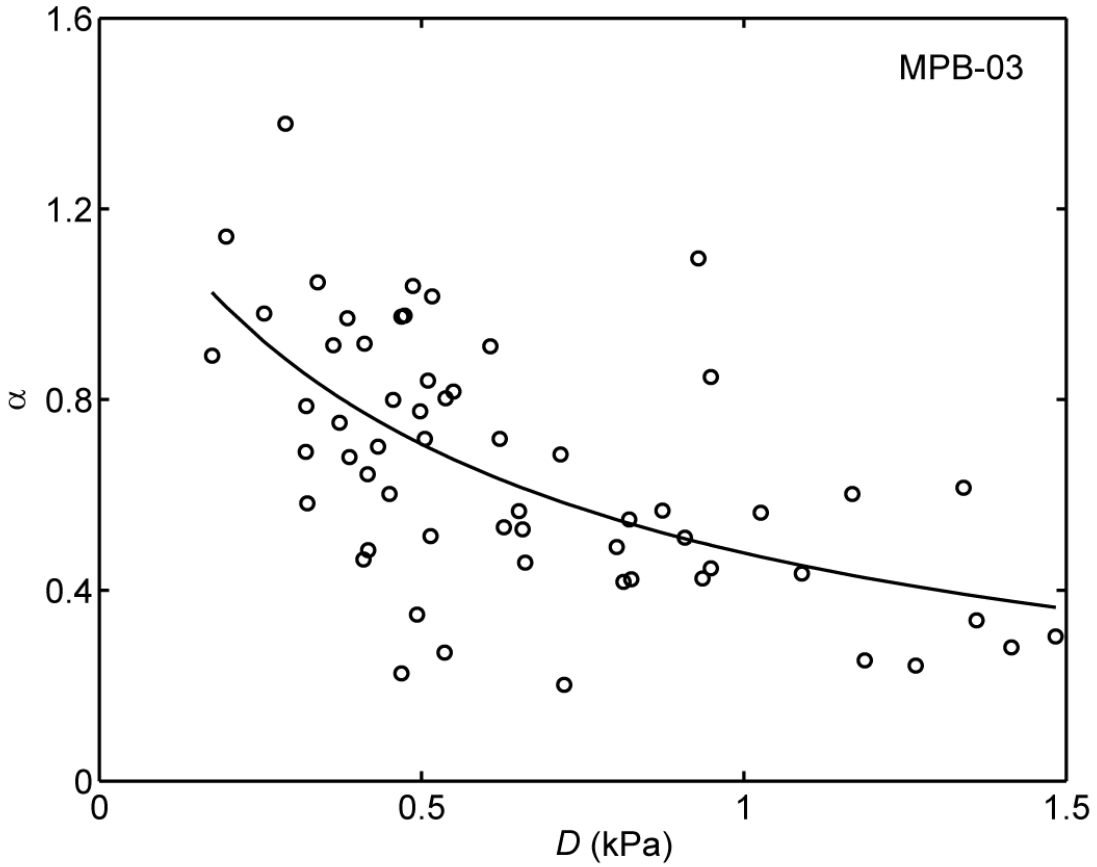

Figure 3.13. Relationship (Eq. 5) between daily values of daytime vapour pressure deficit (*D*) and daily Priestley-Taylor α at daytime soil water content > 0.10 m^3 m^{-3} from 15 May to 30 September 2008 at MPB-03.

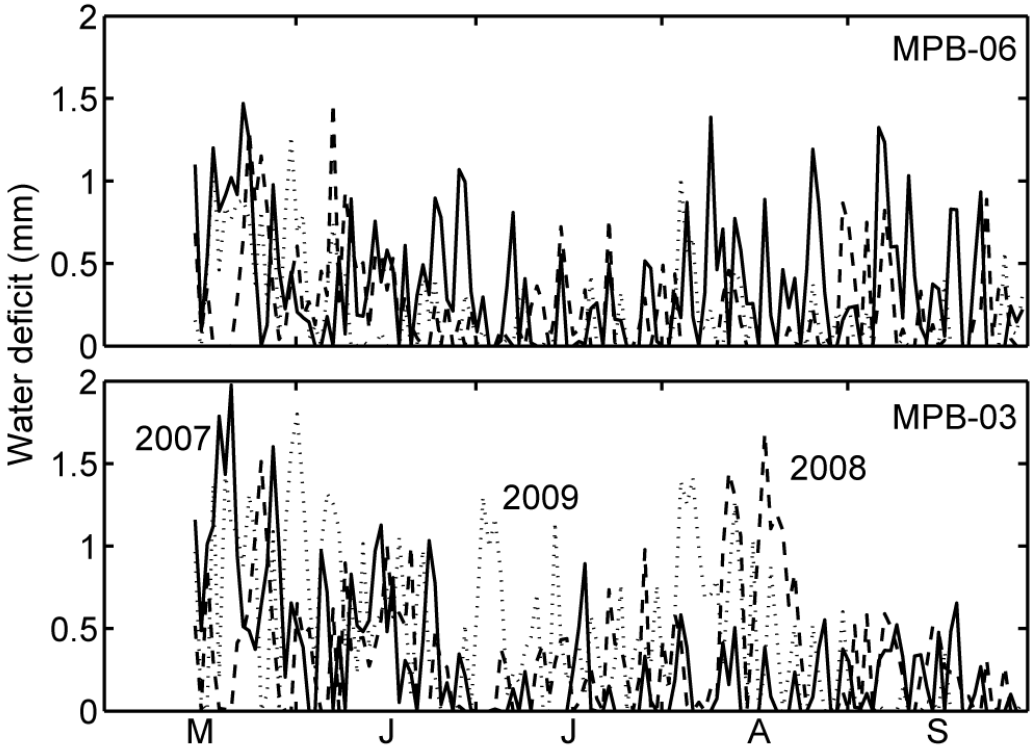

Figure 3.14. Daily water deficit (WD), calculated as daily potential evapotranspiration (E_{pot}) – daily evapotranspiration (E), from 15 May to 30 September at MPB-06 and MPB-03.

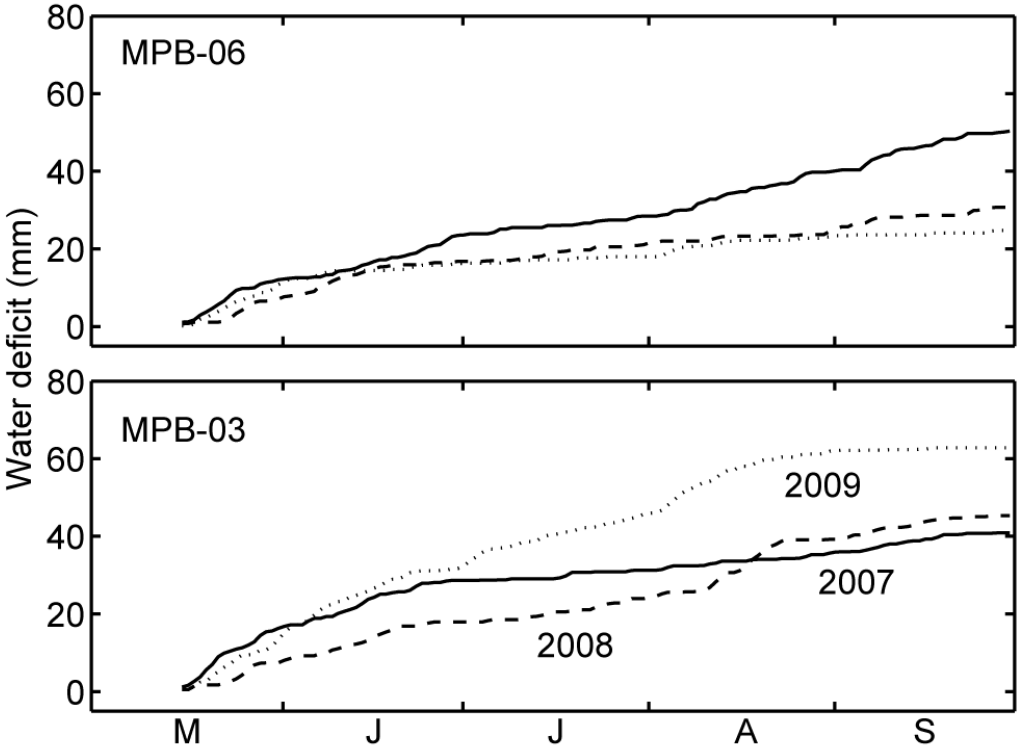

Figure 3.15. Cumulative water deficit (WD) (i.e., Σ(daily E_{pot} – daily E)) from 15 May to 30 September at MPB-06 and MPB-03.

3.4 Discussion

3.4.1 Energy balance

The energy balance values presented here are typical of coniferous forests growing on well-drained sandy soils (Baldocchi *et al.* 2000). Although energy balance closure values are relatively high, complete closure was not achieved. Kidston *et al.* (2010) found, in a 14-m tall boreal jack pine stand, that a lack of complete closure can result from a loss of low-frequency covariance due to an insufficient averaging time. However, they pointed out that the use of

longer averaging times to capture the low-frequency covariance would likely result in a loss of the high-frequency covariance. *E* values in this paper have not been "corrected" for lack of closure. Correction would have resulted in < 15% increase in *E*.

Surprisingly, the progression of the beetle attack did not appear to have an influence on the annual energy balance at either site, as R_n, *H* and λE were similar in magnitude during all three years. In addition, fluxes were not significantly different at MPB-06 in August and September 2006 just after the stand was attacked. This shows that as these sites recover the amount of water being used in the flux of latent heat is rather constant. There were changes in the radiation distribution within the canopy. As the attacked trees died, the needles began to fall which resulted in an increase in the transmissivity of short and long-wave radiation through the canopy. At MPB-06, between 2007 (prior to any loss of needles) and 2009, direct and diffuse solar radiation transmissivity increased from 29 to 44% and from 41 to 51%, respectively, while at MPB-03 solar radiation transmissivity increased from 48% in 2007 to 60% in 2009. Regarding albedo, there was a 16% decrease in the August value between 2007 and 2008 at MPB-06 (from 0.092 to 0.079), and while at MPB-03 the August value remained unchanged (0.074) over the three years (O'Halloran *et al.* 2010). Growing season albedo at MPB-06 was 0.10 in 2007 and 0.08 in 2008 and 2009, while at MPB-03 growing season albedo averaged 0.08 each year (2007 - 2009). During the winter, MPB-03 had higher albedo values than MPB-06 due to more needle-fall having occurred in the former, exposing more of the snow-covered ground surface (O'Halloran *et al.* 2010). Conversely, increased needle fall during the winter can lead to increased litter on the snow surface which can lower albedo (Winkler *et al.* 2010).

The energy balance at these sites could change dramatically when the dead trees fall in significant numbers. The winter albedo of both sites will likely increase, resulting in a reduction

in net radiation compared to the stands before attack (O'Halloran *et al.* 2010). Tree-fall is expected to become frequent about 5 years after attack (Mitchell and Preisler, 1998) and had already started at MPB-03 in 2008.

3.4.2 Evapotranspiration

The values of *E* reported here are similar to those reported for other northern coniferous forests where the interannual variability in *E* has also been quite low. Between 1998 and 2006 in a 90-year-old jack pine stand (OJP) in Saskatchewan, Canada, when annual *P* was 472 mm, annual *E* was also conservative, averaging 300 mm with a range of 62 mm (Zha *et al.* 2010). In a scots pine (*Pinus sylvestris*) forest in southern Finland where annual *P* averaged 692 mm, EC measured annual *E* averaged 295 mm, ranging from a low of 235 mm to a high of 356 mm over a 9 year period (Ilvesniemi *et al.* 2010). Baldocchi *et al.* (1997) reported daily *E* from OJP to typically range between 0.5 and 2.5 mm day^{-1} during the growing season and Kelliher *et al.* (1998) measured *E* from a Siberian scots pine forest over 18 days during the growing season and found a maximum of 2.3 mm day^{-1} . Comparing jack pine with black spruce commonly found in the same area as pine, Brümmer *et al.* (2010) reported a range in *E* from 221 and 288 mm in a dry year (2003) (when *P* = 257 and 315 mm $year^{-1}$) to 301 and 316 mm in wet years (2004 and 2006) (*P* = 611 and 618 mm $year^{-1}$) at OJP and a black spruce stand (SOBS) in Saskatchewan. Average annual *E* was 280 and 308 mm $year^{-1}$ at black spruce stands in Manitoba and Quebec, where average annual *P* was 493 and 917 mm $year^{-1}$ (Brümmer *et al.* 2010). Though these values tend to be slightly higher than at MPB-06, they are very similar to MPB-03.

Evapotranspiration has long been reported to be a conservative process with relatively small interannual variation (Roberts 1983), even as stands develop in leaf area and species

composition (Phillips and Oren 2001; Oishi et al. 2010). As noted by Roberts (1983) and Kelliher *et al*. (1993), the understory, as well as evaporation from the soil, can play an important role in equalizing *E* from stands of varying leaf area. In these recovering stands the accelerated growth of the secondary structure and understory, including the moss and lichen layer, appears to compensate for the reduction in transpiration from tree death. Reid *et al.* (2006) found that lodgepole pine in stands thinned five years prior had higher sap flow rates and mean transpiration rates per unit leaf area than trees in un-thinned stands showing a sustained elevated productivity of trees in thinned stands. The lack of a reduction in *E* in response to the dry conditions in 2009 is a phenomenon that has also been observed in other studies. Oishi *et al.* (2010) found drought conditions in a oak-hickory (*Quercus – Carya*) forest in North Carolina, USA, did not reduce *E* significantly from non-drought years. The authors found that rainy days during drought free periods were characterized by low *D*, which led to low *E*, but during the drought periods *D* was high, leading to moderate levels of *E* despite the dry conditions. Similarly, in these MPB attacked stands, higher values of *D* during the 2009 growing season likely compensated for reductions in *E* due to water limitations and the observed stomatal closure, leading to annual totals of *E* similar to the previous non-drought years.

3.4.3 Canopy characteristics and controls

Decoupling coefficient, *Ω*, values at these sites were low, indicating a high degree of coupling to the *D* of the atmosphere. Low values of *Ω* are typical of the relatively aerodynamically rough surfaces of coniferous forests (Jassal *et al*. 2010). For instance, Brümmer *et al.* (2010) reported *Ω* to range between 0.11 and 0.19 at OJP, SOBS and at black spruce forests in Quebec and Manitoba. Values of g_a were also comparable to other conifer stands of these heights. The old

jack pine site (OJP) in Saskatchewan, with a canopy height of 13.5 m had typical growing season g_a values of ~75 mm s^{-1} (Baldocchi *et al.* 1997) and Kelliher *et al.* (1993) note that forests characteristically have a g_a of about 200 mm s^{-1}. *E* from aerodynamically rougher surfaces tends to be controlled by *D* while *E* from smoother vegetative surfaces is more controlled by R_a (Jarvis and McNaughton 1986). The values of Ω reported here shows that *D* plays a dominant role in controlling *E* (Jarvis and McNaughton 1986).

Priestley-Taylor α values for these sites are similar to those reported in other studies in coniferous stands and much lower than those from well-watered vegetation with a closed canopy which tend to have an α near 1.26 (Jarvis and McNaughton 1986). OJP was found to have values of α of ~ 0.5 (Baldocchi *et al.* 1997) and SOBS values between 0.5 and 0.7 during the peak of the growing season (Arain *et al.* 2003). An aspen forest (SOA) (near OJP and SOBS) had a daytime mean α of 0.91 during the full leaf period (Blanken *et al.* 1998) and a Douglas-fir stand harvested in 1949 had a mean monthly α of 0.62 (Jassal *et al.* 2010).

The values of g_c reported in these sub-boreal forest stands are similar to those from studies in the boreal forest. Baldocchi *et al.* (1997) reported daytime g_c values for OJP to be typically < 3.8 mm s^{-1} and concluded that those values were low as result of a stomatal closure due to low soil moisture, high *D* and a low photosynthetic capacity of jack pine needles. Low θ can decrease g_c via the release of the phytohormone, abscisic acid (ABA), from the roots which is then sensed by the stomata causing them to close (Lambers *et al.* 1998; Baldocchi *et al.* 1997). In the stands in this study, most years there was a positive linear relationship between daytime means of g_c and θ (the r^2 was 0.36, 0.24 and 0.00 at MPB-06, and 0.26, 0.06 and 0.17 at MPB-03, in 2007, 2008 and 2009, respectively), although the relationship was strongest when θ was greater than ~0.08 m^3 m^{-3} at MPB-06 and ~0.15 m^3 m^{-3} at MPB-03. Below these levels, g_c tended

to be low, and there was a lot of scatter in the relationship. Bernier *et al.* (2006) found that in Saskatchewan, relative soil water content explained approximately 46% of the variation in E for SOA but only 10% for OJP due to very low values of θ in the latter. They concluded that the relationship between g_c and θ is significantly affected by soil texture (i.e., the soil water retention curve) which determines the amount of water available to the trees. In the MPB attacked stands, the sandy and fast draining soils limited the growing season variation in θ (fine soil volumetric fraction); the total range in growing season θ (following snowmelt) over the three years was 0.08 $m^3\ m^{-3}$ (0.04 – 0.12 $m^3\ m^{-3}$) at MPB-06, and 0.04 $m^3\ m^{-3}$ (0.12 – 0.18 $m^3\ m^{-3}$) at MPB-03. It is also possible that the lack of a strong response of g_c to θ indicates the trees are able to access water from deeper in the soil profile. However, since g_c did not appear to plateau at the higher values of θ, θ was likely almost always limiting g_c. Comparing with a conifer stand with relatively little soil water limitation, the SOBS stand in Saskatchewan had a typical growing-season mid-day g_c of 5 – 10 mm s^{-1} from 1999 to 2001 (Arain *et al.* 2003) indicating a higher g_c under non-water limiting conditions.

Vapour pressure deficit and Q were able to explain more than half of the variation in half hourly g_c. It was observed that at the highest values of g_c (~> 10 mm s^{-1}; Fig. 3.9), g_{cmod} consistently underestimated g_c, resulting in E_{mod} underestimating E when E was highest. These high values of g_c did not occur consistently under the same conditions of D and Q thus other factors also must have influenced g_c. These could include the varying response of the overstory, understory and moss and lichen layer to D and Q, as well as the influence of the beetle attack. Nevertheless, when half-hourly values of E and E_{mod} were summed for 15 May – 30 September, the agreement was very good.

Like the growing season values of g_c, growing season measurements of conifer stomatal conductance (g_s) made at the leaf level, as described in Chapter 2, did not vary significantly over the three years at MPB-06 (Fig. 3.16). At MPB-03, conifer g_s also followed a trend similar to g_c, increasing slightly in 2008 and then falling in 2009 due to the effects of drought.

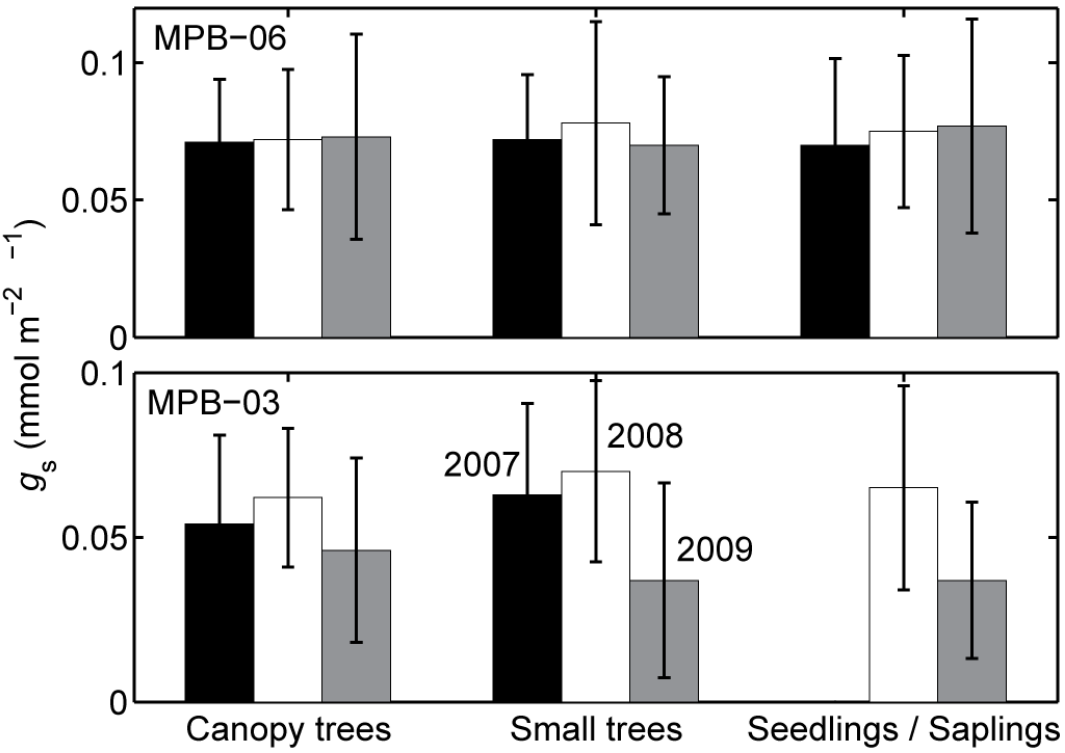

Figure 3.16. Average growing season stomatal conductance (g_s) of canopy trees, small trees, and seedling and saplings. Bars are standard deviations. Average g_s of broadleaf vegetation was 0.15 (0.06), 0.14 (0.07) and 0.27 (0.71) mmol H_2O m^{-2} s^{-1} from 2007-2009 at MPB-06, and 0.13 (0.07), 0.13 (0.09) and 0.14 (0.16) mmol H_2O m^{-2} s^{-1} from 2007-2009 at MPB-03 (numbers in parentheses are standard deviations).

3.4.4 Water balance

MPB-03 had much higher drainage values than MPB-06 due to higher rainfall. At MPB-06 there was a steady decrease in D_r over the three years, due to decreasing totals of P. Despite this decrease, E actually increased from 2007 to 2009 (1 June – 30 September) causing ΔS to be negative in 2009. Uunila *et al.* (2006) suggested that there would be an increase in annual water yield and late summer/fall low flows in even-aged stands without secondary structure following MPB attack but at MPB-06 this has not been the case. Although there are few studies on the effects of beetle attack on the hydrology of forested stands (Hélie *et al.* 2005), the assumption that beetle attack would led to an increase in θ and runoff due to earlier snowmelt, and lower rates of transpiration (BCMFR 2008) were not observed in this study. Although EC measurements were not made before the site was first attacked, E during August and September 2006 and 2007 was 1.91 mm day^{-1} and 2.24 mm day^{-1}, respectively, suggesting E was not much different prior to attack (Appendix 1). This lack of a difference in E could be due to a soil water limitation in 2006, as average θ was 0.05 $m^3\ m^{-3}$ and 0.11 $m^3\ m^{-3}$ during August and September 2006 and 2007, respectively. As evidence that the August 2006 measurements were representative of pre-attack stand conditions, foliar photosynthesis and stomatal conductance of attacked trees were not significantly different than those of the non-attacked trees sampled during that period (see Chapter 2 for details).

The values of α_{max} at high values of D were much less than the theoretical maximum α of 1.26 identified by Priestley-Taylor (1972) for well- watered vegetation. Shuttleworth and Calder (1979), however, noted that using the value of 1.26 is likely unrealistic in forest ecosystems due to physiological controls, which under dry conditions reduce E to levels much lower than those observed over well-watered crops. At MPB-06 in 2009 there were only 19 days when θ was >

$\theta_{threshold}$, thus using only data from that year to model α_{max} was likely not as robust as combining data from all three years, even though the cumulative WD was similar using the two methods. This was likely not an issue in 2009 at MPB-03, as there were a larger number of values available for calculating α_{max} (N = 59).

By including an α_{max} term that varied with D, Eq.4 was able to produce values of E_{pot} that incorporate both the influence of R_a and D on the capacity vegetation to transpire. For instance, under well-watered conditions low D resulted in higher α values, as the stomata were more open during these times, which acted as a positive forcing on E. However, R_a tended to be low under such conditions, which limited E. This interplay of the influences of D and R_a helps explain the low variability in interannual E, despite the variation in climate. The growing season WD shows that these stands are water limited and thus the stomata must close to restrict water loss. However, since the WD was small, even if θ remained high throughout this period, E would not have been dramatically higher. The WD was likely low because E_{pot} would have been less than if the stands had not been attacked by the beetle. The effect of beetle on the WD depends on how much the effect of the beetle reduces E_{pot} (i.e., E when θ is not limiting) compared to how much it reduced E. The observation of a WD indicates that in spite of the beetle attack, stands with either an understory or un-killed trees respond to the atmospheric demand for water.

3.5 Conclusions

Although it has been predicted that the MPB outbreak in BC would significantly alter transpiration rates and thus induce changes in annual water yields (BCMFR 2008; Hélie *et al.* 2005), there has not been a significant change in E at these two sites over the tree years EC measurements were made. The increase in E from the growth release of the secondary structure,

understory vegetation and mosses and lichens at MPB-03 has compensated for the reductions in E due to the death of the overstory. At MPB-06, the growth of the surviving trees and understory vegetation, and mosses and lichens in response to the beetle attack maintained E at relatively stable levels over the three years following attack. Canopy conductance was largely controlled by D but the response varied with Q. The use of the Priestley-Taylor equation with a varying α resulted in reasonable values of E_{pot} for these stands at their current stage of recovery from MPB attack. As the stands continue to recover and canopy closure is once again attained, E_{pot} will likely increase. The large difference in growing season drainage between sites was due to difference in P at the two sites, with MPB-03 having the higher P and D_r.

4. The carbon balance of two lodgepole pine stands recovering from mountain pine beetle attack in British Columbia

4.1 Introduction

Recently, the impact of disturbance on forest carbon (C) cycling in North America is receiving increased attention from researchers (e.g. Amiro *et al*. 2010, Coops and Wulder 2010, Kurz *et al*. 2008). Forests fires, insect attacks and harvesting can all shift forests from C sinks to sources (Amiro *et al.* 2010). In Canada, insect infestations can result in greater annual tree mortality than either fires or harvesting (Kurz *et al*. 2008), thus quantifying their impact is central to furthering our understanding of forest C dynamics. The recent mountain pine beetle (MPB) (*Dendroctonus ponderosae*) outbreak in British Columbia (BC) is unprecedented in terms of tree mortality and area affected and could severely impact the C balance of BC's forests. Lodgepole pine (*Pinus contorta* var. *latifolia*), the main host of the beetle, is found throughout the interior of BC. A 2009 aerial survey reported just under 9 million ha of forests showing some current beetle impact, down from the peak infestation of 10 million ha in 2007 (Westfall and Ebata 2009). Insect attacks can influence net ecosystem production (NEP), the net uptake of atmospheric CO_2 by the forest, via their impact on gross ecosystem photosynthesis (P_g) and ecosystem respiration (R_e). The reduction in leaf area associated with tree mortality would likely lead to a decline in P_g, and the increase in dead organic matter (needles, roots, stems and branches) would be expected to lead to an increase in decomposition. However, the time scale at which these processes occur is not well known. While P_g might be expected to show an immediate response to attack, an increase in R_e could take years.

There are few published results of the impact of insect attacks on C cycling. Eddy covariance (EC) measurements made in a hardwood forest in Wisconsin that had been 37% defoliated by forest tent caterpillars (*Malacosoma disstria*) suggested a 24% reduction in P_g compared to non-outbreak years (Cook *et al.* 2008). Similarly, Clark *et al*. (2010) reported a decrease in the magnitude of annual net ecosystem exchange (NEE) in New Jersey oak (*Quercus* sp.) and pine (*Pinus* sp.) dominated upland forests defoliated by the Gypsy moth (*Lymantria dispar*), though the impact varied among three sites. A modelling study predicted the cumulative impact of the BC MPB outbreak from 2000-2020 to be a net loss 270 Mt C, with the impact peaking in 2009 with a net biome production (NEP plus the impacts of disturbance but excluding the effects of additional harvesting) of -53 g C m^{-2} (Kurz *et al*. 2008). MODIS-based estimates of P_g over the BC MPB infestation area from 2002 to 2005 showed a decrease of 10-20% from pre-outbreak levels (Coops and Wulder 2010), with more severely attacked stands having a greater reduction in P_g.

Although the previous two studies cited reported a decline in P_g, previous results of eddy covariance measurements from two beetle-attacked stands in the central interior of BC showed that in the first two years of measurement (first and second and fourth and fifth years after initial attack) NEP was negative but then increased following a boost in the productivity of the residual trees and vegetation (Chapter 2). These two sites also showed little change in evapotranspiration following the attack, a result of the compensating effect of the surviving trees and below-canopy vegetation (Chapter 3). This study examines how these two stands continue to recover from the attack using four years of EC data focusing on how P_g and R_e have responded by examining their relationships with climate variables.

4.2 Methods

4.2.1 Site description

NEP and climate measurements were made in two stands dominated by lodgepole pine (*Pinus contorta* Dougl. Ex Loud. var. *latifolia* Engelm.), located in the northern interior of BC, in the Sub-Boreal Spruce biogeoclimatic zone (Meidinger and Pojar 1991). The first stand (MPB-06) (55°06'42.8''N, 122°50'28.5''W) is located at Kennedy Siding, approximately 35 km southeast of the town of Mackenzie. The first large scale attack by the beetle at this ~80-year-old stand was in the summer of 2006. This site contained few non-pine trees, and the understory consisted mainly of pine seedlings, scattered shrubs and a ground cover of moss and lichen. The second, ~110 year-old stand (MPB-03) (54°28'24.8''N, 122°42'48.4''W) is in Crooked River Provincial Park, approximately 70 km north of Prince George, BC and approximately 100 km south of MPB-06. The overstory was comprised of about 92% lodgepole pine and 8% subalpine fir (*Abies lasiocarpa*), and had a developed secondary structure (tree seedlings and saplings, and sub-canopy and canopy trees that survive the attack) consisting of lodgepole pine, subalpine fir and hybrid white spruce (*Picea glauca)* sub-canopy trees and saplings, and seedlings of all three tree species. The ground cover was dominated by mosses, lichens and dwarf shrubs. MPB-03 was first attacked in 2003, and by March 2007, when NEP measurements began, more than 95% of the pine canopy had been killed by the beetle. Both sites are flat and on coarse textured gravelly soils of glacio-fluvial origin. The fine soil bulk density is approximately 1180 and 1160 kg m^{-3} and soil coarse fragment content is about 34 and 70 % (by volume >2 mm) at MPB-06 and MPB-03, respectively. In 2007, stand density was ~1235 and ~560 stems ha^{-1} and stand basal area was 12.0-20.1 m^2 ha^{-1} and 8.8-17.9 m^2 ha^{-1} (live and dead trees with height > 10 m) at MPB-06 and MPB-03, respectively. LAI decreased at MPB-06 from 1.4 in 2007 to 1.3 in 2010. Live

LAI at MPB-06 was 0.42, 0.31, 0.30 and 0.22 in 2007, 2008, 2009 and 2010, respectively. At MPB-03, LAI decreased from 0.9 in 2007 to 0.55 in 2010. For further information on stand characteristics see Chapter 2.

4.2.2 Flux, climate and ecophysiological measurements

A 32-m-tall scaffold flux tower (~2.1 m long x ~1.5 m wide) was established at each of MPB-06 and MPB-03 in July 2006 and March 2007, respectively. Flux and climate measurements began on 18 July 2006 and 20 March 2007 at the respective sites. Fluxes of CO_2 (F_c), sensible (H) and latent heat (λE) were measured directly using the EC technique. A 3-dimensional ultrasonic anemometer (model CSAT3, Campbell Scientific Inc. (CSI), Logan, Utah) was used to measure the three components of the wind vector, and turbulent fluctuations of CO_2 and H_2O concentration were measured using an open-path infrared gas analyzer (IRGA) (model LI-7500, LI-COR, Inc, Lincoln, Nebraska,). Signals were measured with a data logger (CSI, model CR1000) with a synchronous-device-for-measurement (SDM) connection. At both sites, EC sensors were mounted at the height of 26 m, which was ~8 m and ~6 m above the top of the canopy at MPB-06 and MPB-03, respectively. Following Webb *et al*. (1980), F_c and λE were calculated as the product of the dry air density and the covariance of the CO_2 and water vapour mixing ratios, respectively, measured at 10 Hz. Further details of the measurements system and the data processing procedure are provided in Chapter 2.

Climate variables measured included above-canopy upwelling and downwelling shortwave and longwave radiation (at 30-m height) and above-canopy upwelling and downwelling (30-m height), and below-canopy downwelling (3-m height) photosynthetically active radiation (PAR), precipitation at just-below-canopy height, wind speed, air temperature

and relative humidity at the 25-m height, soil temperature at depths of 5, 10, 20 and 50 cm, soil heat flux at a depth of 5 cm and water content at the 0-10 cm and 30-50 cm depths at MPB-06 and at the 10-cm, 20-cm and 50-cm depths at MPB-03. Meteorological measurements were made every second, and 30-min average values calculated. Snow-pack depth was also measured at a clearcut weather station located ~1 km from MPB-06, using an acoustic distance sensor and precipitation calculated from these data and manual measurements of liquid water equivalent. Instrument names and model numbers can be found in Chapter 2. Leaf area index (LAI) was calculated for the canopies at both sites using a LI-COR Plant Canopy Analyzer (model LAI-2000, LI-COR Inc.) as well as a TRAC (Tracing Radiation and Architecture of Canopies) instrument (Third Wave Engineering, Nepean, Ontario, Canada), hemispherical photography (Egginton *et al.* 2008). Live LAI at MPB-06 was determined by canopy photo analysis. Photographs of the forest canopy were taken each year in 8 directions from the tower. The images were adjusted to ensure the same area of the canopy was analysed each year and the fraction of green leaf area was determined by overlaying a 240-point grid on each image and counting the number of grid points on green forest canopy. Each year, live LAI was determined as the LAI measured in 2006 adjusted by the fraction of green canopy from the photographic analysis.

Foliar gas-exchange (CO_2 and water vapour) measurements were made every two to four weeks throughout the 2007-2009 growing seasons (1 May- 30 September) at MPB-06 and 2007-2010 growing seasons at MPB-03 (Bowler 2010). The measurement periods were 23 May – 23 September 2007, 27 May – 11 September 2008, 27 May - 14 September 2009, and 14 July – 13 August 2010 (measurements were made at MPB-03 only in 2010). Shoots were clipped at random from the lower branches of the canopy exposed to sun at a height of approximately 6 m

using a pruning pole and shoots from smaller understory trees were clipped using handheld shears from random branches and measured within 5 minutes of sampling. Samples were taken from the same trees on consecutive occasions. Measurements were made between 10:00 and 16:00h PST in ambient light conditions. Foliar net assimilation (A_n) and stomatal conductance (g_s) measurements were made using a portable photosynthesis measurement systems (model LI-6400, LI-COR Inc.) with a clear acrylic conifer chamber (model 6400-05, LI-COR Inc.), following the approach of Pypker and Fredeen (2002). Needles intact to the branchlet were placed in the conifer chamber under ambient light conditions. Broadleaf vegetation gas-exchange measurements began in early June when leaves were estimated to be fully expanded. Samples were randomly selected from many different species of several classes of vegetation including small trees such as trembling aspen (*Populus tremuloides*), deciduous and evergreen shrubs, herbaceous annuals, and lycopods (the latter occur at MPB-03 only). The physiological response to excision of broadleaves has been found to be more rapid than needles (Richardson and Berlyn 2002); therefore to minimize stomatal closure due to leaf water potential changes following excision, broadleaf gas-exchange measurements were conducted on intact foliage, except for very small evergreen shrubs such as wintergreens (*Pyrola* spp.). These species were too close to the ground to effectively enclose in the conifer chamber. It was assumed the effects of excision were minimal due to the similarity in leaf structure and cuticle thickness compared to conifers (Taneda and Tateno 2005). During the measurements a CO_2 concentration and air flow rate was maintained for 3 min at 380 ppmv and 500 μmol s^{-1} (300 mL min^{-1}), respectively. Air temperature, vapour pressure deficit (D) and PAR were continuously recorded during each measurement along with A_n and g_s. Area-based estimates of A_n were calculated after determining half the total leaf area, using the volumetric displacement technique, for each branchlet sampled

and leaf area to dry leaf biomass ratios (specific leaf area, SLA) were determined. Broadleaf sample one-side surface areas were determined optically using a flat bed scanner (Epson Expression 1640 XL) and analyzed using WinFolia (version Pro 2003d) image processing software (Régent Instrument Inc., Quebec, Canada).

There are three main stages to MPB attack in terms of its effects on the host tree. The green attack stage generally occurs during the first year of attack, when the needles remain green. The red attack stage occurs after the first winter of attack when the tree has been killed and the needles turn red. Finally, the tree enters the grey attack stage one or two years later when the needles begin to fall. By 2007, MPB-03 was already in the red and grey stage of attack. Tree health status inventories at MPB-06 were conducted each year from 2006 to 2010 (Fig. 4.1). The attack status of individual trees was determined along two 350-m long x 2-m wide transects. Green attack was identified by the presence of beetle core holes, while red attack was identified by foliage colour and grey attack by the transition to grey colour. Inventories were also conducted in June and October 2007 by Hilker *et al.* (2009). In addition, independent tree health assessments were also made annually in August by biologists evaluating woodland caribou response to partial retention logging of MPB attacked stands (Seip and Jones 2007). Tree health was also determined by canopy photo analysis.

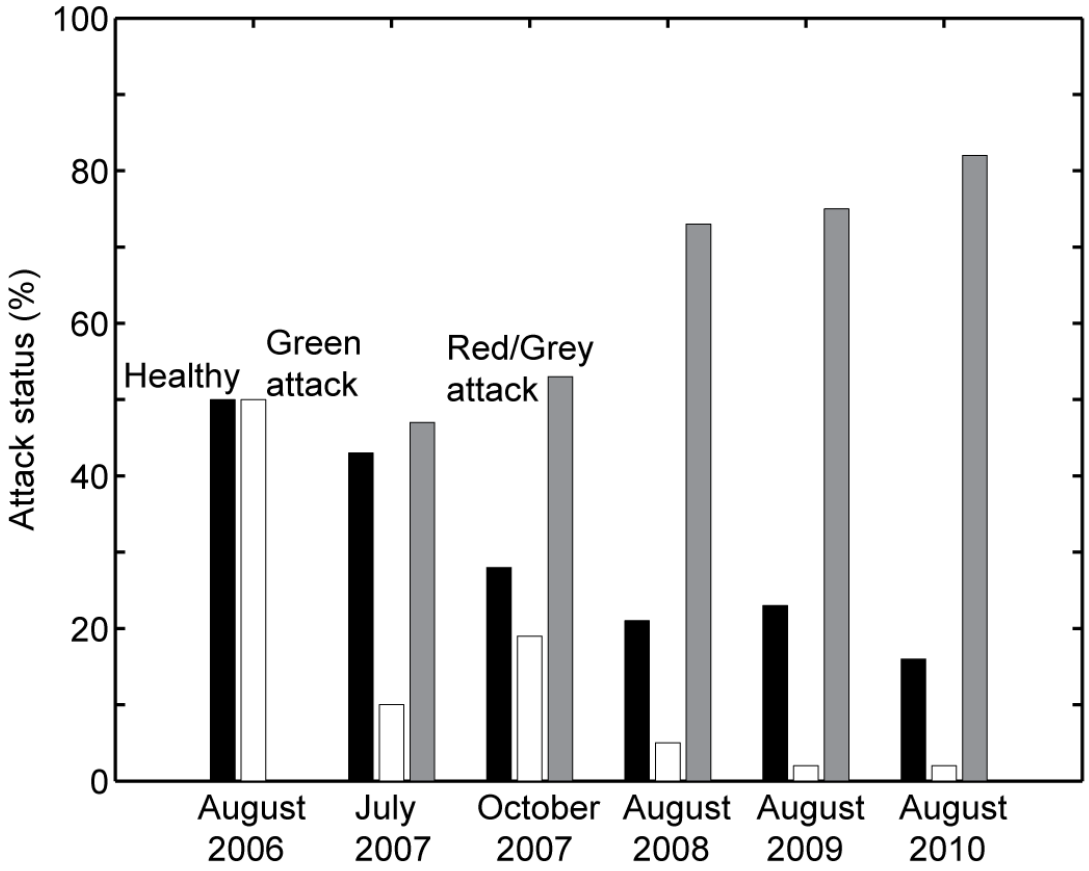

Figure 4.1. Mountain pine beetle attack status at MPB-06. July and October 2007 are values from Hilker *et al.* (2009). August 2007-2009 are mean values from this study and of Seip and Jones (2008). August 2010 are mean values of Spittlehouse *et al.* (2010) and Dale Seip (personal communication).

4.2.3 Flux quality control and data analysis

Quality control procedures included rejection of flux data when a 30-minute period had more than 30% of an individual trace with an instrument diagnostic warning flag that indicated a bad measurement, and setting minimum (300 µmol mol^{-1}) and maximum (1000 µmol mol^{-1}) bounds on CO_2 concentrations as measured by the open-path IRGA. Fluxes were not rejected on the basis of wind direction since the fetch of beetle-affected forest was greater than 1 km in all directions around the tower, and when wind passed through the tower before passing through the

sonic anemometer array, which was rare, there was no detectable effect. An additional quality control procedure was applied to winter flux data to address the issue of wintertime CO_2 uptake commonly observed with the use of the LI-7500 open-path IRGA (described in detail in Chapter 2).

Nighttime EC measurements provide a direct measure of R_e (van Gorsel *et al.* 2008). At both sites, only nighttime EC data when friction velocity (u_*) was greater than the threshold u_* (u_{*th}) of 0.30 m s^{-1} were considered for analysis, thus ensuring sufficient turbulent mixing (Baldocchi 2003). The value of u_{*th} was determined by plotting half-hourly CO_2 flux against u_* and selecting the value for which a further increase in u_* no longer led to an increase in the flux (Massman and Lee 2002). The value was not clearly defined, which, unfortunately, is common-place in EC studies (Gu *et al.* 2005); however, it was within ±0.05 m s^{-1} of 0.30 m s^{-1}. Daytime R_e was estimated using the standard algorithm established by the Fluxnet Canada Research Network (FCRN) of the Canadian Carbon Program (Barr *et al.* 2004) which assumes the following empirical logistic relationship between nighttime R_e ($u_* > u_{*th}$) and soil temperature at 5-cm depth (T_s) can be applied to the daytime:

$$R_e = \frac{r_1}{1+\exp[r_2(r_3 - T_s)]} \quad (1)$$

where r_1, r_2 and r_3 are parameters set by the model. Following the FCRN protocol, a moving window parameter ($r_w(t)$), which estimates the seasonal variation of the parameters in Eq. (1) was added so that:

$$R_e = \frac{r_w(t) r_1}{1+\exp[r_2(r_3 - T_s)]} \quad (2)$$

The moving window parameter is calculated as the slope of the linear regression between estimates of R_e obtained from the annual relationships (Eq. 1) and R_e from the measurements

Barr *et al.* (2004). The window is 100 data points wide and is moved in an increment of 20 points at a time.

P_g was calculated as daytime NEP + daytime R_e. Gaps in the daytime NEP data were filled with the difference between modelled P_g and R_e. P_g was modelled using the following FCRN standard algorithm, which assumes a rectangular hyperbolic (Michaelis–Menten) relationship between P_g and downwelling PAR (Q):

$$P_g = \frac{\alpha_P Q P_{g\max P}}{\alpha_P Q + P_{g\max P}} \quad (3)$$

where α_P is the quantum yield, $P_{g\mathrm{maxP}}$ is ecosystem photosynthetic capacity (i.e., asymptotic value when Q approaches infinity). An additional moving window parameter ($p_w(t)$) is added, resulting in:

$$P_g = \frac{p_w(t)\alpha_P Q P_{g\max P}}{\alpha_P Q + P_{g\max P}} \quad (4)$$

where the moving window parameter was used as in Eq (2) above. The gap-filling procedure was altered from that described in Barr *et al.* (2004) in that, the moving window was not applied during the winter (when T_s was <1 °C). Ideally, each window would cover a period of a few days. However, during the winter at these sites, when NEE measurements were sparse due to the screening procedure (Chapter 2 (Brown *et al*. 2010), a single 100 point window was found to span weeks or 2-3 months. Over such time spans climatic variability, such as changes in air temperature (T_a), resulted in variations in R_e even though T_s varied little. To fill gaps in H and λE a procedure described in Chapter 3 was used.

In this paper, the seasonal and annual C balance values of R_e and P_g were obtained using the nighttime R_e - T_s relationship (Eq. (2)) and the P_g and Q relationship (Eq. (4)) when daytime NEP values were missing.

The growing season photosynthetic and respiratory characteristics of the two ecosystems were also determined without using the nighttime relationship (Eq. 1) to obtain daytime R_e. These estimates were obtained by applying the Michaelis–Menten light response relationship to daytime NEP measurements as follows:

$$\mathrm{NEP} = \frac{\alpha_N Q P_{g\max N}}{\alpha_N Q + P_{g\max N}} - R_{edN} \qquad (5)$$

where α_N is the quantum yield, $P_{g\mathrm{maxN}}$ is ecosystem photosynthetic capacity and R_{edN} is the daytime ecosystem respiration.

To examine the seasonal variation in daytime ecosystem respiration and its response to T_s, 3-day values of daytime ecosystem respiration (R_{ed}) were determined as the intercept of the linear relationship between 3-day half-hourly values of measured NEP and Q when Q was <300 μmol m^{-2} s^{-1} (Jassal *et al*. 2007). R_{ed} values binned by a width of 2.0 °C were then used with average 3-day daytime T_s (5-cm depth) to develop a R_{ed} function using Eq. 1. Only values of R_{ed} were included for the analysis when the r^2 was > 0.2 for the 3-day fitting procedure. Annual and growing season totals of R_{ed} were calculated by applying this R_{ed} function to nighttime and daytime half-hourly T_s values.

The light response parameters of the foliage were determined using the following equation:

$$A_n = \frac{\alpha_l Q A_{\max}}{\alpha_l \ Q + A_{\max}} - R_{ld} \qquad (6)$$

where α_l is the leaf quantum yield, A_{max} is the leaf photosynthetic capacity R_{ld} is the leaf daytime respiration.

In the ecosystem respiration and light response analysis the fitted models (Eq. (1) and (3)) were compared to null models (containing only an intercept parameter) with a likelihood ratio test (Seber and Wild 2003). *P*-values were determined by comparing the change in the log likelihood between the full and null models to a chi-squared distribution with degrees of freedom equal to the difference in the number of model parameters. To test for changes in the models over time, models with parameters being constant across years were compared to fitting separate models to each year's data using a likelihood ratio test. The log likelihood for the temporally constant model was compared to the sum of the log likelihoods for the separate models, with the difference compared to a chi-squared distribution with degrees of freedom equal to the number of extra parameters used when fitting separate models for each year.

The quality of the EC data was assessed by determining energy balance closure, although a closure correction was not applied. A detailed energy balance closure analysis was reported in Chapter 3. Briefly, half-hourly measurements of net radiation flux (R_n), surface soil heat flux (G), H and λE were used together with estimates of the rate of change in energy storage (per unit ground area) in the air and biomass between the EC sensors and the ground surface (S_t). The slopes of plots of half-hourly values of $H + \lambda E$ vs. available energy flux ($R_n - G - S_t$) for both sites were always >0.89 on an annual basis, and >0.92 for the growing season data.

4.3 Results

4.3.1 Climate

The main difference between the climates at the two sites is the precipitation, with approximately twice as much growing season rainfall at MPB-03 compared to MPB-06 (Fig. 4.2) due to the presence of convective storms which frequently pass over MPB-03. Despite the large difference in precipitation, the region of both sites often experiences a period with little rainfall in late July and August. While rainfall during the 2007 and 2008 occurred quite steadily throughout the growing seasons, 2009 and 2010 were quite dry. At MPB-06 soil fine fraction (soil particle size < 2 mm) volumetric water content (θ) was at its lowest level (< 0.05 m^3 m^{-3}) from 29 July to 7 September 2009, during which time there was a total of 29 mm of rainfall. In 2010 between 24 July and 22 August, MPB-06 received only 1 mm of rainfall and θ fell to 0.05 m^3 m^{-3}. MPB-03 also experienced a prolonged drought in 2010, lasting from 13 July to 22 August (10 mm of rainfall), during which time θ was approximately 0.12 m^3 m^{-3}. There was a similar, though shorter drought at MPB-03 in 2009 lasting from 17 July to 10 August. Over the four years, 2009 had the warmest growing season at both sites (Fig. 4.2; Table 4-1) when T_a, Q and daytime D were all highest. The winter was much milder in 2010 than the previous years, with 5-day-average T_a never falling below -8 °C after 10 January at both sites. While snowmelt was not complete until mid-May in 2007 to 2009, it was complete by late April in 2010 at MPB-06, while at MPB-03 snowmelt was complete by 20 April in 2007 and 2010, and by 15 May and 7 May in 2008 in 2009. Wintertime daily T_s (5-cm depth) never fell below -1.0 °C at MPB-06 and 0.0 °C at MPB-03. Further climate details are provided in Chapters 2 and 3.

Table 4-1. Average values of climate variables for the growing season.

	MPB-06				MPB-03			
	2007	2008	2009	2010	2007	2008	2009	2010
Air temperature (26-m height) (° C)	11.8	12.4	12.9	12.0	12.8	13.0	14.0	12.7
Soil temperature (5-cm depth) (° C)	10.4	11.1	11.9	11.7	10.3	10.3	10.8	10.9
Rainfall total[3] (mm)	246	250	177	219	576	620	477	422
θ (m^3 m^{-3}) (0-10-cm depth)	0.11	0.11	0.08	0.09	0.17	0.16	0.15	0.15
Q (μmol m^{-2} s^{-1})	396	396	421	396	413	410	442	418
D[1] (kPa)	0.80	0.83	0.94	0.88	0.86	0.84	1.04	0.92
GSL[2] (days)	136	141	134	147	143	160	155	162
R_n[3] (GJ m^{-2})	1.49	1.57	1.57	1.50	1.70	1.63	1.72	1.60

[1] Daytime average values.
[2] Growing season length (half-hourly values of air temperature and soil temperature (5-cm depth) > 0 and 1°C, respectively).
[3] Growing season total.

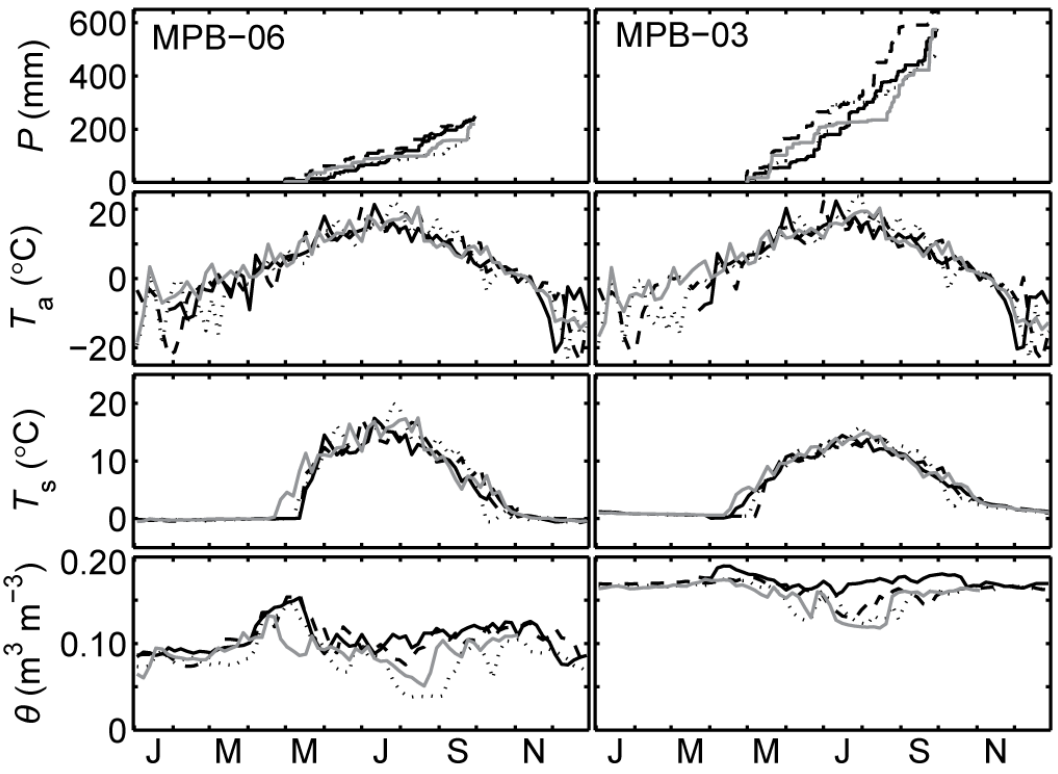

Figure 4.2. Cumulative totals of growing season precipitation (P) and 5-day-averages of air temperature at 26 m (T_a), soil temperature at 5-cm depth (T_s) and volumetric water content 0-30-cm depth (θ) for 2007 (black line), 2008 (dashed line), 2009 (dotted line) and 2010 (grey line).

4.3.2 Ecosystem respiration analysis: based on the nighttime approach

The logistic relationship between nighttime half-hourly measured R_e and T_s at the 5-cm depth (Eq. (1)) was significant (P <0.001) at both sites each year and varied significantly between successive years at both sites (Fig. 4.3 and Table 4-2) (P <0.001). To compare with the logistic equation, the response of R_e to T_s using the following exponential equation was also determined,

$$R_e = R_{e10} Q_{10}^{(T_s - 10)/10} \quad (7)$$

where R_{e10} and Q_{10} are the respiration rate at 10 °C and the relative increase in respiration per 10 °C increase in T_s, respectively (Table 4-2). The logistic equation (Eq. (1)) provided a slightly better fit than the exponential equation at both sites. R_e normalized to 10 °C (R_{e10}) calculated with the logistic equation was highest at MPB-06 and MPB-03 in 2008 and 2007, respectively, and lowest in 2010 at both sites. At MPB-06, when T_s was < 10 °C, the rate of increase in R_e with T_s was most rapid in 2010 and most gradual in 2008, but at higher T_s, R_e increased most rapidly in 2010. Although there was a smaller variation in the response of R_e to T_s between years at MPB-03, R_e was both highest for T_s < 5.0 °C and lowest for T_s > 10 °C in 2010. Over the four years the annual totals of R_e calculated using the logistic equation were approximately 15 and 5% lower than those calculated with the exponential equation at MPB-06 and at MPB-03, respectively. Q_{10} values (Eq. (7)) were between 2.70 and 2.93 at MPB-06 and 2.48 and 4.27 at MPB-03. There was no direct relationship observed between half-hourly R_e and θ. While θ has often been found to have a positive impact on R_e (Krishnan *et al.* 2006), the negative correlation between T_s and θ can make determining the nature of its influence problematic. When values of half-hourly measured R_e were normalized by dividing by modelled R_e (R_{eN}) and plotted against θ (Jassal *et al.* 2007), a significant relationship was observed at MPB-06 when θ was > 0.13 m^3 m^{-3} in 2007 and 2008 and >0.11 m^3 m^{-3} in 2009 and 2010, and for θ > 0.17 m^3 m^{-3} in 2007 at MPB-03 (Fig. 4.4). The rate of the increase in R_{eN} with θ was greatest at MPB-06 in 2008 and 2010. There was also a significant decline in R_{eN} for θ < 0.085 m^3 m^{-3} at MPB-06 in 2009.

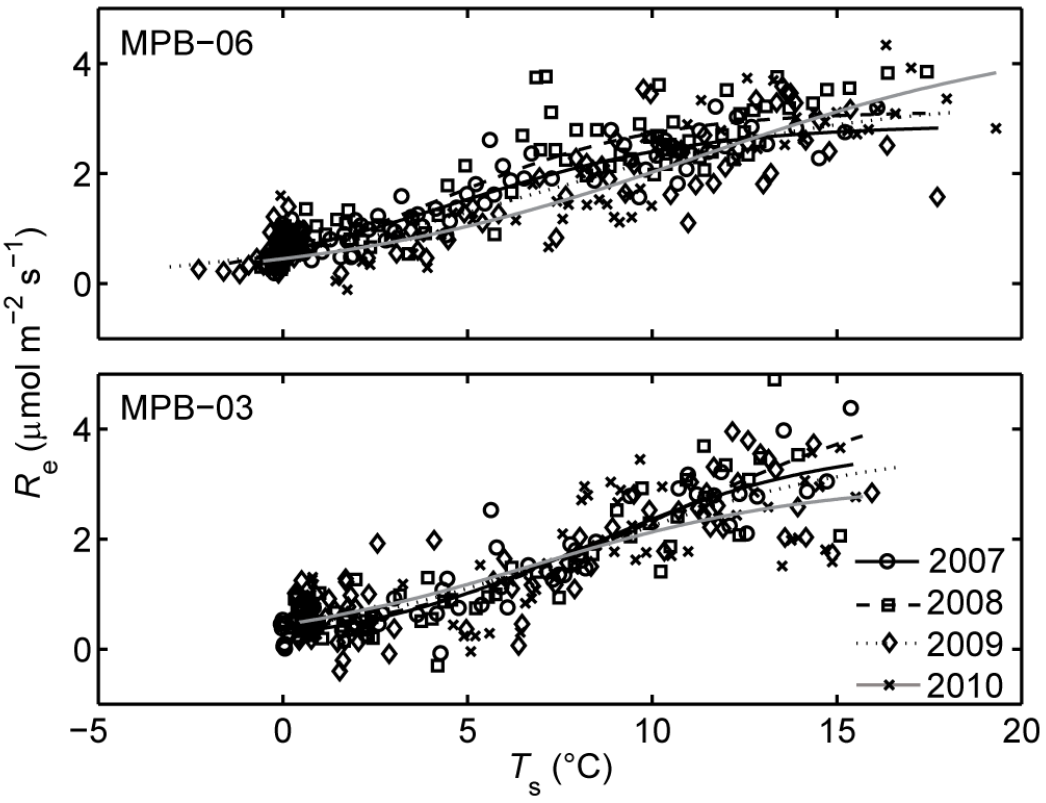

Figure 4.3. Relationship between annual measured half-hourly values of ecosystem respiration (R_e) and soil temperature at the 5-cm depth (T_s) (Eq.1). Values are bin averages of 10 measurements starting from the smallest value.

Table 4-2. Parameters from the annual relationships between half-hourly values of measured nighttime ecosystem respiration (R_e) and soil temperature at the 5-cm depth (T_s) and daily daytime derived respiration (R_{ed}) and daily daytime T_s. R_{10} values are ecosystem respiration at 10 °C. R_{tot} and R_{totd} are the annual totals (g C m^{-2}) of modelled ecosystem respiration using the nighttime and daytime methods.

	MPB-06				MPB-03			
	2007	2008	2009	2010	2007	2008	2009	2010
R_e (logistic)								
a	2.88	3.13	3.37	4.61	3.71	4.95	3.69	2.99
b	0.30	0.345	0.23	0.19	0.31	0.25	0.26	0.27
c	4.56	4.39	7.07	11.23	8.18	10.51	8.32	6.60
r^2	0.47	0.50	0.42	0.49	0.43	0.39	0.32	0.17
R_{e10}	2.40	2.73	2.22	2.03	2.36	2.32	2.24	2.15
R_e[1]	503	557	495	497	489	515	497	507
	(516, 481)[3]	(573, 538)	(538, 473)	(516,477)	(519, 462)	(554, 482)	(532, 473)	(549, 478)
R_e[2]	354	407	370	376	378	392	377	349
R_e (exponential)								
R_{e10}	2.06	2.28	1.92	1.80	2.04	2.08	1.95	1.90
Q_{10}	2.70	2.93	2.73	2.90	3.87	4.27	3.20	2.50
r^2	0.43	0.46	0.40	0.47	0.40	0.37	0.30	0.16
R_e[1]	566	660	600	560	518	530	529	545
R_{ed} (logistic)								
a	2.79	173	5.09	3.34	2.64	5.86	243.45	45.83
b	0.36	0.12	0.18	0.16	0.33	0.27	0.09	0.06
c	5.49	48.65	14.03	12.77	5.32	12.75	58.78	61.22
r^2	0.74	0.92	0.84	0.87	0.86	0.92	0.81	0.47
R_{ed10}	2.34	1.88	1.65	1.31	2.17	1.90	2.39	2.13
R_{ed}[1]	427	542	421	342	481	420	668	659
R_{ed}[2]	336	400	340	244	336	346	431	358

R_{e10} and R_{ed10} values are in μmol m^{-2} s^{-1}.
[1] Annual totals (g C m^{-2}).
[2]Growing season totals (1 May – 30 September) (g C m^{-2}).
[3] Numbers in parentheses are upper and lower 95% confidence intervals.

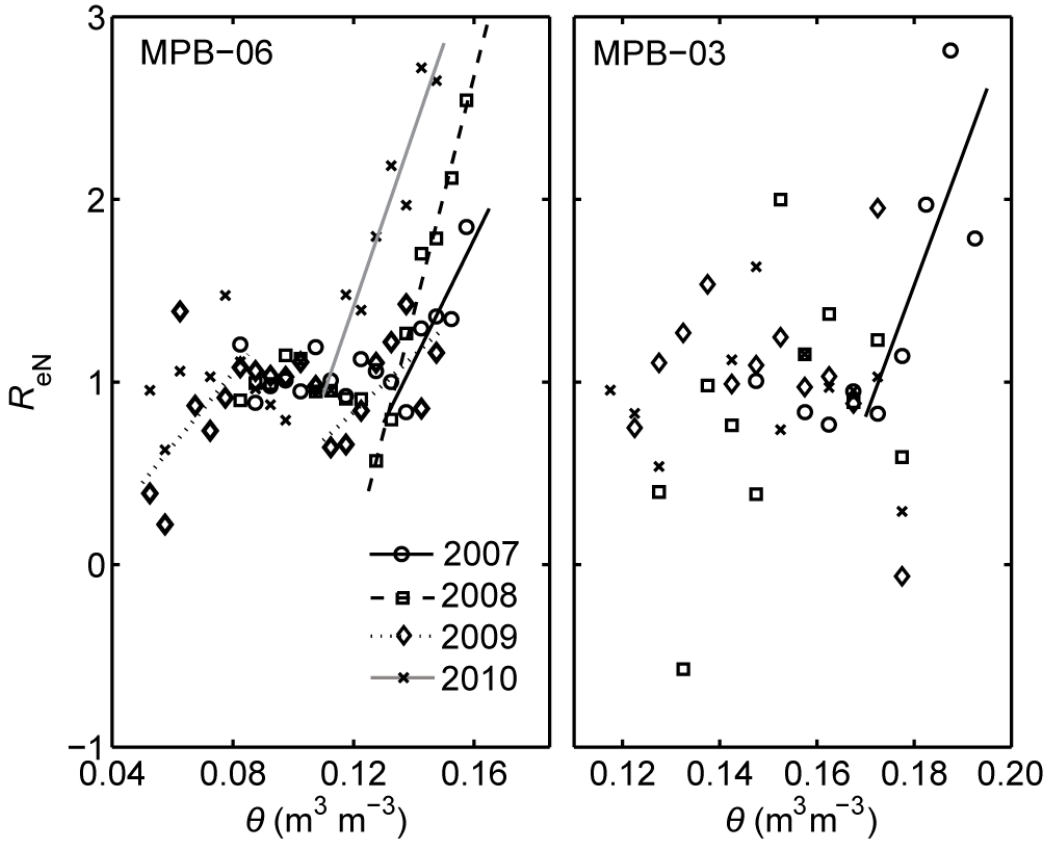

Figure 4.4. Relationship between annual measured half-hourly values of normalized ecosystem respiration (R_{eN} (measured R_e /modelled R_e) and soil volumetric water conent (θ). Data were sorted into 0.05 m^3 m^{-3} wide bins. The lines represent the linear regression (significant relationships): $R_{eN} = a\ \theta - b$. The a, b and r^2 parameters for MPB-06 were 33.47, -3.57 and 0.80 ($0.13 < \theta < 0.165$ m^3 m^{-3}) in 2007, 64.97, -7.72 and 0.98 ($0.12 < \theta < 0.165$ m^3 m^{-3}) in 2008, 15.42, -1.02 and 0.45 ($0.11 < \theta < 0.15$ m^3 m^{-3}) and 20.04, -0.55 and 0.30 ($0.05 < \theta < 0.085$ m^3 m^{-3}) in 2009 and 48.10, -4.36 and 0.91 ($0.11 < \theta < 0.15$ m^3 m^{-3}) in 2010, and were 71.86, -11.41 and 0.54 ($0.17 < \theta < 0.195$ m^3 m^{-3}) in 2007 for MPB-03.

4.3.3 Comparison of ecosystem respiration derived using the nighttime and daytime approaches

T_s explained most of the variation in R_{ed} for the majority of the years at both sites and the response varied significantly between successive years (P <0.001) (Fig. 4.5 and Table 4-2). The values of R_{ed10} were less than those of R_{e10} at both sites, with the exception of 2009 at MPB-03.

Over the four years, the ratio of the annual total ecosystem respiration obtained using the daytime approach to that obtained using the nighttime approach varied from 0.69 to 0.97 at MPB-06 and from 0.81 to 1.34 at MPB-03. As can be seen in Fig. 4.6, the agreement between R_e and R_{ed} was worse during the winter at both sites, with winter R_{ed} being about 35% lower and 100% higher in 2009 at MPB-06 and MPB-03, respectively.

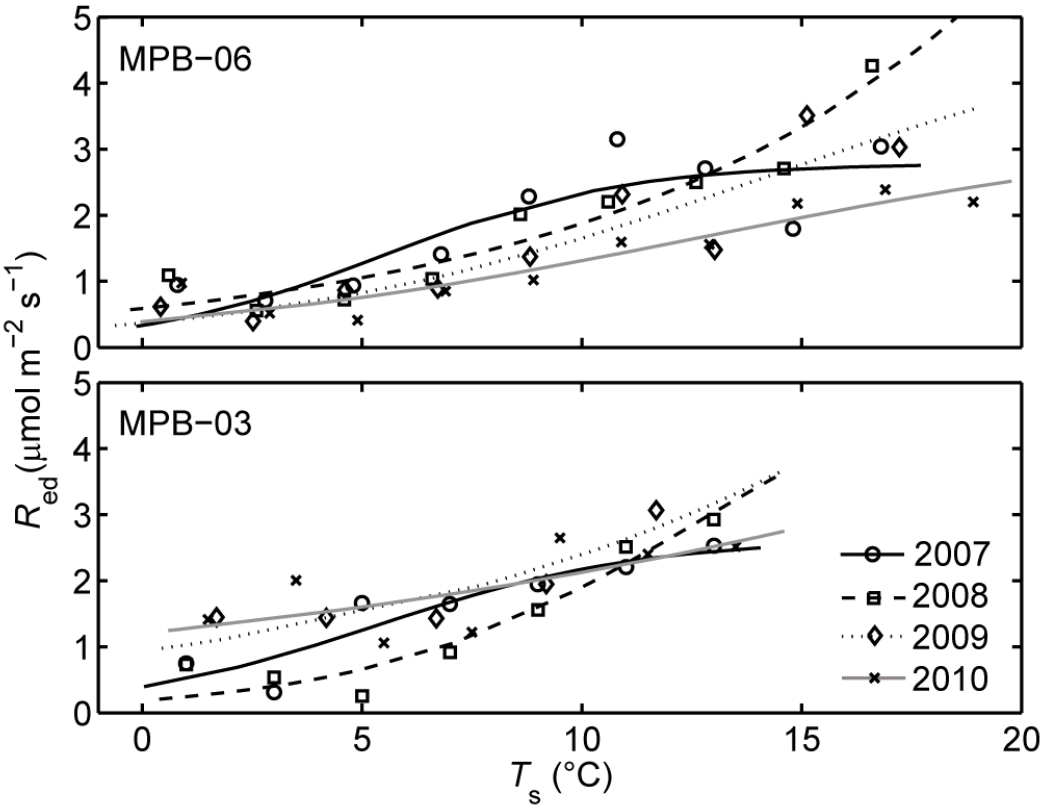

Figure 4.5. Relationship between annual 3-day daytime values of ecosystem respiration (R_{ed}) and daily daytime soil temperature at the 5-cm depth (T_s) (Eq. 1). Data were sorted into 2 °C wide bins.

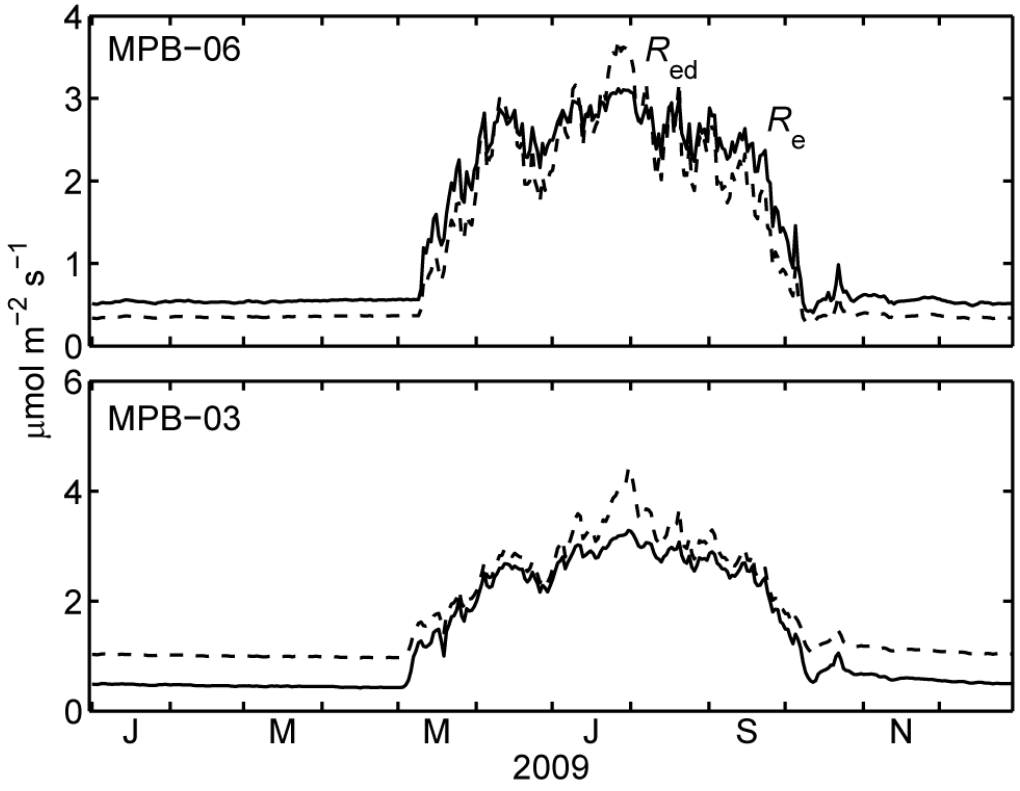

Figure 4.6. Daily values of ecosystem respiration calculated using the nighttime ecosystem respiration (R_e) and daytime ecosystem respiration (R_{ed}) approaches.

4.3.4 NEP and P_g light response analysis

At both sites Q was an important determinant of NEP and P_g (calculated using the nighttime R_e – T_s relationship) during the growing season (Eqs. (3) and (5); Table 4-3), with the relationship being significant each year at both sites and varying significantly between successive years (P <0.001). However, the proportion of NEP and P_g variance explained by Q was greater at MPB-06 than MPB-03. In every year, both P_{gmaxN} and P_{gmaxP} were higher at MPB-06 than MPB-03. At MPB-06, P_{gmaxN} increased from a low value in 2007 to similar values in 2008, 2009 and 2010, while P_{gmaxP} was highest in 2010. At MPB-03, both P_{gmaxN} and P_{gmaxP} were highest in 2008 and

lowest in 2010. The agreement between P_{gmaxN} and P_{gmaxP} was very good, especially at MPB-03 where the values were within 0.3 μmol m^{-2} s^{-1} of each other every year. Growing season values of α_N and α_P also agreed very well at both sites. As the PAR reflectivity was ~4.5 and 5% at MPB-06 and MPB-03, respectively, and given that some Q was absorbed by dead needles and tree boles, actual α values were likely slightly higher than those reported here. At both sites, the relationship between both daytime NEP and P_g and Q levelled off at a Q of approximately 1400 μmol m^{-2} s^{-1} (Fig. 4.7). In 2007 at Q values higher than this there was a significant reduction in NEP and P_g at both sites. There was also a slight decline in NEP at high Q in 2008, 2009 and 2010, more strongly at MPB-03 than MPB-06. Growing season R_{edN} values were highest in 2008 and lowest in 2010 at both sites.

Table 4-3. Regression parameters (Eqs.3 and 5) for the growing season (1 May -30 September) for net ecosystem production (NEP) and gross ecosystem photosynthesis (P_g) (nighttime method).

	MPB-06				MPB-03			
	2007	2008	2009	2010	2007	2008	2009	2010
NEP								
P_{gmaxN}[1]	6.69	7.64	7.62	7.46	6.29	7.51	6.77	6.00
α_N	0.021	0.024	0.023	0.019	0.029	0.037	0.031	0.029
R_{edN}[1]	2.36	2.47	2.19	1.80	2.56	2.79	2.37	2.22
r^2	0.29	0.31	0.32	0.38	0.19	0.16	0.16	0.14
P_g								
P_{gmaxP}[1]	6.97	8.04	8.63	9.59	6.07	7.39	6.93	6.02
α_P	0.021	0.026	0.024	0.022	0.026	0.034	0.031	0.030
r^2	0.34	0.30	0.34	0.43	0.16	0.14	0.14	0.14

Only measured daytime values (Q > 5 μmol m^{-2} s^{-1}) were used in the analysis.
[1] values are in μmol m^{-2} s^{-1}.

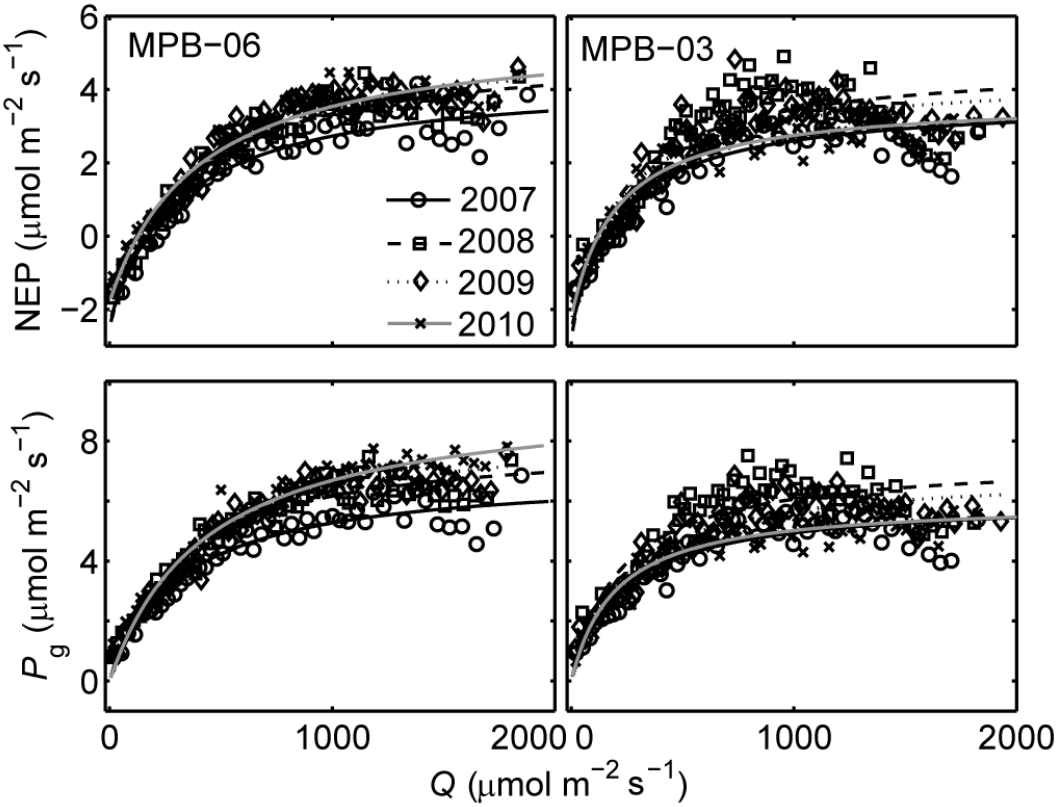

Figure 4.7. Relationship between daytime (Q > 5 μmol m^{-2} s^{-1}) measured net ecosystem production (NEP) and photosynthetically active radiation (Q) (Eq. 3) (upper panels) and gross ecosystem photosynthesis (P_g) (calculated using nighttime R_e –T_s relationships) and Q (Eq. 5) (lower panels) during the growing season. Symbols are bins of 50, starting with the smallest value while the lines have been fit to all the data (see Table 4-3 for parameter values).

4.3.5 Seasonal and annual NEP, R_e and GEP: based on the nighttime approach

Wintertime (1 January to 31 March and December) average daily NEP, which is comprised almost entirely of R_e, averaged -0.57, -0.49, -0.53 and -0.29 g C m^{-2} day^{-1} at MPB-06 and -0.45, -0.39, -0.49 and -0.42 g C m^{-2} day^{-1} at MPB-03, in 2007 to 2010, respectively (Fig. 4.8). Small rates of P_g did occasionally occur in the winter, mainly in March and especially in 2010, when T_a warmed above freezing. Higher rates of P_g typically began to occur in April, when daytime T_a

was often several degrees above freezing. During this time NEP was often quite high as R_e was limited because the ground was still covered with snow, keeping T_s just slightly above 0 °C. Once the snow melted and the ground surface was exposed, both T_s and R_e increased rapidly. During the mid-summer, maximum 5-day average NEP increased from 0.8 g C m^{-2} day^{-1} in 2007 to 1.4 g C m^{-2} day^{-1} in 2009 and 2010 at MPB-06. Maximum 5-day average P_g ranged from 3.6 in 2007 to 4.3 g C m^{-2} day^{-1} in 2010, while maximum 5-day R_e increased from 3.1 g C m^{-2} day^{-1} in 2007 to 3.8 g C m^{-2} day^{-1} in 2010. At MPB-03, maximum 5-day average NEP was 1.0, 1.8, 1.6 and 1.6 g C m^{-2} day^{-1} for 2007 to 2010, respectively, while maximum 5-day average P_g increased from 4.0 g C m^{-2} day^{-1} in 2007 to 5.3 g C m^{-2} day^{-1} in 2008 before falling to 4.7 and 4.2 g C m^{-2} day^{-1} in 2009 and 2010, respectively. 5-day average R_e ranged from a high of 3.4 g C m^{-2} day^{-1} in 2007 and 2010 to 3.8 g C m^{-2} day^{-1} in 2008.

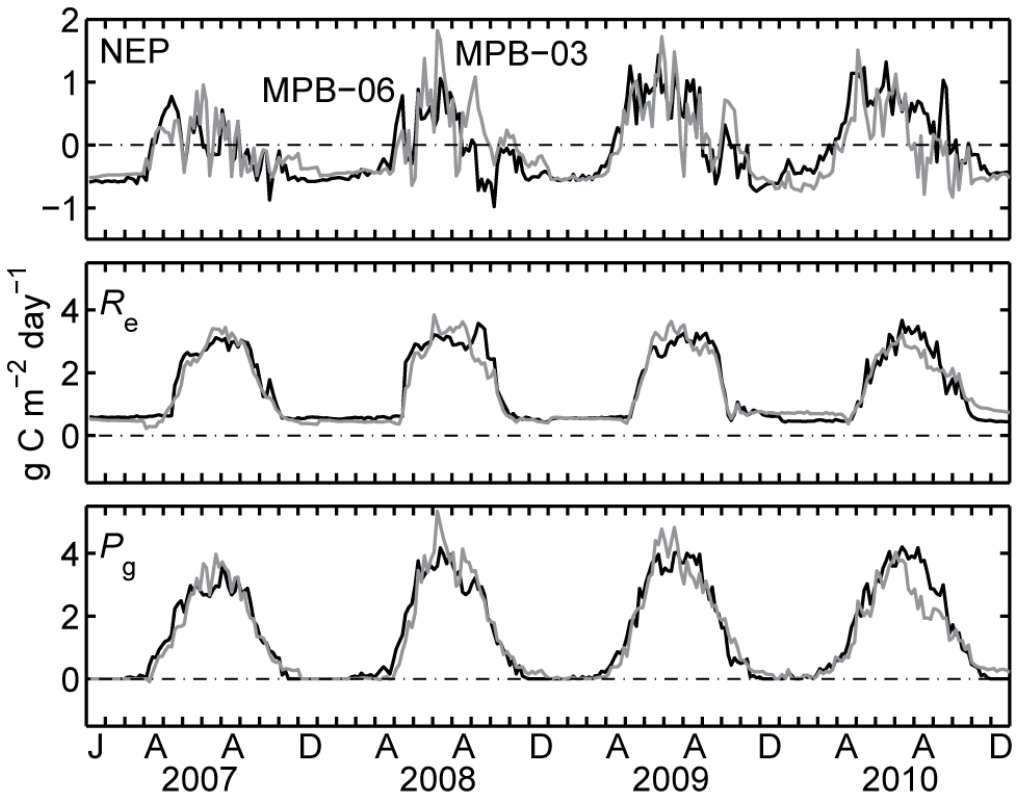

Figure 4.8. 5-day average net ecosystem production (NEP), ecosystem respiration (R_e) and gross ecosystem photosynthesis (P_g) (nighttime R_e-T_s relationship).

At both sites, annual total NEP increased each year from 2007, when both sites were small C sources, to 2009 when both were C sinks (Fig. 4.9; Table 4-4). In 2010 annual NEP diverged at the two sites, increasing considerably at MPB-06, but becoming negative at MPB-03. At MPB-06, the yearly increase in annual NEP was due to increasing photosynthesis, as annual P_g increased by 136 g C m^{-2} over the four years. Annual R_e was very stable at MPB-06, varying by just 36 g C m^{-2} over the four years. The relatively low annual R_e in 2010 helped lead to the high NEP that year. At MPB-03, annual P_g increased from 2007 to 2008, was stable in 2009 and then fell in 2010. At MPB-03, annual R_e was also very stable ranging from 487 to 513 g C m^{-2}

between 2007 and 2010. Annual P_g was similar at both sites each year, except in 2010 when P_g was much higher at MPB-06. Growing season NEP was highest in 2010 and 2009 at MPB-06 and MPB-03, respectively (Table 4-4). The growing season accounted for 88 and 87% of annual P_g and 74 and 75% of R_e at MPB-06 and MPB-03 over the four years.

Table 4-4. Annual and growing season totals of net ecosystem production (NEP), gross ecosystem photosynthesis (P_g) and ecosystem respiration (R_e) (nighttime method).

	MPB-06			MPB-03		
	NEP	P_g	R_e[1]	NEP	P_g	R_e[1]
Annual (g C m^{-2})						
2007	-81	440	521	-57	430	487
	(-71, -84)	(450, 435)	(527, 514)	(-43, -60)	(440, 423)	(496, 477)
2008	-58	499	557	3	516	513
	(-40, -60)	(516, 491)	(571, 537)	(15, -8)	(525, 498)	(526, 492)
2009	10	535	525	6	509	503
	(21, 6)	(578, 522)	(569, 508)	(13, -10)	(523,495)	(527, 490)
2010	64	576	512	-26	484	510
	(71, 59)	(571, 548)	(520, 496)	(-19, -38)	(492, 469)	(524, 491)
Growing season (g C m^{-2})						
2007	13	388	375	14	383	369
2008	32	448	416	65	463	398
2009	90	478	388	67	446	379
2010	98	487	389	38	398	360

[1] Annual and growing season totals of R_e differ from R_{etot} values in Table 4-2 in that these values include the effect of the moving-window parameter (Eq. 2).

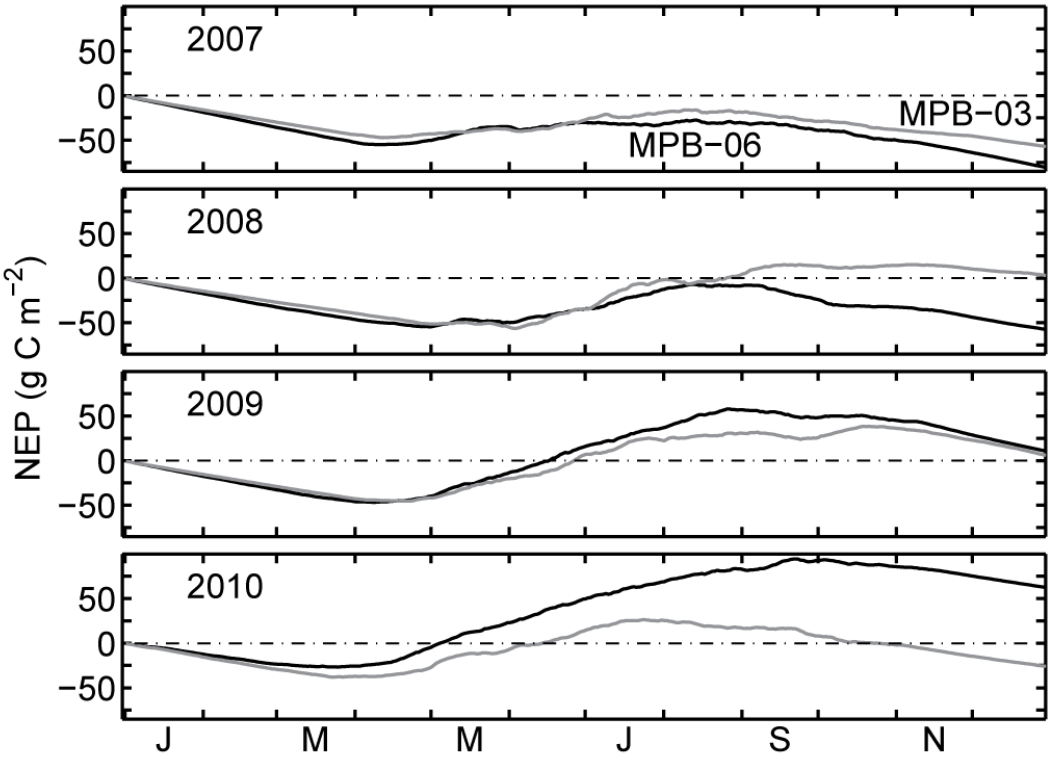

Figure 4.9. Annual courses of cumulative net ecosystem production (NEP) for 2007 to 2010.

4.3.6 Foliar CO_2 exchange

Growing season averages of net foliar photosynthesis (A_n) of un-attacked canopy trees (dbh > 9 cm, height > 1.3 m), small trees (< 9 cm dbh, > 1.3 m tall), seedlings/saplings (< 9 cm dbh, < 1.3 m tall) and broadleaf vegetation are shown in Fig. 4.10. Broadleaf A_n values were highest at both sites, having higher values than each of the conifer classes. At MPB-06, A_n for all conifer classes increased from 2007 to 2009 and each year the small trees had slightly higher A_n than the other two conifer classes. The small trees in 2009 had the highest average A_n (6.2 μmol m^{-2} s^{-1}) of all the conifer classes over the three years. Average broadleaf A_n was greatest in 2008 at 7.5 μmol m^{-}

^{2} s^{-1}, although the variation was high in all years. At MPB-03, A_n for all conifer classes was greatest in 2008 and lowest in 2010, and was similar among conifer classes each year. Broadleaf A_n was greatest in 2007 with an average of 7.5 μmol m^{-2} s^{-1} and was slightly lower in the following years, although in each year there was a large variation.

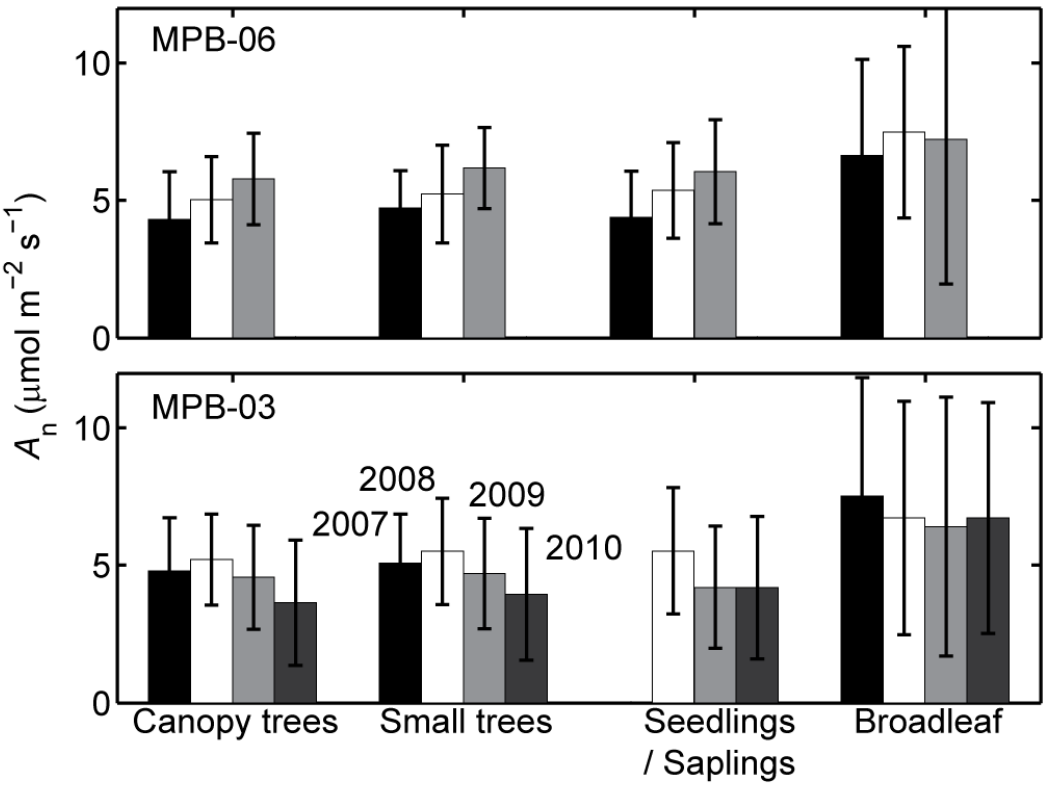

Figure 4.10. Growing season averages of foliar net photosynthesis (A_n) for canopy trees, small trees, seedling and saplings and broadleaf vegetation. Mean photosynthetically active radiation for all conifer and broadleaf measurements was 845 and 613 μmol m^{-2} s^{-1} in 2007, 752 and716 μmol m^{-2} s^{-1} in 2008 and 863 and 650 μmol m^{-2} s^{-1} in 2009 at MPB-06, and 1195 and 924 μmol m^{-2} s^{-1} in 2007, 922 and 869 μmol m^{-2} s^{-1} in 2008 and 1042 and 937 μmol m^{-2} s^{-1} in 2009, and 1009 and 774 in 2010 at MPB-03. Measurements were not made at MPB-06 in 2010 and were not made on seedlings and saplings at MPB-03 in 2007. Bars are standard deviations.

There was a significant relationship between Q and A_n for 2007-2009 at MPB-06 and in 2008 at MPB-03 (P <0.05) (Fig. 4.11), and there was a significant difference in the relationships

between years at MPB-06 (P <0.05). No measurements were made at MPB-03 in 2007 and 2009 when Q was < 220 μmol m^{-2} s^{-1} making it difficult to fit a light response curve to the data. Generally there was little response to increasing Q for Q > 500 μmol m^{-2} s^{-1}. There was much more variation in A_n at MPB-03, especially for Q > 1100 μmol m^{-2} s^{-1} when values were often low. At MPB-06, A_{max}, α_l, and R_{ld} were all highest in 2008.

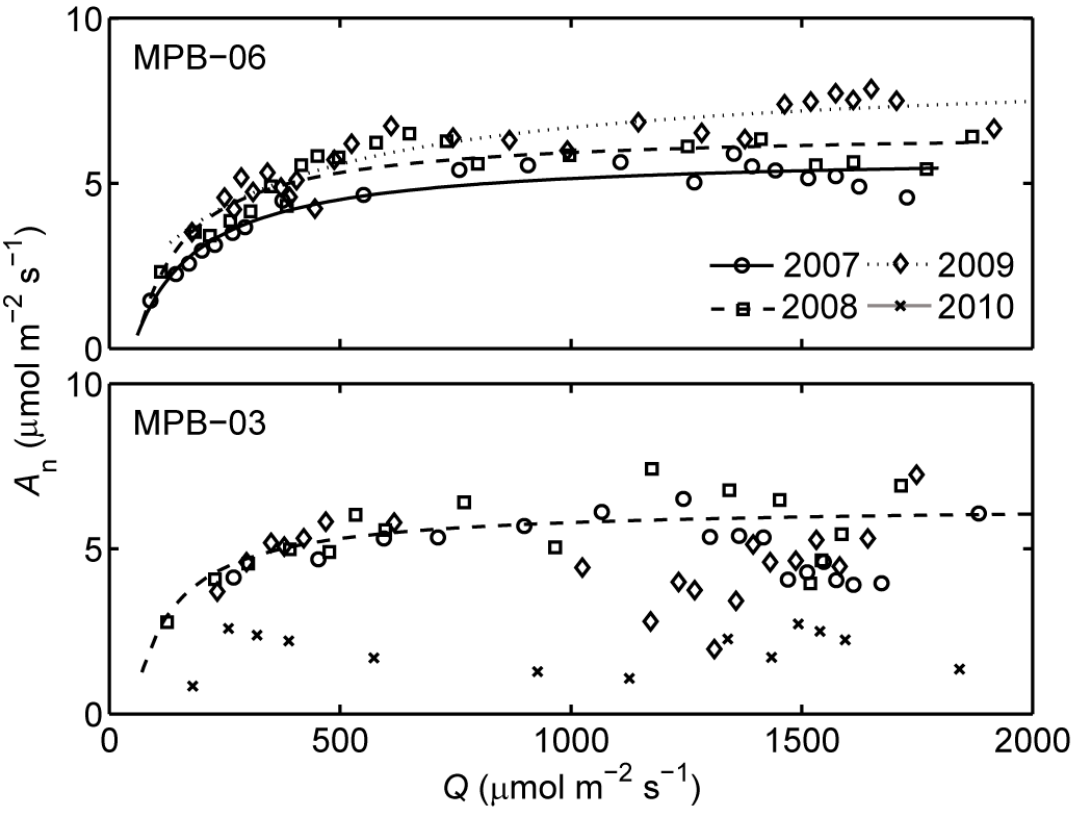

Figure 4.11. Relationship between net foliar photosynthesis (A_n) (half of the total needle area basis) and photosynthetically active radiation (Q) of (coniferous) trees. Values are binned averages of 10 starting with the smallest value. Leaf photosynthetic capacity (A_{max}), leaf quantum yield (α_l), leaf daytime respiration (R_{ld}) and the r^2 were 9.4 μmol m^{-2} s^{-1}, 0.11, 3.5 μmol m^{-2} s^{-1} and 0.53 in 2007, 14.2 μmol m^{-2} s^{-1}, 0.29, 7.6 μmol m^{-2} s^{-1} and 0.39 in 2008 and 7.5 μmol m^{-2} s^{-1}, 0.02, -1.0 μmol m^{-2} s^{-1} and 0.44 in 2009 at MPB-06 and 15.1 μmol m^{-2} s^{-1}, 0.42, 8.8 μmol m^{-2} s^{-1} and 0.21 in 2008 at MPB-03.

4.3.7 Water use efficiency

Monthly April to October water use efficiency (WUE = P_g / E), varied from a low of 0.9 g C (kg H_2O) $^{-1}$ in April 2008 to a high of 3.3 g C (kg H_2O) $^{-1}$ in August 2010 at MPB-06, and from 0.1 g C (kg H_2O) $^{-1}$ in April 2008 to 2.5 g C (kg H_2O) $^{-1}$ in October 2009 at MPB-03 (Fig. 4.12). At MPB-06, monthly E varied conservatively over the years (Chapter 3) causing interannual differences in monthly values of WUE to be dominated by changes in P_g. Growing season average WUE was lowest in 2007 at both sites due to low P_g. Maximum growing season WUE occurred in 2010 at MPB-06 and in 2008 and 2009 at MPB-03 (Table 4-5). At MPB-06, the highest monthly WUE, which occurred in August 2010, was a result of high P_g and a slightly low E due to drought. At MPB-03 variation in WUE was due to changes in both P_g and E. Maximum interannual variation in monthly E occurred in July and August, where values were low in 2009 (August) and 2010 (July and August) due to drought. In August 2009, P_g did not respond as strongly to drought as E did, resulting in a slightly high WUE, while the 2010 drought resulted in a decline in both P_g and E, leading to little change in WUE.

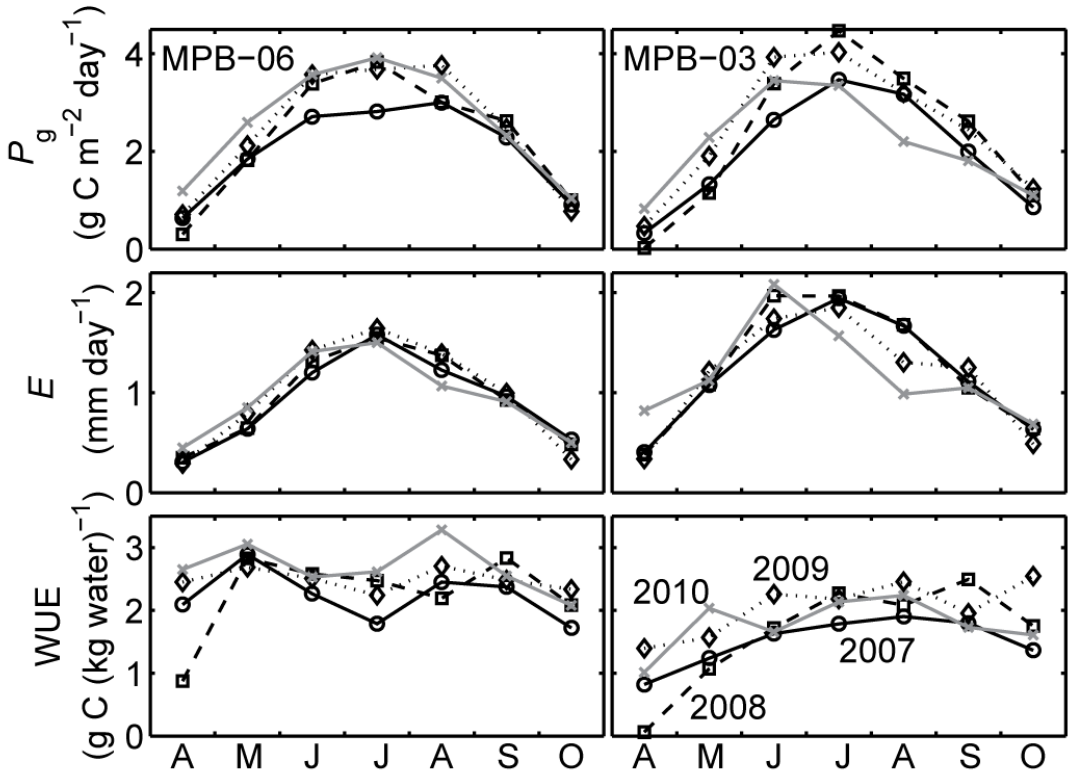

Figure 4.12. Monthly means of gross ecosystem photosynthesis (P_g), evapotranspiration (E), and water use efficiency (WUE).

Table 4-5. Growing season evapotranspiration (E), gross ecosystem photosynthesis (P_g) and water use efficiency (WUE).

	MPB-06				MPB-03			
	2007	2008	2009	2010	2007	2008	2009	2010
E (mm)	176	177	191	176	228	236	226	208
P_g (g C m^{-2})	388	448	478	487	383	463	446	399
WUE (g C (kg H_2O)$^{-1}$)	2.2	2.5	2.5	2.8	1.7	2.0	2.0	1.9

4.4 Discussion

4.4.1 The response of R_e, P_g and NEP to environmental variables

The larger proportion of R_e explained by T_s at MPB-06 than MPB-03 could be a result of the latter site having a high fraction of subalpine fir and white spruce and greater abundance of broadleaf vegetation whose respiratory response to T_s might differ from that of lodgepole pine, which dominates MPB-06. The logistic equation best described the response of R_e to T_s. Annual totals of R_e calculated using the exponential equation were unrealistically high due to an overestimation of R_e when T_s was high. This conclusion was reinforced by the annual totals of R_{ed} which were more similar to those of R_e calculated using the logistic equation than those calculated using the exponential equation. Q_{10} values obtained using the exponential equation were higher at MPB-03 than MPB-06 every year, except 2010, showing a greater temperature sensitivity of respiration at that site. The decline in Q_{10} in 2009 and 2010 at MPB-03 was likely due to low θ. Normalized R_e (R_{eN}) showed that at MPB-06, once θ exceeded the threshold of approximately 0.12 m^3 m^{-3}, R_e increased rapidly with θ. In 2009, when growing season θ reached the lowest values over the four years at MPB-06, R_{eN} declined significantly, showing a clear water limitation of R_e. At MPB-03, θ only had a positive influence on R_{eN} in 2007, the year θ reached the highest values, suggesting that had similar values been reached in the following years, R_{eN} would also have responded positively.

At MPB-06, annual totals of R_{ed} were consistently less than, and outside the 95% confidence intervals of the R_e annual totals, with the exception of 2008 when the totals agreed well (Table 4-2). At MPB-03, annual totals of R_{ed} were also outside the bounds of the R_e annual totals 95% confidence intervals (below in 2008 and above in 2009 and 2010), except in 2007 when the agreement was very good. Much of the disagreement between the two approaches at

MPB-06 occurred during the winter. When restricted to the growing season, the agreement between the two approaches was much better, with the exception of 2010 when the R_e annual total was considerably higher than the R_{ed} annual total. At MPB-03, the agreement between growing season totals of R_e and R_{ed} was also much better than that for the annual totals. Still, the annual totals of R_{ed} seemed unreasonably high at MPB-03 in 2009 and 2010. While the flux footprint of daytime and nighttime measurements was quite different (the 80% cumulative flux contour was typically 400 and 1500 m upwind of the tower along the longitudinal axis of the footprint during the daytime and nighttime, respectively (Appendix 2)), since the stand is relatively homogenous this would not be expected to have much effect on NEP measurements. Although the r^2 of the fit between binned values of R_{ed} and T_s was high at MPB-03, the average number of 3-day R_{ed} values included in the analysis over the four years was only 32, adding some uncertainty in the R_{ed} estimates. Annual totals of R_{ed} may have been less than those of R_e because leaf respiration has been found to be lower during the day than night due to light inhibition of dark respiration (Brooks and Farquhar 1985); however, annual totals of R_{ed} were not consistently lower at MPB-03. The good agreement between P_{gmaxN} and P_{gmaxP} indicates values of R_{eN} were similar to daytime R_e obtained from the nighttime approach and provides confidence in using the nighttime approach to estimate daytime R_e.

While the response of R_e to T_s and θ did vary over the years at both sites, it is difficult to attribute this to the impact of the beetle attack. At MPB-06, the ratio of autotrophic (R_a) to heterotrophic (R_h) respiration might have fallen as a result of the dramatic reduction in the fraction of un-attacked trees from 2007. However, the strong growth of the surviving trees may have had the opposite effect of increasing R_a. Although no measures of R_a and R_h were made, their relative contributions to R_e can be estimated (Amiro *et al.* 2010). Assuming that R_a is about

55% of P_g, as various studies have suggested (e.g., Waring *et al*. 1998; Jassal *et al.* 2007), annually, R_a comprised 46, 50, 56 and 61% of R_e from 2007 to 2010 at MPB-06, and 49, 55, 56 and 52% of R_e at MPB-03 from 2007 to 2010. The increase in the contribution of R_a to R_e at MPB-06 seems likely, given the large increase in P_g over the four years.

At MPB-06, the steady annual increase in P_g resulted in the corresponding increase in NEP. At MPB-03, variation in NEP was also mainly controlled by changes in P_g, as R_e varied little over the four years. The decline in P_g in 2010 at MPB-03 corresponded to a significant reduction in $P_{g\text{maxN}}$ and $P_{g\text{maxP}}$. The mid-growing season drought in 2009 and 2010 limited P_g at MPB-03. As reported in Chapter 3, at MPB-03 there was a significant drop in canopy conductance during the growing season drought in 2009, and there was an even greater drop in 2010 as the stomata closed to limit water loss. The resulting decline in P_g and NEP during late July and August 2009 and 2010 can be seen in Fig. 4.8. At a 78-year old jack pine (*Pinus Banksiana*) stand in Saskatchewan, Kljun *et al.* (2006) observed little effect of a three year drought on P_g owing to the trees being able to access water at deep soil depths. During the growing season at MPB-03, θ increased slightly (~1.5%) from the 10 cm to 20 cm soil depths and then decreased 0.5% from the 20 to 50 cm soil depth. At MPB-06, although θ was also lowest during the mid-growing season droughts in 2009 and 2010, there was not a significant impact on P_g. Perhaps the different response to drought observed at the two sites is due to the trees being almost exclusively lodgepole pine at MPB-06, which are known to be drought tolerant, while at MPB-03 a large fraction of the remaining live trees were subalpine fir and white spruce, which are more vulnerable to drought (Bigler *et al.* 2007). Also, although θ was always higher at MPB-03, the soil coarse fragment content is 70% by volume, compared to 35%

at MPB-06, much of which is composed of large rocks, resulting in a smaller quantity of fine soil from which tree roots could extract water.

In 2010, the spring months of April and May were extremely productive at MPB-06 (Fig. 4.13). It was during this period when NEP in 2010 mainly differed from the previous years, although NEP was also high during April-May in 2009. During this period T_a was high in 2010, averaging 6.5 °C, compared to the 5.0 °C average of the previous three years. T_a was particularly high between 14-20 April 2010, when maximum daytime values were between 15 and 22 °C, compared to the same period in 2007-2009 when T_a never reached 14 °C. Similar values of spring T_a at MPB-03 also led to a high April-May NEP in 2009 and 2010. Spring growing conditions are thus an important determinant of the annual C balance of these sites.

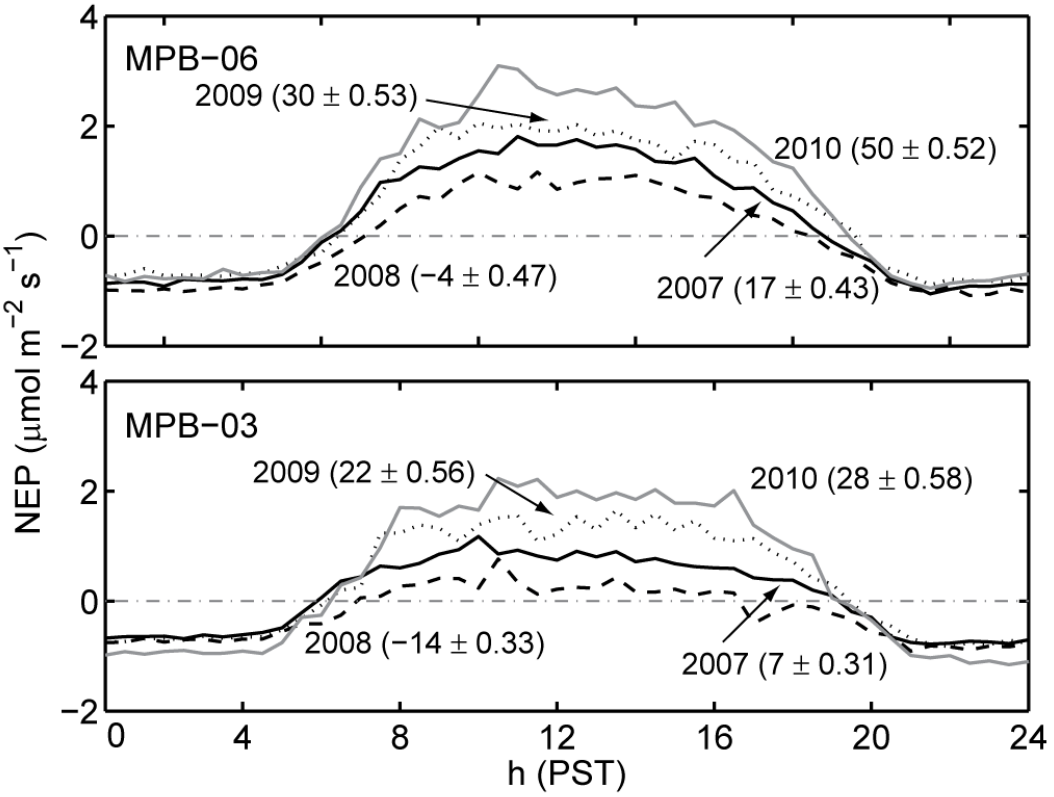

Figure 4.13. Ensemble-average half-hourly values of net ecosystem production (NEP) for April and May. Values in parentheses are the total NEP (g C m^{-2}) and standard deviation for the two-month period.

4.4.2 Foliar CO_2 exchange

Foliar gas-exchange measurements provided an important validation of the tower-based NEP measurements and helped determine how the different components of the stand responded to the beetle attack. A_n followed similar trends as P_g at both sites. Although the sampling frequency was much lower than the continuous tower-based measurements, there was a clear annual increase in average A_n of all conifer classes at MPB-06, comparing well with the growing season P_g trends. Both the EC and foliar gas-exchange data showed the surviving MPB-06 canopy trees,

as well as younger sub-canopy trees and broadleaf vegetation increasing photosynthesis as the stand recovered. At MPB-03, the trend in A_n was also similar to that of growing season P_g, although the decline in 2009 in A_n was greater than that observed with the EC data. This discrepancy in 2009 could be due to the low sampling frequency of A_n. Average A_n from the broadleaf vegetation, which was much more developed at MPB-03, was relatively stable during the four years; however, the large variation in the measurements made it difficult to determine any trends. The light response analysis of conifer A_n also agreed well with that of P_g at MPB-06, both showing an increase in the photosynthetic response to Q. Conifer α_L values were greater than values of α_P in 2007 and 2009 at MPB-06 but the agreement between the two was good in 2008 at both sites. In 2008 at MPB-03, conifer A_n showed a strong response to Q, and values were the highest of the three years, agreeing well with P_g. A relationship between A_n and Q could not be determined for 2007, 2009 and 2010. During these years there was high variability in the measurements, but like P_g, A_n decreased at high Q. The low A_n values in 2010 were a result of measurements only being made during the drought period. Thus, both the foliar gas-exchange and NEP measurements showed the effects of water stress on photosynthesis during the 2010 growing season at MPB-03.

4.4.3 Interannual variability in WUE

While the surviving trees increased their P_g, the total amount of water transpired and evaporated from the ground surface remained rather constant, leading to an increase in growing season WUE at MPB-06. At MPB-03, growing season E followed the same as pattern as P_g, increasing from 2007 to 2008, and then decreasing in 2009 and 2010, although the magnitude of change was much less. The higher WUE at MPB-06 was due to the lower E and generally higher P_g

compared to MPB-03. During the drought in August 2009, WUE remained relatively high at MPB-03 because P_g remained similar to previous August values despite the drop in E in 2009, while in 2010, both P_g and E decreased in July and August, probably because the drought was more severe that year, keeping WUE similar to non-drought years. This reduction in both E and P_g in response to water stress is not surprising given that trees must optimize the trade off between C uptake and transpiration (Beer *et al*. 2009) and has been frequently observed in other forests (Ponton *et al*. 2006; Barr *et al*. 2007). As the stomata close to restrict water loss, a reduction in photosynthesis also occurs.

4.4.4 Recovery of NEP following MPB attack

Both these stands demonstrated resilience to MPB attack. The prediction that stands in the central interior of BC would quickly become C sources and remain so for several years (Kurz *et al.* 2008) has not proven to be true at these two contrasting sites. While MPB-06 was a moderate C source for the first two years following attack, the surviving trees and vegetation showed increased vigour in the third and fourth years resulting in an increase in P_g and as a result, NEP. At MPB-03, measurements were not made until the fourth year following attack, and that year the site was also a moderate C source. While NEP was slightly positive in the following two years, the site became, as a result of drought, a C source in the seventh year (2010) after attack. While the fraction of healthy trees at MPB-06 decreased rapidly in 2007 and 2008, and almost the entire canopy had been killed at MPB-03, the surviving trees and vegetation appeared to benefit from a reduction in competition for nutrients and soil water and an increase in Q reaching the lower levels of the canopy crown and understory (Mitchell *et al.* 1983; Waring and Pitman 1985). At MPB-06, between 2007 (prior to any loss of needles) and 2009, direct and diffuse solar

radiation transmissivity increased from 29 to 44% and 41 to 51%, respectively, while at MPB-03 solar radiation transmissivity increased from 48% in 2007 to 60% in 2009. Evidence suggests that in beetle-attacked stands nutrient levels remain similar to undisturbed stands, increasing the availability for surviving trees (Knight *et al.* 1991). In a clearcutting and thinning by girdling experiment where 40% of the trees were left alive, Knight *et al.* (1991) found that a thinned lodgepole stand retained nitrates and total nitrogen, while there was large decrease in both in the clearcut stand. Although the drop in NEP at MPB-03 appeared to be a response to drought, it may be the start of a longer term trend if the initial growth release following attack slows down. However, Berg *et al.* (2006) found that in spruce forests which had experienced spruce-beetle (*Dendroctonus rufipennis*) outbreaks, the surviving trees experienced rapid growth for decades, until the canopies began to close and competition suppressed annual growth. Thus, it seems likely the trees at these two sites will continue to experience high rates of growth until the canopies begin to close and there is more competition for light and nutrients. In both stands most of the killed trees remained standing. However, as tree fall increases and the stems, branches and roots begin to decompose, there could be a significant increase in R_e, negating any increase in NEP from the enhanced P_g. Tree fall began to occur in 2008 and 2009 (5 and 6 years after attack) and many more fell in 2010 at MPB-03, while at MPB-06 a few trees began to fall in 2009 and 2010, but not in great numbers. In Oregon, trees killed by the beetle began falling five years following death and 50% had fallen after nine years and 90% after 14 years (Mitchell and Preisler 1998). Busse (1994) reported that MPB-killed trees in Oregon took a minimum of 26 years for 50% of their wood biomass to decompose after they had fallen. They did not detect any decomposition in tree boles that were either standing or elevated above the soil surface by branches, but once the boles were in contact with the soil surface the decay was relatively rapid.

Similarly, Brown *et al.* (1998) reported wind-thrown lodgepole pine boles in a subalpine forest in Colorado persist on the forest floor for many decades with most of their volume intact. A 10-year-old clearcut (CC-97; see Chapter 2 for site details) located 1 km from MPB-06 still had dead branches and coarse woody debris on the ground left from when the site was harvested a decade ago, indicating the decay of the dead organic material could take many years at both these sites.

4.5 Conclusion

The logistic equation provided a consistently better description of the response of R_e to T_s than the exponential equation at both sites. The good agreement between α_N and α_P and between P_{gmaxP} and P_{gmaxN} indicates that P_g and daytime R_e derived using the nighttime approach, were realistic estimates of the true fluxes. Foliar gas-exchange measurements of A_n validated tower-based estimates of P_g, with both increasing from 2007 to 2009 at MPB-06, and decreasing in response to drought in 2009 and 2010 at MPB-03. The annual C balance of both sites was strongly affected by spring NEP.

The recovery of NEP from beetle attack occurred much quicker than hypothesized, with MPB-06 and MPB-03 reaching C neutrality in the third year and fifth years after attack. The increase in NEP at both sites was due to an increase in P_g. Furthermore, NEP and foliar gas-exchange measurements indicated a significant increase in the photosynthetic capacity of both stands. In neither stand was there a significant increase in R_e as it recovered, indicating slow decomposition of the large amounts dead organic matter. In both stands solar radiation transmissivity increased significantly from 2007 to 2009. As these stands continue to open, more light will reach the lower tree crowns and understory, enhancing the growth of the surviving

trees, seedlings and saplings, as well as shrubs, mosses and lichens. Thus, the future C status of these sites depends on the interplay between the individual responses of P_g and R_e.

5. Conclusions

This study has examined four years of EC data from two MPB-attacked lodgepole pine stands in the central interior of BC. The differences in the characteristics of MPB-06 and MPB-03, and the several years over which NEP was measured provided insight on the spatial and temporal effects of the MPB outbreak, and the effect of climate variability on C and water cycling in these stands. The major findings of this study are presented below.

1. The recovery of NEP from beetle attack occurred much more quickly than hypothesized at the onset of this study. MPB-06 was a moderate C source for the first two years following attack, but became a sink in the third and fourth years. MPB-03 was a moderate C source in the fourth year, had a slight C uptake in the fifth and sixth years, and, due to drought, was a C source in the seventh year after attack. The increase in NEP was due to an increase in P_g from the canopy trees that survived the beetle attack, the seedlings and saplings and other understory vegetation at MPB-06, and from the canopy subalpine fir, the sub-canopy trees, the seedlings and saplings and the other understory vegetation at MPB-03. The increase in the photosynthetic capacity (P_{gmax}) of the surviving vegetation was likely a response to the canopy transmissivity of solar radiation, as well as a reduction in competition for nutrients and soil water due to tree mortality. Foliar gas-exchange measurements of A_n for canopy trees, small trees, seedling and saplings and broadleaf vegetation confirmed the increase in the P_{gmax} observed at stand level P_g, although the response varied among the stand classes.

2. Ecosystem respiration did not increase significantly in both stands, indicating slow decomposition of the large amounts of dead organic matter. Although R_e did increase from a low in 2007 at MPB-03, there was not a significant increase in R_{e10} values between 2007 and 2010. While R_h is expected to increase in the coming years due to the decomposition of the fallen dead needles and dead roots, the killed trees will likely take several years to fall and decades to decompose. Studies in Oregon and Colorado suggest that R_h will likely increase following tree fall at MPB-06 and MPB-03 due to an increase in decomposition. The increase could be small, but could be sustained for many years. Autotrophic respiration could also increase if the growth release of the stands continues, which would further augment R_e.

3. Drought had a major effect on NEP at MPB-03 in 2009 and 2010, as shown by reductions in both P_g and A_n. The reduction in P_g was likely due to a reduced C uptake by the subalpine fir and white spruce trees, which are drought sensitive and made up a significant fraction of the live trees at MPB-03. MPB-06 did not show the same response to drought as MPB-03, likely because it contained few non-lodgepole pine trees. As a result, if less drought tolerant trees, such as subalpine fir and white spruce become more dominant than prior to the beetle outbreak, drought could play a more important role in determining the future C balance of these stands.

4. The good agreement between P_{gmaxP} and P_{gmaxN} indicated that values of P_g and daytime R_e derived using the nighttime approach were likely representative of the actual fluxes.

Furthermore, the relatively good agreement between growing season totals of R_e and R_{ed} also provided confidence in the use of the nighttime approach to determine daytime R_e.

5. NEP measurements at the site harvested in 1997 (CC-97) showed that ten years following harvesting this replanted stand remained a growing-season C source. As expected, the site harvested in 2005 (CC-05) was a significant C source during the 2007 growing season, since the stand was clearcut harvested only two years earlier. The comparison of growing season NEP from the harvested and beetle-attacked stands showed the potential consequence of the increase in forest harvesting approved by the British Columbia Ministry of Forests and Range following the beetle outbreak, which could lead to much higher C emissions over extended time periods than if stands were allowed to recover naturally.

6. Increased *E* from the growth release of the surviving trees and understory vegetation at MPB-06 and MPB-03 appeared to compensate for a reduction in *E* due to the tree mortality from beetle attack. The result was little change in *E* at either of these sites between 2007 and 2010. It had been predicted that the MPB outbreak in BC would significantly alter transpiration rates and thus induce changes in annual water yields. During August and September 2006, shortly after MPB-06 was first attacked, *E* was slightly less than the following year when 50% of the trees had been killed (Appendix 2). As evidence that the August and September 2006 measurements were representative of pre-attack stand conditions, foliar photosynthesis and stomatal conductance of attacked

trees were not significantly different than those of the non-attacked trees sampled in late August 2006 (Table 2-3). However, θ was low in 2006, which may have limited E.

7. The growing season WD showed both stands were water limited, even though a high proportion of the trees were dead, implying that the remaining live vegetation was consuming a significant amount of water. The variability in the WD between 2007 and 2009 was small due to little year-to-year variability in values of E_{pot} and E during the 15 May – 30 September period. There was no apparent increase in D_r in both stands due to the beetle attack; however, if E had been greater at MPB-03 prior to the beetle attack, it is possible D_r has increased since then. There is no evidence for this at MPB-06, as E did not change significantly in the first two years following the first year of attack, and in August and September 2006, shortly after MPB-06 was first attacked, E was not higher than the following year. The large difference in growing season D_r between sites was due to the similarly large difference in P, with MPB-03 having both higher P and D_r.

Both of these stands were still in the early stages of recovery from beetle attack when NEP measurements were made. The future C balance of these stands will depend on the individual responses of R_e and P_g. A modelling study by Kurz *et al*. (2008) predicted the cumulative impact of the BC MPB outbreak from 2000-2020 to be a net loss 270 Tg C (36 g C m^{-2} $year^{-1}$) over 374, 000 km^2 of forest, due to a decrease in net primary production ($P_n = P_g - R_a$) and an increase in R_h. That study predicted both the direct effects of the beetle and the additional salvage harvesting response to reduce P_n from pre-outbreak values of 440 g C m^{-2} $year^{-1}$ to 391 g C m^{-2} $year^{-1}$ during the 2015-2018 period, after which, P_n was predicted to recover. R_h was

predicted to increase from 408 to 424 g C m^{-2} $year^{-1}$ during the 2003 to 2007 period. These values were calculated for a much larger area than the stand level at which NEP measurements were made, and thus the two results are not directly comparable; however, they predict a different trend than observed in this study. MODIS-based estimates of P_g (at a 1-km spatial resolution) over the BC MPB infestation area from 2002 to 2005 showed a decrease of 10-20% from pre-outbreak values (Coops and Wulder 2010), with more severely attacked stands experiencing a greater reduction. While NEP measurements were not made at MPB-06 or MPB-03 prior to the beetle attack, measurements made at MPB-06 shortly after the site was first attacked in 2006 were not significantly different than those made during the same period in 2007, when 50% of the trees were dead (Fig. 2-3). While it is possible the stands studied here were not representative of the MPB infestation region as a whole, it is important to note that while the EC technique provides a direct measure of NEP at the stand level, MODIS-based estimates of P_g are made at a coarser spatial and temporal resolution and rely on an algorithm relating P_g to the fraction of absorbed Q through a radiation-use conversion efficiency term which depends on vegetation type (Running *et al.* 2004, Coops and Wulder 2010). The contrasts in the results of these approaches highlight the importance of continuing EC measurements at the stand scale, as well as using other techniques, such as MODIS-based and modelling approaches, to study the landscape-scale recovery from the beetle outbreak.

The results presented here indicate that the future C status of these forests is not yet clear and a number of research areas can be indentified which merit further work. EC measurements should continue at both of these stands to continue to track the recovery. The trees will fall in the coming years, which will increase the canopy transmissivity of solar radiation and enhance forest re-growth, as well as add a large supply of dead organic matter to the soil surface. Soil

respiration measurements in both control and root exclusion plots (e.g., Gaumont-Guay *et al*. 2008) would enable R_e to be partitioned into R_h and R_a and the response of R_h to the influx of dead organic matter (roots, needles, branches and boles) to be tracked. Foliar gas-exchange measurements should also be continued as they can play an important role in determining the recovery of various components of the stand, as demonstrated in this study. Finally, EC measurements made in healthy stands as well as other beetle-attacked stands that differ from these two, but are still representative of the infestation region, would provide important information on the variability of the impacts of the outbreak and help advance our understanding of the processes involved in this type of forest disturbance.

References

Allard V, Ourcival JM, Rambal S, Joffre R, Rocheteau A. 2008. Seasonal and annual variation of carbon exchange in an evergreen Mediterranean forest in southern France. Global Change Biology 14, 714-725.

Amiro BD, Ian MacPherson J, Desjardins RL, Chen JM, Liu J. 2003. Post-fire carbon dioxide fluxes in the western Canadian boreal forest: Evidence from towers, aircraft and remote sensing. Agricultural and Forest Meteorology 115(1-2):91-107.

Amiro BD, Barr AG, Black TA, Iwashita H, Kljun N, McCaughey JH, Morgenstern K, Murayama S, Nesic Z, Orchansky AL, and others. 2006. Carbon, energy and water fluxes at mature and disturbed forest sites, Saskatchewan, Canada. Agricultural and Forest Meteorology 136(3-4):237-251.

Amiro BD, Barr AG, Barr JG, Black TA, Bracho R, Brown M, Chen J, Clark KL, Davis KJ, Desai AR, and others. 2010. Ecosystem carbon dioxide fluxes after disturbance in forests of North America. Journal of Geophysical Research. 115:G00K02.

Arain MA, Black TA, Barr AG, Griffis TJ, Morgenstern K, Nesic Z. 2003. Year-round observations of the energy and water vapour fluxes above a boreal black spruce forest. 17(18):3600.

Aukema BH, Carroll AL, Zhu J, Raffa KF, Sickley TA, Taylor SW. 2006. Landscape level analysis of mountain pine beetle in British Columbia, Canada: Spatiotemporal development and spatial synchrony within the present outbreak. Ecography 29: 427-441.

Baldocchi DD, Vogel CA, Hall B. 1997. Seasonal variation of carbon dioxide exchange rates above and below a boreal jack pine forest. Agricultural and Forest Meteorology 83(1-2):147-170.

Baldocchi D, Kelliher FM, Black TA, Jarvis P. 2000. Climate and vegetation controls on boreal zone energy exchange. Global Change Biology 6(S1):83.

Baldocchi, DD. 2003. Assessing the eddy covariance technique for evaluating carbon dioxide exchange rates of ecosystems: past, present and future. Global Change Biology 9, 479-492.

Baldocchi DD 2008. Breathing of the terrestrial biosphere: lessons learned from a global network of carbon dioxide flux measurement systems. Australian Journal of Botany 56, 1–26.

Barr AG, Black TA, Hogg EH, Kljun N, Morgenstern K, Nesic Z. 2004. Inter-annual variability in the leaf area index of a boreal aspen-hazelnut forest in relation to net ecosystem production. Agricultural and Forest Meteorology 126(3-4):237-255.

Barr AG, Morgenstern K, Black TA, McCaughey JH, Nesic Z. 2006. Surface energy balance closure by the eddy-covariance method above three boreal forest stands and implications for the measurement of the CO_2 flux. Agricultural and Forest Meteorology 140(1-4):322-337.

Barr AG, Black TA, Hogg EH, Griffis TJ, Morgenstern K, Kljun N, Theede A, Nesic Z. 2007. Climatic controls on the carbon and water balances of a boreal aspen forest, Global Change Biology 13(3):561-576.

Beer C, Ciais P, Reichstein M, Baldocchi D, Law BE, Papale D, Soussana J-, Ammann C, Buchmann N, Frank D, Gianelle D, Janssens IA, Knohl A, Köstner B, Moors E, Roupsard O, Verbeeck H, Vesala T, Williams CA and Wohlfahrt G. 2009. Temporal and among-site variability of inherent water use efficiency at the ecosystem level. Global Biogeochemical Cycles 23(2):GB2018.

Berg EE, David Henry J, Fastie CL, De Volder AD, Matsuoka SM. 2006. Spruce beetle outbreaks on the Kenai Peninsula, Alaska, and Kluane National Park and Reserve, Yukon Territory: Relationship to summer temperatures and regional differences in disturbance regimes. Forest Ecology and Management 227(3):219-232.

Bergeron O, Margolis HA, Black TA, Coursolle C, Dunn AL, Barr AG, Wofsy SC. 2007. Comparison of carbon dioxide fluxes over three boreal black spruce forests in Canada. Global Change Biology 13(1):89-107.

Bernier PY, Bartlett P, Black TA, Barr A, Kljun N, McCaughey JH. 2006. Drought constraints on transpiration and canopy conductance in mature aspen and jack pine stands. Agricultural and Forest Meteorology 140(1-4):64-78.

Bigler C, Gavin DG, Gunning C, Veblen TT. 2007. Drought induces lagged tree mortality in a subalpine forest in the Rocky Mountains. Oikos 116(12):1983-1994.

Black TA, Hartog G, Neumann HH, Blanken PD, Yang PC, Russell C, Nesic Z, Lee X, Chen SG, Staebler R, Novak MD. 1996. Annual cycles of water vapour and carbon dioxide fluxes in and above a boreal aspen forest. Global Change Biology 2, 219-229.

Blanken P.D, T.A. Black, H.H. Neumann, G. Den Hartog, P.C. Yang, Z. Nesic, R S, W. Chen, M.D. Novak. 1998. Turbulent flux measurements above and below the overstory of a boreal aspen forest. Boundary-layer Meteorology 89(1):109 .

Bond-Lamberty B, Peckham SD, Ahl DE, Gower ST. 2007. Fire as the dominant driver of central Canadian boreal forest carbon balance. Nature 450(7166):89-92.

Bonneville M, Strachan IB, Humphreys ER, Roulet NT. 2008. Net ecosystem CO_2 exchange in a temperate cattail marsh in relation to biophysical properties. Agricultural and Forest Meteorology 148(1):69-81.

British Columbia Ministry of Forests and Range. 2006. The State of British Columbia's Forests 2006. Forest Practices Branch, Ministry of Forests and Range, Victoria, BC. 182 p.

British Columbia Ministry of Environment. 2008. Mountain pine beetle infestation: Hydrological impacts.http://www.llbc.leg.bc.ca/public/pubdocs/bcdocs/445817/finishdownloaddocument.pdf.

British Columbia Ministry of Forests and Range. 2010. Facts about B.C.'s mountain pine beetle. http://www.for.gov.bc.ca/hfp/mountain_pine_beetle/Updated-Beetle-Facts_Mar2010.pdf

Brooks A and Farquhar G. 1985. Effect of temperature on the CO_2/O_2 specificity of ribulose-1,5-bisphosphate carboxylase/oxygenase and the rate of respiration in the light. Planta 165(3):397-406.

Brown M, Black TA, Nesic Z, Foord VN, Spittlehouse DL, Fredeen AL, Grant NJ, Burton PJ, Trofymow JA. 2010. Impact of mountain pine beetle on the net ecosystem production of lodgepole pine stands in British Columbia. Agricultural and Forest Meteorology 150(2):254-264.

Brown, P.M., W.D. Shepperd, S.A. Mata, and D.L.McClain. 1998. Longevity of windthrown logs in a subalpine forest of central Colorado. Canadian Journal of Forest Research 28:932–936.

Brümmer C, Black TA, Jassal RS, Grant NJ, Spittlehouse DL, Chen B, Nesic Z, Amiro BD, Arain MA, Barr AG, Bourque CPA, Coursolle C, Dunn AL, Flanagan LB, Humphreys ER, Lafleur PM, Margolis HA, McCaughey JH, Wofsy SC. 2010. Effects of climate and vegetation type on evapotranspiration and water use efficiency in Canadian forest, peatland and grassland ecosystems. (*Submitted to Agricultural and Forest Meteorology*).

Burba GG, Anderson DJ, Xu L, McDermitt DK. 2006. Additional term in the Webb–Pearman–Leuning correction due to surface heating from an open-path gas analyzer. EOS Transactions AGU 87, C12A-03.

Burba GG, McDermitt DK, Grelle A, Anderson DJ, Xu L. 2008. Addressing the influence of instrument surface heat exchange on the measurements of CO_2 flux from open-path gas analyzers. Global Change Biology 14: 1854-1876.

Busse MD. 1994. Downed bole-wood decomposition in lodgepole pine forests of central Oregon. Soil Science Society of America Journal. 58(1):221-227.

Campbell GS, Norman JM. 1998. An Introduction to Environmental Biophysics. Springer, New York.

Chen J, Chen W, Liu J, Cihlar J, Gray S. 2000. Annual carbon balance of Canada's forests during 1895–1996. Global Biogeochemical Cycles 14(3):839-849.

Clark KL, Skowronski N, Hom J. 2010. Invasive insects impact forest carbon dynamics. Global Change Biology 16(1):88-101.

Coates KD, DeLong C, Burton PJ, Sachs DL. 2006. Abundance of secondary structure in lodgepole pine stands affected by the mountain pine beetle. Report for the Chief Forester, May 2006. Bulkley Valley Centre for Natural Resources Research and Management. Unpublished report, 17 pp.

Cook B, Bolstad P, Martin J, Heinsch F, Davis K, Wang W, Desai A, Teclaw R. 2008. Using light-use and production efficiency models to predict photosynthesis and net carbon exchange during forest canopy disturbance. Ecosystems 11(1):26-44.

Egginton VN, Spittlehouse DL, Brown M. 2008. Determining solar and longwave radiation in mountain pine beetle attacked stands using hemispherical photography. BC Ministry of Forests and Range, Prince George, BC. Draft interim report.

Ensminger I, Sveshnikov D, Campbell DA, Funk C, Jansson S, Lloyd J, Shibistova O, Öquist G. 2004. Intermittent low temperatures constrain spring recovery of photosynthesis in boreal Scots pine forests. Global Change Biology 10: 995-1008.

Friedlingstein P, Houghton RA, Marland G, Hackler J, Boden TA, Conway TJ, Canadell JG, Raupach MR, Ciais P, Le Quere C. 2010. Update on CO2 emissions. Nature Geoscience 3(12):811-812.

Gaumont-Guay D, Black TA, Barr AG, Jassal RS, Nesic Z. 2008. Biophysical controls on rhizospheric and heterotrophic components of soil respiration in a boreal black spruce stand. Tree Physiology 28(2):161-171.

Gorte RW, Ramseur JL. 2008. Forest carbon markets: potentials and drawbacks, CRS Report for Congress, RL 34560. Washington, DC, Congressional Research Service.

Grelle A and Burba G. 2007. Fine-wire thermometer to correct CO_2 fluxes by open-path analyzers for artificial density fluctuations. Agricultural and Forest Meteorology 147(1-2):48-57.

Griffis TJ, Black TA, Morgenstern K, Barr AG, Nesic Z, Drewitt GB, Gaumont-Guay D, McCaughey JH. 2003. Ecophysiological controls on the carbon balances of three southern boreal forests. Agricultural and Forest Meteorology 117(1-2):53-71.

Gu L, Falge EM, Boden T, Baldocchi DD, Black TA, Saleska SR, Suni T, Verma SB, Vesala T, Wofsy SC, Xu LK. 2005. Objective threshold determination for nighttime eddy flux filtering. Agricultural and Forest Meteorology 128(3-4):179-197.

Heath R, and Alfaro RI, 1990. Growth response of a Douglas-fir/lodgepole pine stand after thinning of lodgepole pine by the mountain pine beetle, Journal of Entomological Society of British Columbia 87, 16–21.

Hélie JF, Peters DL, Tattrie KR, Gibson JJ. 2005. Review and synthesis of potential hydrologic impacts of mountain pine beetle and related harvesting activities in British Columbia. Natural Resources Canada, Canadian Forest Service, Pacific Forestry Centre, Mountain Pine Beetle Initiative Working Paper 2005-23, Victoria, BC.

Hilker T, Coops NC, Coggins SB, Wulder MA, Brown M, Black TA, Nesic Z, Lessard D. 2009. Detection of foliage conditions and disturbance from multi-angular high spectral resolution remote sensing. Remote Sensing of Environment 113(2):421-434.

Humphreys ER, Black TA, Ethier GJ, Drewitt GB, Spittlehouse DL, Jork E-, Nesic Z, Livingston NJ. 2003. Annual and seasonal variability of sensible and latent heat fluxes above a coastal Douglas-fir forest, British Columbia, Canada. Agricultural and Forest Meteorology 115(1-2):109-125.

Humphreys ER, Black TA, Morgenstern K, Li Z, Nesic Z. 2005. Net ecosystem production of a Douglas-fir stand for 3 years following clearcut harvesting. Global Change Biology 11, 1-15.

Ilvesniemi H, Pumpanen J, Duursma R, Hari P, Keronen,P, Kolari P, Kulmala M, Mammarella I, Nikinmaa E, Rannik Ü, Pohja T, Siivola E, Vesala T. 2010. Water balance of a boreal Scots pine forest. Boreal Environment Research. 15: 375–396.

IPCC. 2007. Climate Change 2007: Synthesis Report. Contribution of Working Groups I, II and III to the Fourth Assessment Report of the Intergovernmental Panel on Climate Change [Core Writing Team, Pachauri, R.K and Reisinger, A. (eds.)]. IPCC, Geneva, Switzerland, 104 pp.

Jarvis PG, McNaughton KG. 1986. Stomatal control of transpiration. Advances in Ecological Research 15:1-49.

Jassal RS, Black TA, Cai T, Morgenstern K, Li Z, Gaumont-Guay D, Nesic Z. 2007. Components of ecosystem respiration and an estimate of net primary productivity of an intermediate-aged Douglas-fir stand. Agricultural and Forest Meteorology 144(1-2):44-57.

Jassal RS, Black TA, Spittlehouse DL, Brümmer C, Nesic Z. 2009. Evapotranspiration and water use efficiency in different-aged Pacific Northwest Douglas-fir stands. Agricultural and Forest Meteorology 149(6-7):1168-1178.

Kelliher FM, Leuning R, Schulze ED.1993. Evaporation and canopy characteristics of coniferous forests and grasslands. Oecologia 95(2):153-163-163.

Kelliher FM, Lloyd J, Arneth A, Byers JN, McSeveny TM, Milukova I, Grigoriev S, Panfyorov M, Sogatchev A, Varlargin A, Ziegler W, Bauer G, Schulze ED. 1998. Evaporation from a central Siberian pine forest. Journal of Hydrology 205(3-4):279-296.

Kidston J, Brümmer C, Black T, Morgenstern K, Nesic Z, McCaughey J, Barr A. 2010. Energy balance closure using eddy covariance above two different land surfaces and implications for CO_2 flux measurements. Boundary-Layer Meteorology 136(2):193-218.

Kirschbaum MUF, Keith H, Leuning R, Cleugh HA, Jacobsen KL, van Gorsel E, Raison RJ. 2007. Modelling net ecosystem carbon and water exchange of a temperate eucalyptus delegatensis forest using multiple constraints. Agricultural and Forest Meteorology 145(1-2):48-68.

Kljun N, Black T, Griffis T, Barr A, Gaumont-Guay D, Morgenstern K, McCaughey J, Nesic Z. 2006. Response of net ecosystem productivity of three boreal forest stands to drought. Ecosystems 9(7):1128-1144-1144.

Knight DH, Yavitt JB, Joyce GD. 1991. Water and nitrogen outflow from lodgepole pine forest after two levels of tree mortality. Forest Ecology and Management 46(3-4):215-225.

Kormann R, Meixner FX. 2001. An analytic footprint model for neutral stratification. Boundary-Layer Meteorology 99:207–224.

Kowalski S, Sartore M, Burlett R, Berbigier P, Loustau D. 2003. The annual carbon budget of a French pine forest (Pinus pinaster) following harvest. Global Change Biology 9, 1051-1065.

Krishnan P, Black TA, Grant NJ, Barr AG, Hogg E(H, Jassal RS, Morgenstern K. 2006. Impact of changing soil moisture distribution on net ecosystem productivity of a boreal aspen forest during and following drought. Agricultural and Forest Meteorology 139(3-4):208-223.

Krishnan P, Black TA, Barr AG, Grant NJ, Gaumont-Guay D, Nesic Z. 2008. Factors controlling the interannual variability in the carbon balance of a southern boreal black spruce forest. Journal of Geophysical Research 113, D09109, doi:10.1029/2007JD008965.

Kurz WA, Apps MJ. 1999. A 70-year retrospective analysis of carbon fluxes in the Canadian forest sector. Ecological Applications 9: 526-547.

Kurz WA, Stinson G, Rampley GJ, Dymond CC, Neilson ET. 2008. Risk of natural disturbances makes future contribution of Canada's forests to the global carbon cycle highly uncertain. Proceedings of the National Academy of Sciences 105(5):1551-1555.

Lafleur PM, Humphreys ER. 2008. Spring warming and carbon dioxide exchange over low Arctic tundra in central Canada. Global Change Biology 14: 740-756.

Lambers H, Chapin FS, Pons TL. 1998. Plant Physiological Ecology. Springer-Verlag, New York, 591 pp.

Lee X, Black TA. 1993. Atmospheric turbulence within and above a Douglas-fir stand. Part II. Eddy fluxes of sensible heat and water vapour. Boundary-Layer Meteorology. 64:369-389.

Lemmen DS, Warren FJ, Lacroix J and Bush E, editors. 2008. From impacts to adaptation: Canada in a changing climate 2007. Government of Canada, Ottawa, ON. 448 p.

Massman WJ and Lee X. 2002. Eddy covariance flux corrections and uncertainties in long-term studies of carbon and energy exchanges. Agricultural and Forest Meteorology, 113(1-4):121-144.

McNaughton KG, Jarvis PG, 1983. Predicting effects of vegetation changes on transpiration and evaporation. In: Kozlowski TT (Ed.), Water Deficits and Plant Growth, Academic Press, New York, pp. 1–47.

Meidinger D, Pojar J, 1991. Ecosystems of British Columbia. Research Branch, Ministry of Forests, 31 Bastion Square, Victoria BC, 330pp.

Mitchell RG, Waring RH, Pitman GB. 1983. Thinning lodgepole pine increases tree vigor and resistance to mountain pine beetle. Forest Science 29:204-211.

Mitchell RG, Preisler HK. 1998. Fall rate of lodgepole pine killed by the mountain pine beetle in Central Oregon. Western Journal of Applied Forestry 13: 23-26.

Mkhabela MS, Amiro BD, Barr AG, Black TA, Hawthorne I, Kidston J, McCaughey JH, Orchansky AL, Nesic Z, Sass A, Shashkov A, Zha T. 2009. Comparison of carbon dynamics and water use efficiency following fire and harvesting in Canadian boreal forests. Agricultural and Forest Meteorology 149(5):783-794.

Monson RK, Sparks JP, Rosenstiel TN, Scott-Denton LE, Huxman TE, Harley PC, Turnipseed AA, Burns SP, Backlund B, Hu J. 2005. Climatic influences on net ecosystem CO_2 exchange during the transition from wintertime carbon source to springtime carbon sink in a high-elevation, subalpine forest. Oecologia 146: 130-147.

Monson RK, Lipson DL, Burns SP, Turnipseed AA, Delany AC, Williams MW, Schmidt SK. 2006. Winter forest soil respiration controlled by climate and microbial community composition. Nature 439, 711-714.

Monteith, JL, Unsworth MH. 2008. Principles of Environmental Physics. 2nd Edition, Elsevier, Amsterdam, 304 pp.

Morgenstern K, Andrew Black T, Humphreys ER, Griffis TJ, Drewitt GB, Cai T, Nesic Z, Spittlehouse DL, Livingston NJ. 2004. Sensitivity and uncertainty of the carbon balance of a pacific northwest Douglas-fir forest during an el Niño/La niña cycle. Agricultural and Forest Meteorology 123(3-4):201-219.

NFI. 2004. Canada's National Forest Inventory - Ground Sampling Guidelines. Retrieved April 10, 2008, from https://nfi.nfis.org/documentation/ground_plot/Gp_guidelines_v4.1.pdf.

O'Halloran TL, Law BE, Wang Z, Barr JG, Schaaf C, Brown M, Goulden M, Fuentes JD, Black TA, Engel V. 2010. Albedo offsets or enhances CO_2 warming from natural disturbances. (*submitted to Nature Geoscience*).

Oishi A, Oren R, Novick K, Palmroth S, Katul G. 2010. Interannual invariability of forest evapotranspiration and its consequence to water flow downstream. Ecosystems 13(3):421-436-436.

Phillips N and Oren R. 2001. Intra- and inter-annual variation in transpiration of a pine forest. Ecological Applications; Ecological Applications 11(2):385-396.

Ponton S, Flanagan LB, Alstad KP, Johnson BG, Morgenstern K, Kljun N, Black TA, Barr AG. 2006. Comparison of ecosystem water-use efficiency among Douglas-fir forest, aspen forest and grassland using eddy covariance and carbon isotope techniques. Global Change Biology 12(2):294-310.

Potts DF. (1984). Hydrologic impacts of a large-scale mountain pine beetle (*Dendroctonus Ponderosae* Hopkins) epidemic. Journal of the American Water Resources Association, 20: 373–37.

Priestley CHB, Taylor RJ. 1972. On the assessment of surface heat flux and evaporation using large-scale parameters. Monthly Weather Review. 100:81-82.

Pypker TG, Fredeen AL. 2002. Ecosystem CO_2 flux over two growing seasons for a sub-boreal clearcut 5 and 6 years after harvest. Agricultural and Forest Meteorology 114: 15–30.

Pypker TG, Fredeen AL. 2003. Below ground CO_2 efflux from cut blocks of varying ages in sub-boreal British Columbia. Forest Ecology and Management 172: 249-259.

Rannik Ü, Altimir N, Raittila J, Suni T, Gaman A, Hussein T, Hölttä T, Lassila H, Latokartano M, Lauri A, Natsheh A, Petäjä T, Sorjamaa R, Ylä-Mella H, Keronen P, Berninger F, Vesala T, Hari P, Kulmala M. 2002. Fluxes of carbon dioxide and water vapour over scots pine forest and clearing. Agricultural and Forest Meteorology 111(3):187-202.

Reid DEB, Silins U, Lieffers VJ. 2006. Sapwood hydraulic recovery following thinning in lodgepole pine. Annals of Forest Science. 63(4):329-338.

Rex J, Dubé S. 2009. Hydrologic effects of mountain pine beetle infestation and salvage-harvesting operations. 2009. Mountain Pine Beetle Working Paper 2009-05. Natural Resources Canada, Canadian Forest Service, Pacific Forestry Centre, Victoria, BC.

Richardson AD and Berlyn GP. 2002. Changes in foliar spectral reflectance and chlorophyll fluorescence of four temperate species following branch cutting. Tree Physiology 22(7):499-506.

Roberts J. 1983. Forest transpiration: A conservative hydrological process? Journal of Hydrology 66(1-4):133-141.

Running SW, Nemani RR, Heinsch FA, Zhao M, Reeves M, Hashimoto H. 2004. A continuous satellite-derived measure of global terrestrial primary production. Bioscience 54(6):547-560.

Safranyik L, Wilson WR. 2006. The mountain pine beetle: A synthesis of biology, management, and impacts on lodgepole pine. Natural Resources Canada, Canadian Forest Service, Pacific Forestry Centre, Victoria, B.C.

Seip D, Jones ES. 2007. Response of woodland Caribou to partial retention logging of winter ranges attacked by mountain pine beetle. Annual Progress Report. FSP Project M07-5049. BC Ministry of Forest and Range, Prince George, BC, Canada. 21 p.

Shuttleworth WJ and Calder IR. 1979. Has the Priestley-Taylor equation any relevance to forest evaporation? Journal of Applied Meteorology; Journal of Applied Meteorology 18(5):639-646.

Smirnova E, Bergeron Y, Brais S. 2008. Influence of fire intensity on structure and composition of jack pine stands in the boreal forest of Quebec: Live trees, understory vegetation and dead wood dynamics. Forest Ecology and Management 255(7):2916-2927.

Taneda H and Tateno M. 2005. Hydraulic conductivity, photosynthesis and leaf water balance in six evergreen woody species from fall to winter. Tree Physiology 25(3):299-306.

Tanner CB, and Thurtell GW. 1969. Anemoclinometer Measurements of Reynolds Stress and Heat Transport in the Atmospheric Boundary Layer. Research and Development Technical Report ECOM-66-G22F. University of Wisconsin, Madison, Wisconsin.

Taylor SW, Carroll AL, Alfaro RE, and Safranyik L. 2006. Forest, climate and mountain pine beetle outbreak dynamics in Western Canada. *In* The mountain pine beetle: a synthesis of biology, management, and impacts on lodgepole pine. Natural Resources Canada, Canadian Forest Service, Pacific Forestry Centre, Victoria, BC. pp. 67-94.

Uunila L, Guy B, Pike R. 2006. Hydrologic effects of mountain pine beetle in the interior pine forests of British Columbia. Streamline watershed management bulletin 9(2):1-6.

van Gorsel E, Leuning R, Cleugh HA, Keith H, Kirschbaum MUF, Suni T. 2008. Application of an alternative method to derive reliable estimates of nighttime respiration from eddy covariance measurements in moderately complex topography. Agricultural and Forest Meteorology 148(6-7):1174-1180.

Veblen TT, Hadley KS, Reid MS, Rebertus AJ. 1991. The response of subalpine forests to spruce beetle outbreak in Colorado. Ecology 72, 213-231.

Walton A, Hughes J, Eng M, Fall A, Shore T, Riel B, Hall P. 2008. BC Ministry of Forest and Range, Provincial-Level Projection of the Current Mountain Pine Beetle Outbreak. (http://www.for.gov.bc.ca/hre/bcmpb/BCMPB.v5.BeetleProjection.Update.pdf),Victoria.

Waring RH and Pitman GB. 1985. Modifying lodgepole pine stands to change susceptibility to mountain pine beetle attack. Ecology 66(3):889-897.

Waring RH, Landsberg JJ, Williams M. 1998. Net primary production of forests: A constant fraction of gross primary production? Tree Physiology 18(2):129-134.

Webb EK, Pearman GI, Leuning R. 1980. Correction of flux measurements for density effects due to heat and water vapour transfer. Quarterly Journal of the Royal Meteorological Society 106(447):85-100.

Westfall J, Ebata T. 2009. 2009 Summary of forest health conditions in British Columbia. Forest Practices Branch, British Columbia Ministry of Forests and Range.

Wilson K, Goldstein A, Falge E, Aubinet M, Baldocchi D, Berbigier P, Bernhofer C, Ceulemans R, Dolman H, Field C, Grelle A., Ibrom A, Law BE, Kowalski AS, Meyers TP, Moncrieff JB, Monson RK, Oechel W, Tenhunen J.D, Valentini R, Verma SB. 2002. Energy balance closure at FLUXNET sites. Agricultural and Forest Meteorology 113(1-4):223-243.

Winkler R, Boon S, Zimonick B, Baleshta K. 2010. Assessing the effects of post-pine beetle forest litter on snow albedo. Hydrological Processes 24(6):812.

Yang RC. 1998. Foliage and stand growth responses of semimature lodgepole pine to thinning and fertilization. Canadian Journal of Forest Research 28: 1794–1804.

Zha T, Barr AG, van der Kamp G, Black TA, McCaughey JH, Flanagan LB. 2010. Interannual variation of evapotranspiration from forest and grassland ecosystems in western Canada in relation to drought. Agricultural and Forest Meteorology 150(11):1476-1484.

Appendix 1: Comparison of evapotranspiration in the year of and the year following the MPB attack at MPB-06

Average daily *E* measured by eddy covariance during 1 August to 30 September was 1.91 and 2.24 mm day^{-1} in 2006 and 2007, respectively (Fig. A.1). During this period θ was 0.05 $m^3 m^{-3}$ and 0.11 $m^3 m^{-3}$ in 2006 and in 2007, respectively.

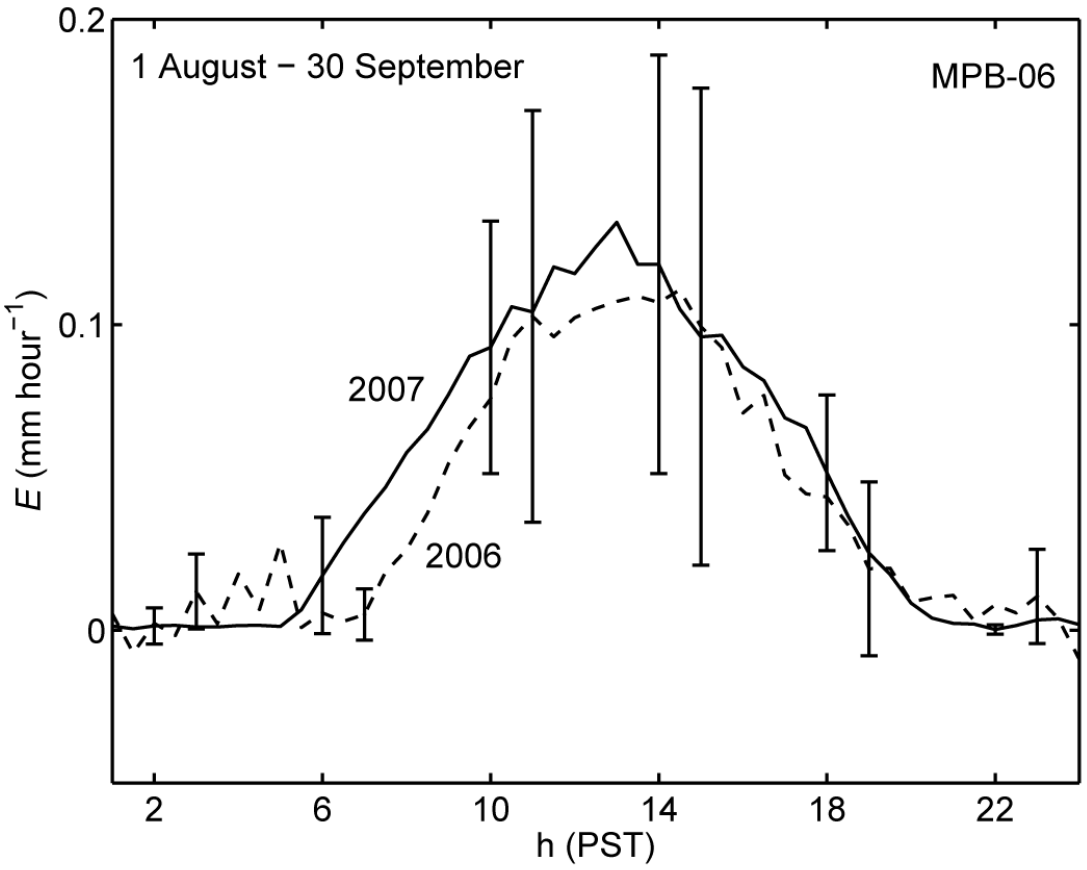

Figure A.1. Evapotranspiration (*E*) at MPB-06. Bars are standard deviation.

Appendix 2: Flux footprint analysis

Flux footprint analysis was conducted following the methods of Kormann and Meixner (2001) who developed a simple analytical model to describe the crosswind integrated and crosswind-distributed footprint under all conditions of atmospheric stability.

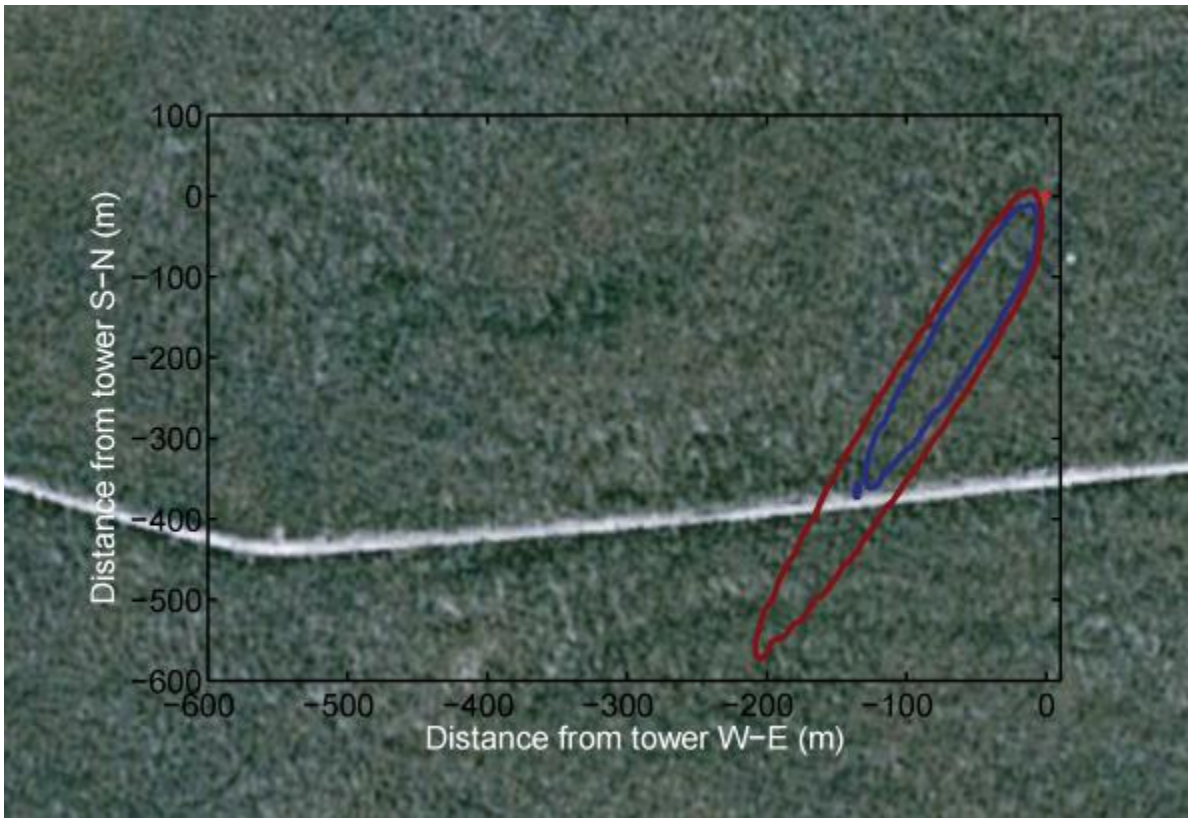

Figure A. 2. A typical daytime source area calculated with input parameters that reflect the average conditions for July (between 10:00 – 14:00 PST) at MPB-06 in 2009. Blue and red lines are the 80 and 90% source area contours.

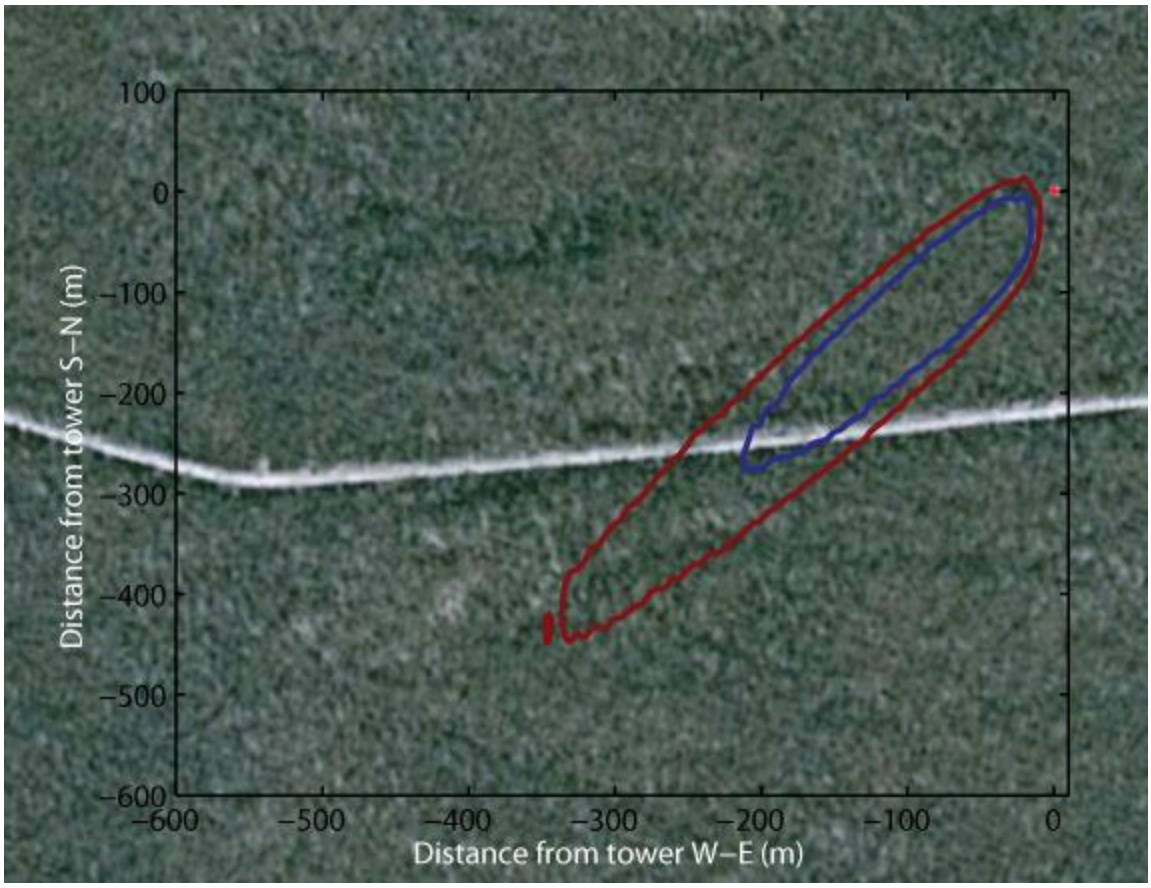

Figure A.3. A typical daytime source area calculated with input parameters that reflect the average conditions for September (between 10:00 – 14:00 PST) at MPB-06 in 2009. Blue and red lines are the 80 and 90% source area contours.

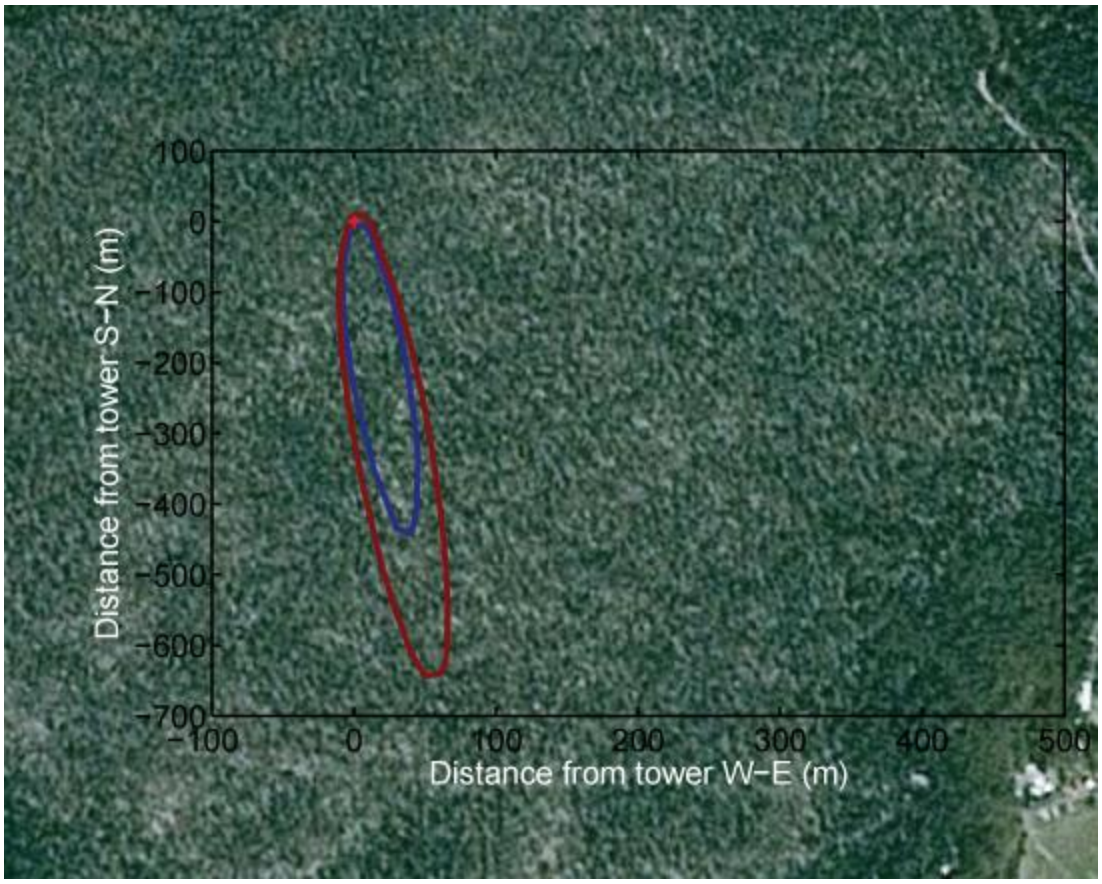

Figure A.4. A typical daytime source area calculated with input parameters that reflect the average conditions for July (between 10:00 – 14:00 PST) at MPB-03 in 2009. Blue and red lines are the 80 and 90% source area contours.

Figure A. 5. A typical daytime source area calculated with input parameters that reflect the average conditions for September (between 10:00 – 14:00 PST) at MPB-03 in 2009. Blue and red lines are the 80 and 90% source area contours.

Table A-1. Mean July and September climate values for MPB-06 and MPB-03 used to calculate the flux source area (Figs. A.2 - A.5).

	MPB-06		MPB-03	
	July	September	July	September
Relative humidity (%)	47	59	45	57
T_a (°C)	20	15	22	16
u (m s^{-1})	2.1	2.9	2.15	2.4
wind direction (°)	200	218	175	232
H (W m^{-2})	250	127	266	133
λE (W m^{-2})	110	77	129	100

T_a is air temperature at 26 m, u is the mean horizontal wind speed at 26 m, H is the sensible heat flux and λE is the latent heat flux.

Appendix 3. Evapotranspiration at clearcut harvested sites

Average daily and daytime (600-1800 PST) measured *E* during the 29 June-23 July measurement period was 3.97 and 3.16 mm day^{-1} and 0.12 and 0.11 mm hour^{-1} at CC-07 and MPB-06, respectively, while during the 24 July – 16 August period, average daily and daytime measured *E* was 4.64 and 2.87 mm day^{-1} and 0.14 and 0.10 mm hour^{-1} at CC-05 and MPB-06, respectively (Fig. A.6). During the first and second period, average daily Q, T_a and total rainfall as measured at MPB-06, were 460 and 405 μmol m^{-2} s^{-1}, 16 and 14 °C and 35 and 32 mm, respectively.

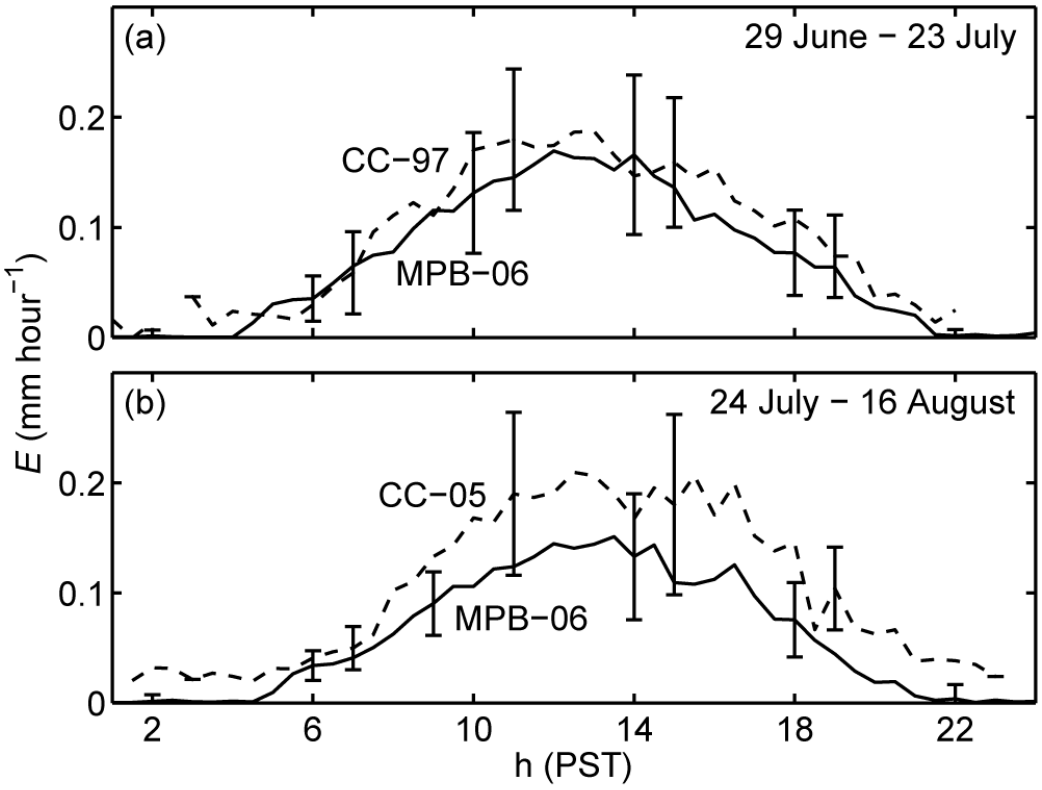

Figure A.6. Evapotranspiration (*E*) at (a) MPB-06 and CC-97 and (b) MPB-06 and CC-05 during the 2007 growing season. Bars are standard deviation.

NEP values during the two measurement periods were -0.37 and -0.87 g C m^{-2} day^{-1} at CC-97 and CC-05, respectively, both slightly lower than MPB-06 values during the same period (Fig 2.10). These negative NEP values suggest that P_g was relatively low at these two harvested stands, although P_g was not estimated due to an insufficient amount of data to fit the R_e and P_g models (Eq. 4.1 and 4.2). Light response characteristics were determined using the following equation:

$$\mathrm{NEP} = \frac{\alpha_N Q P_{\max N}}{\alpha_N Q + P_{\max N}} - R_{dN} \qquad (1)$$

where α_N is the quantum yield P_{maxN} is ecosystem photosynthetic capacity and R_{dN} is the daytime ecosystem respiration. The photosynthetic capacity of the sites was low (Fig. A.7), thus, the higher daytime *E* at the harvested stands was likely from evaporation from the soil surface rather than from transpiration. This was likely especially true at CC-05 which was only harvested two years before the measurements were made and only had a sparse covering of lichen and moss, as well as planted seedlings of lodgepole pine and hybrid white spruce. Had the vegetation cover been greater, the photosynthetic uptake during the day might have been higher. Under such conditions there would have probably been a higher contribution of transpiration to *E*. Still, *E* was higher than expected considering the sandy soils of the site.

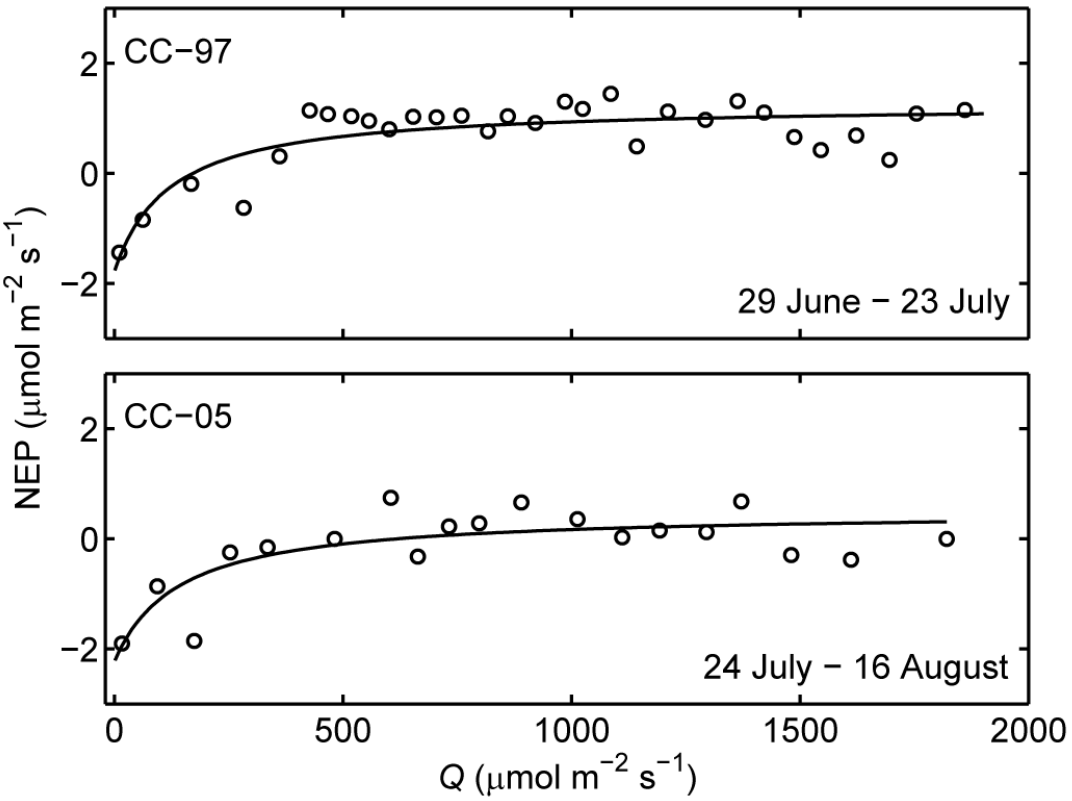

Figure A.7. Relationship between net ecosystem production (NEP) and photosynthetically active radiation (Q) during the 2007 growing season. P_{maxN}, α_N and R_{dN} were 3.05 μmol m^{-2} s^{-1}, 0.025 and 1.79 μmol m^{-2} s^{-1} at CC-97, and 2.74 μmol m^{-2} s^{-1}, 0.020 and 2.24 μmol m^{-2} s^{-1} at CC-05.

Appendix 4: Climate and eddy covariance measurement system design

A 32-m-tall scaffold flux tower (~2.1 m long x ~1.5 m wide) (Fig.A.8) was erected at each of MPB-06 and MPB-03 in July 2006 and March 2007, respectively (Fig. A.8). Flux and climate measurements began on 18 July 2006 and 20 March 2007 at the respective sites. A 3-dimensional ultrasonic anemometer (model CSAT3, Campbell Scientific Inc. (CSI), Logan, Utah) was used to measure the three components of the wind vector, and turbulent fluctuations of CO_2 and H_2O were measured using an open-path infrared gas analyzer (IRGA) (model LI-7500, LI-COR, Inc, Lincoln, Nebraska,) (Fig. A.9). At both sites, EC sensors were mounted at the height of 26 m, which was ~8 m and ~6 m above the top of the canopy at MPB-06 and MPB-03, respectively. Signals were measured with a data logger (CSI, model CR1000) with a synchronous-device-for-measurement (SDM) connection (Fig. A.10). High frequency (10 Hz) data were stored on a compact flash card that was replaced every 2-4 weeks. During the winter the sampling rate was reduced to 5 Hz to conserve power. Half-hourly covariances and other statistics were calculated on the data logger and transmitted with climate data daily by cell phone to the laboratory. Following Webb *et al*. (1980), F_c and λE were calculated as the product of the dry air density and the covariances of vertical velocity and CO_2 mixing ratio and vertical velocity and water vapour mixing ratio, respectively, measured at 10 Hz (see Appendix 7).

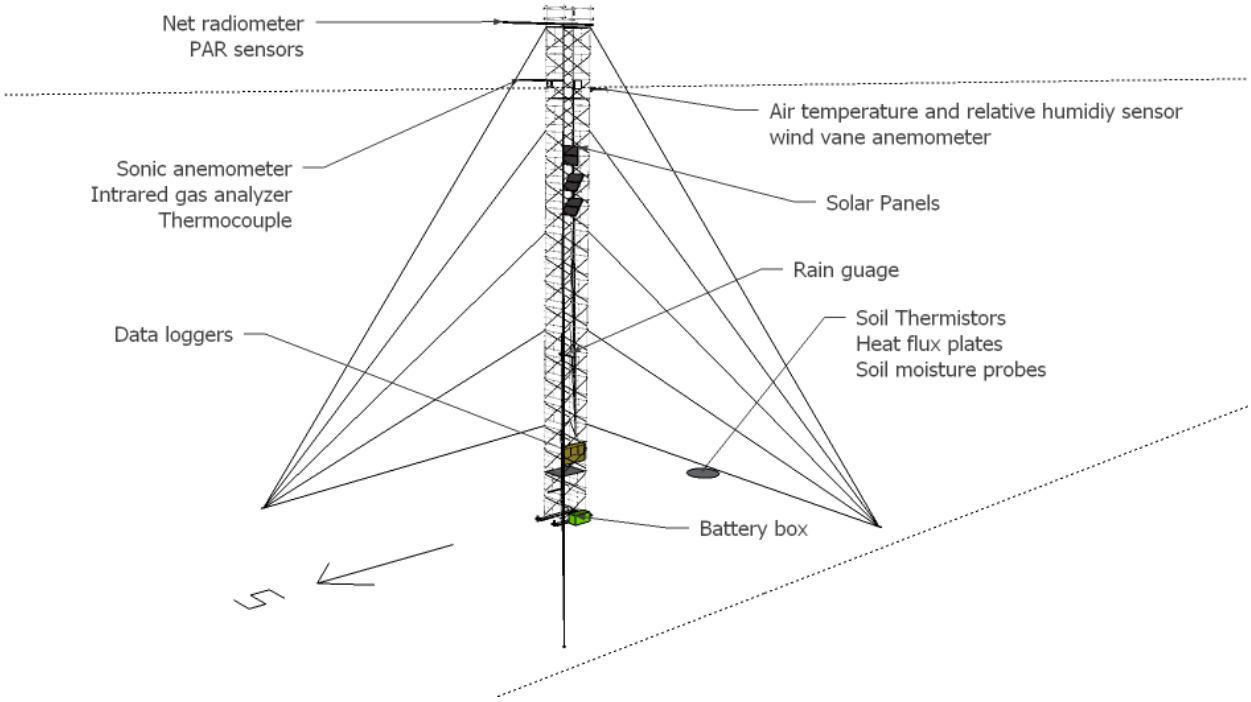

Figure A.8. Diagram of the flux tower design at MPB-06 and MPB-03.

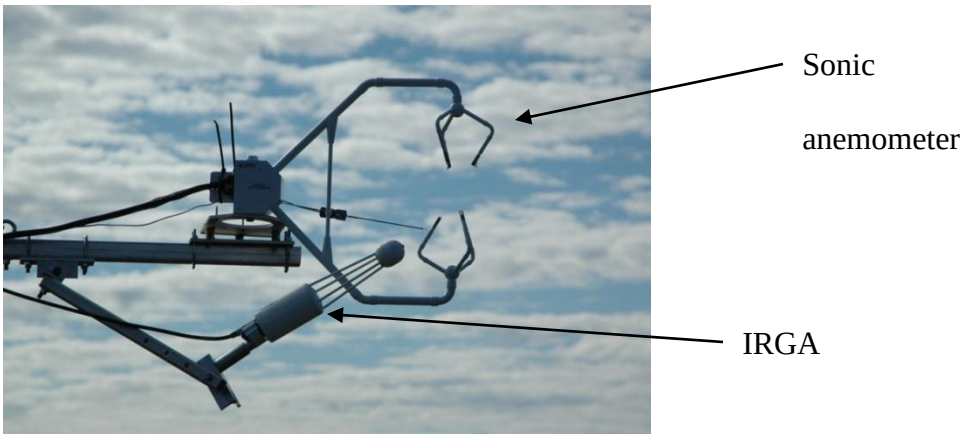

Figure A.9. Sonic anemometer, infrared gas analyser (IRGA) and fine-wire thermocouple (at 26-m height) at MPB-06.

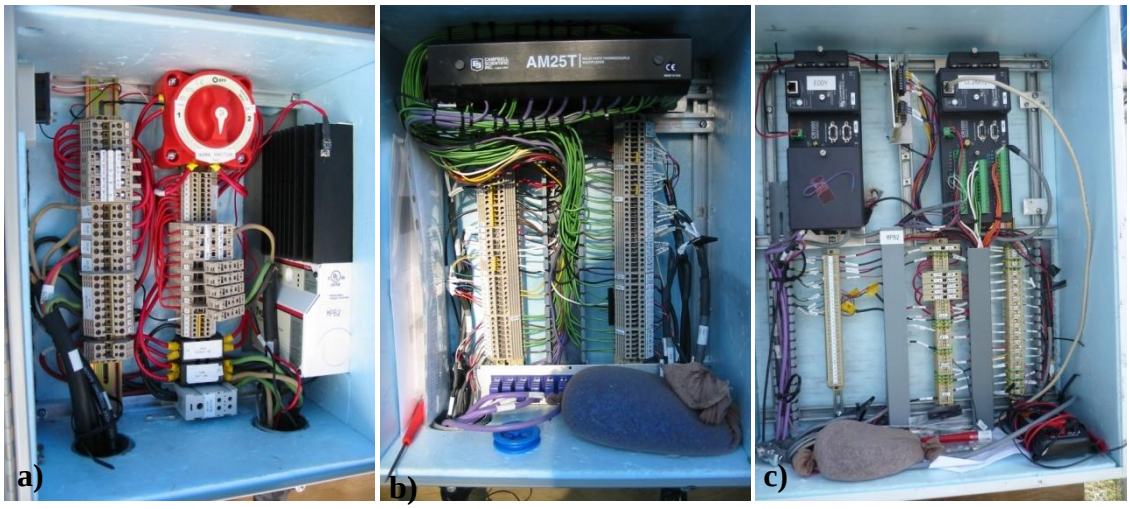

Figure A.10. a) Power, b) multiplexer and c) data logger boxes at MPB-03.

Climate variables measured included above-canopy upwelling and downwelling shortwave and longwave radiation (model CNR1, Kipp and Zonen B.V., Delft, The Netherlands) (at 30-m height) and above-canopy upwelling and downwelling (30-m height), and below-canopy downwelling (3-m height) photosynthetically active radiation (PAR) (model LI-190AS, LI-COR Inc.), precipitation at canopy height (tipping bucket rain gauges, model TE525WS-L, CSI at MPB-03 and model 2501, Sierra Misco, Berkeley, CA at MPB-06), wind speed (model 05103 R.M. Young Inc., Traverse City, MI), air temperature and relative humidity (model HMP45C, Vaisala Oyj, Helsinki, Finland) at the 25-m height, soil temperature (chromel-constantan 30 gauge thermocouple wire, Omega Engineering Stamford, Connecticut) at depths of 5, 10, 20 and 50 cm, soil heat flux (3 heat-flux plates model HP01, Hukseflux Delft, The Netherlands) at a depth of 5 cm and water content (model CS616, CSI) at the 0-10 cm and 30-50 cm depths at MPB-06 and (model EC-5, Decagon Devices Inc, Pullman, Washington) at the 10-cm, 20-cm and 50-cm depths at MPB-03. Climate instruments were connected to a data logger (CSI, model CR1000) via a multiplexer (CSI, model AM25T) (Fig.A.8). Meteorological measurements were made every second and 30-min average values calculated.

The systems were powered using 3 100-W solar panels (CTI-130, Carmanah Technologies Corp., Victoria, BC) (Fig. A.11) with an 800-Ah battery unit consisting of 8 absorbent glass mat batteries (EX-1000, Carmanah Technologies Corp.) stored in an insulated box (63.5 cm tall, 122 cm wide and 61 cm deep) (2448, Greenlee Textron, Inc., Providence, Rhode Island) (Fig. A.12). The system consumed 1A continuous current (12 W), and 24-Ah during per day. 1 hour of summer charging was enough to power the system for a full day. The reserve provided > 20 days of power without any additional solar charging. During the winter, when the power drained below 11.7 V, due to a lack of solar charging, the climate program turned off the IRGA, which reduced the power consumption to ~0.2 A. When the batteries reached 14.4 V from solar recharging, the IRGA was automatically switched back on. As the open-path IRGA often does not make reliable measurements under adverse weather conditions (raining, snowing or ice or condensation on the instrument), during such times, the IRGA was often manually switched off to conserve power. The IRGA was switched back on when weather conditions were generally clear and accurate measurements could be made. Although insulated, the temperature inside the power box during the winter would occasionally reach a minimum of -10 °C, which reduced the capacity of the batteries. At a flux tower similar to MPB-06 and MPB-03, located near Summit Lake, ~30 km south of MPB-03, burying the power box to a soil depth of 30 cm and covering it with an insulated plywood box kept wintertime temperatures inside the box several degrees warmer than at MPB-06 and MPB-03 (temperature was not measured inside the box at Summit Lake). This increased the battery capacity at this site and enabled the IRGA to run continuously through the winter.

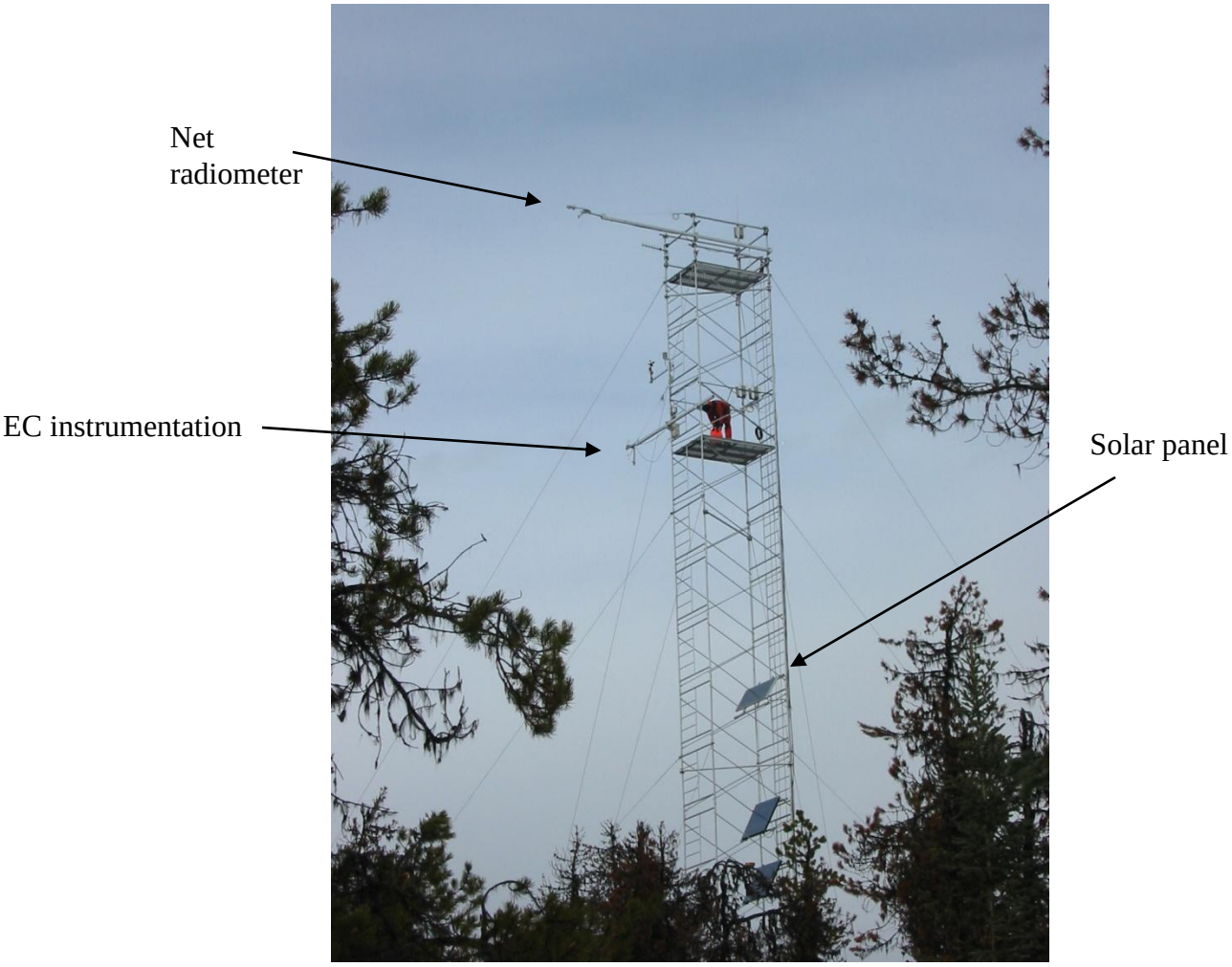

Figure A.11. MPB-06 32-m-tall tower with eddy covariance (EC) and net radiometer booms and three solar panels.

Figure A.12. Insulated battery box with batteries at MPB-03.

NEP measurements were also made in two harvested stands during the summer of 2007. They (CC-05 and CC-97) are located approximately 1 km E and 2 km SW, respectively, of the MPB-06 flux tower (Fig. A.13). CC-97 is a 10-year-old clearcut, which was left to naturally regenerate. The same 0.25-m x 3-m tall triangular tower was used at each site, first at CC-05 and then at CC-97. Measurements included the same EC instrumentation as used on the two main towers as well as above-canopy upwelling and downwelling shortwave and longwave radiation (model CNR1, Kipp and Zonen B.V.) (at 3-m height), air temperature and relative humidity (model HMP45C, Vaisala Oyj) at the 3-m height, soil temperature (chromel-constantan 30 gauge thermocouple wire) at depths of 2, 10, 20 and 50 cm, soil heat flux (3 heat-flux plates) at a depth of 5 cm and water content (model EC-5, Decagon Devices Inc, Pullman, Washington) at the 5-cm, 15-cm and 30-cm depths. EC and climate signals were measured with a data logger (CSI, CR5000). The system was powered using a 100-W solar panels (CTI-130, Carmanah

Technologies Corp.) with an 100-Ah battery unit consisting of 1 absorbent glass mat battery (EX-1000, Carmanah Technologies Corp.).

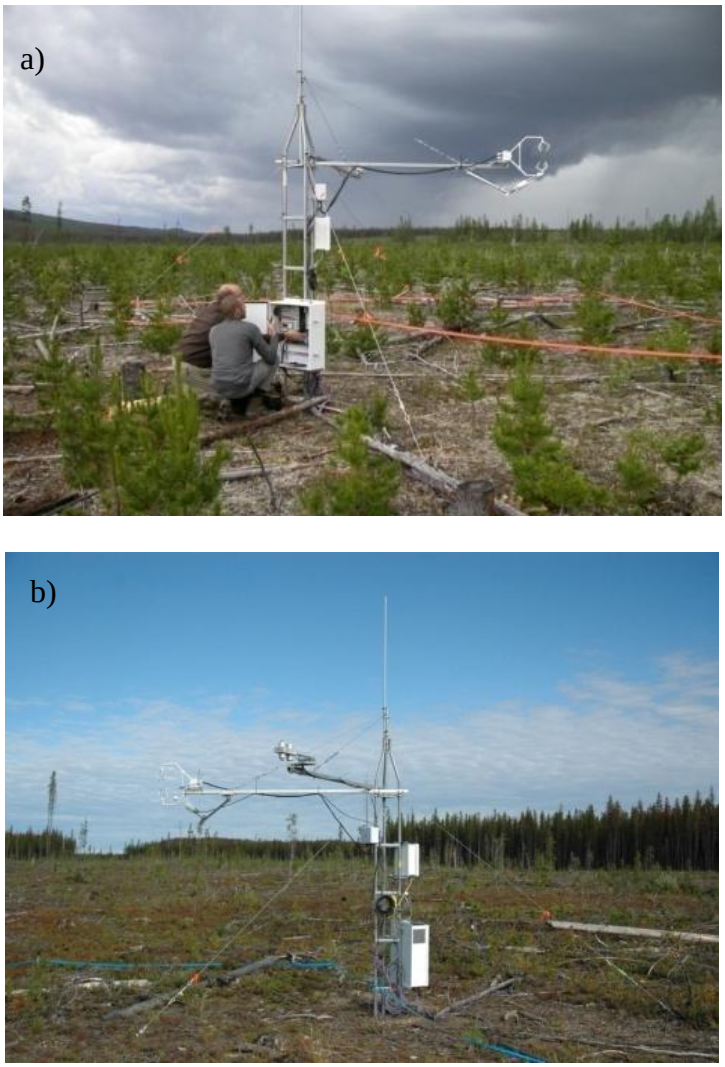

Figure A.13. Eddy covariance and climate measurement tower at a) CC-97 and b) CC-05 during the 2007 growing season.

Appendix 5: Canopy photographs

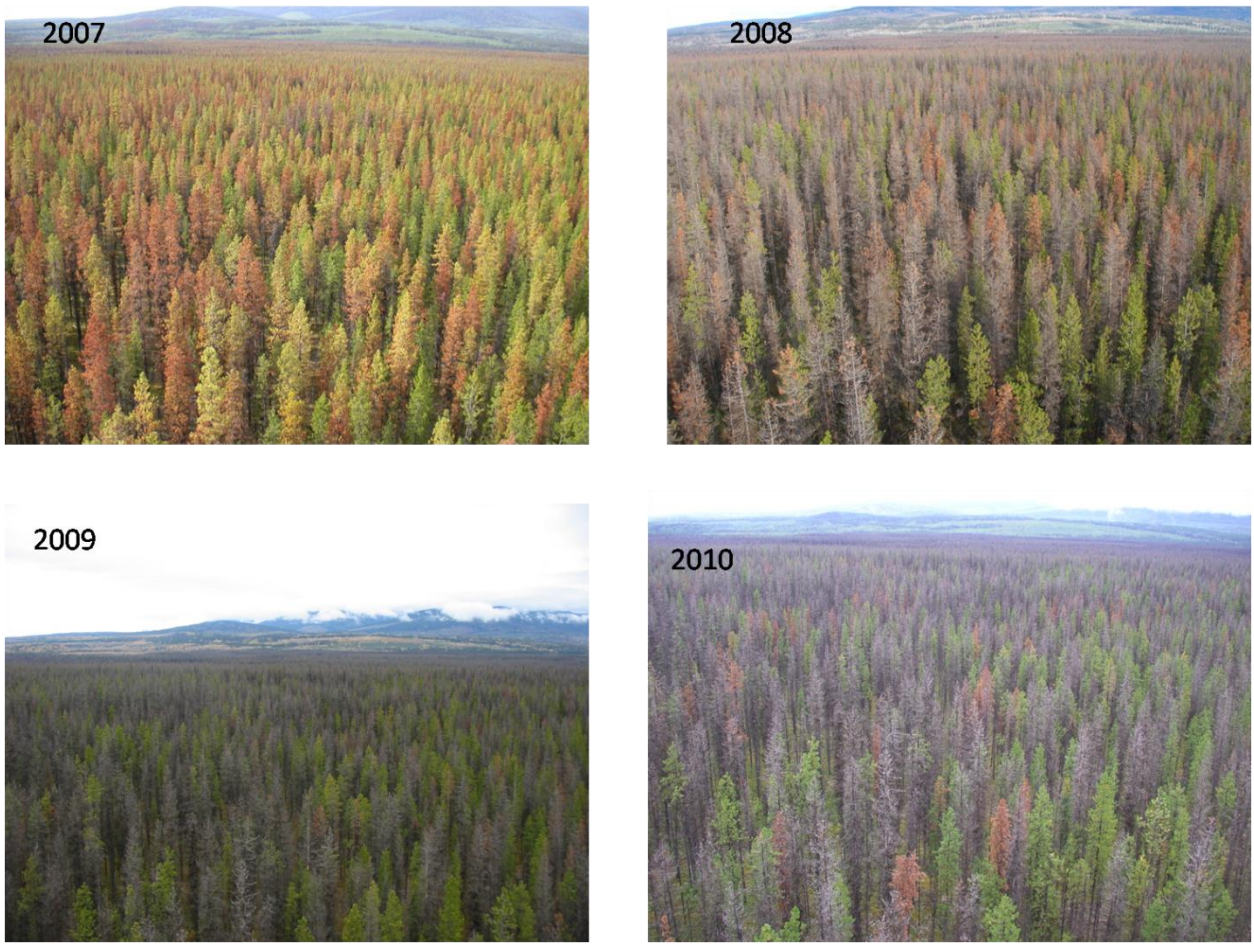

Figure A.14. MPB-06 canopy photographs.

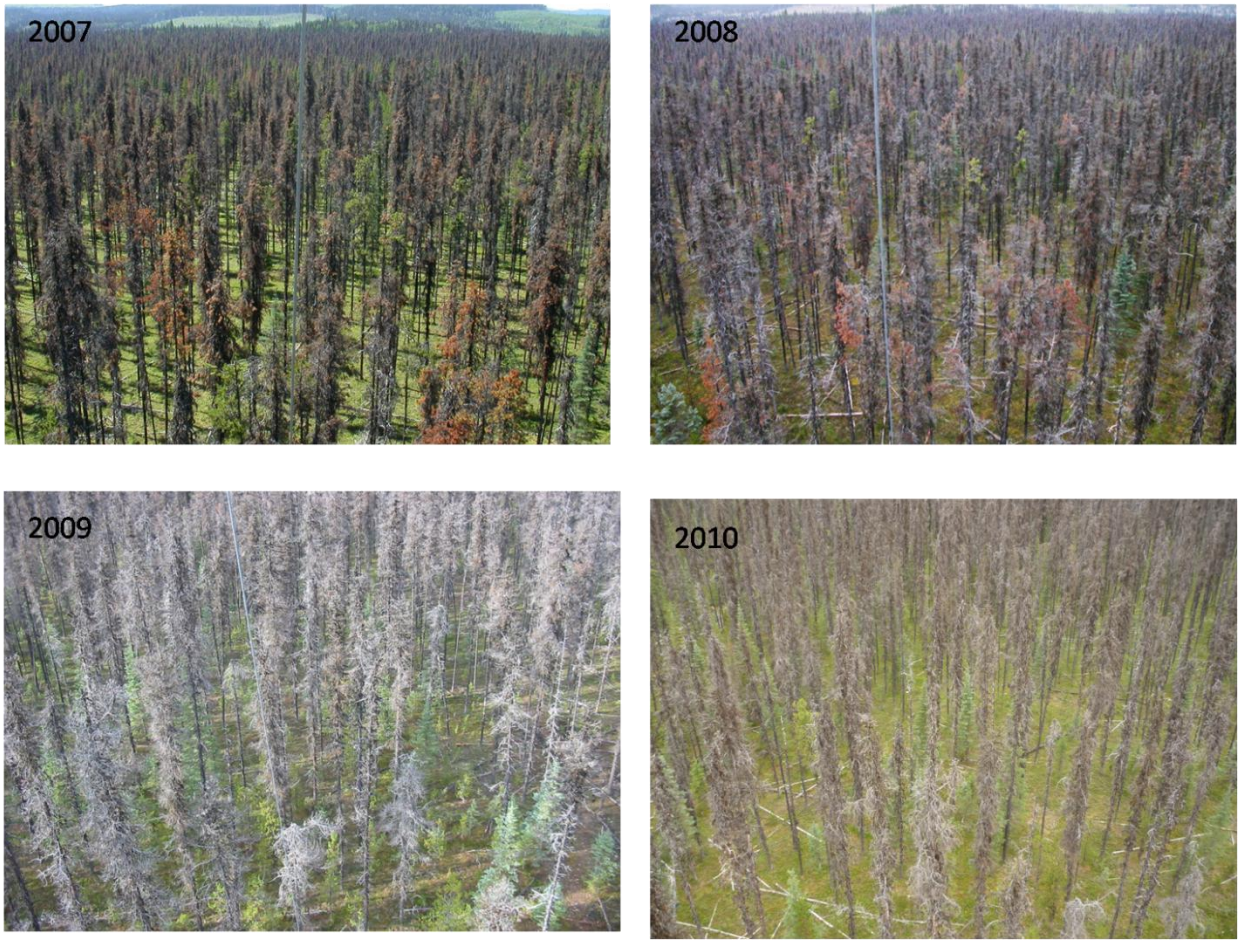

Figure A.15. MPB-03 canopy photographs.

Appendix 6: Test of significance

In the ecosystem respiration and light response analysis the fitted models (Eq. (1) and (3)) were compared to null models (containing only an intercept parameter) with a likelihood ratio test (Seber and Wild 2003). *P*-values were determined by comparing the change in the log likelihood between the full and null models to a chi-squared distribution with degrees of freedom equal to the difference in the number of model parameters. To test for changes in the models over time, models with parameters being constant across years were compared to fitting separate models to each year's data using a likelihood ratio test. The log likelihood for the temporally constant model was compared to the sum of the log likelihoods for the separate models, with the difference compared to a chi-squared distribution with degrees of freedom equal to the number of extra parameters used when fitting separate models for each year.

Matlab code for determining significance in R_e between years at MPB-06:

```
%%
MPB_NEP_annual;
MPB1_ts
=[siteDataMPB1_2007.ts;siteDataMPB1_2008.tssiteDataMPB1_2009.ts;siteDataMPB1_
2010.ts];
MPB1_R_meas =[siteDataMPB1_2007.erm;
siteDataMPB1_2008.ermsiteDataMPB1_2009.erm; siteDataMPB1_2010.erm];
% FCRN R Model
    fTs2R               = inline(['b(1)./(1+exp(b(2)*(b(3)-Ts)))'],'b','Ts');
    bRGuess             = [20 0.10 20];
    iReg                    = find(~isnan(MPB1_R_meas+MPB1_ts));
    nReg                    = length(iReg);

   [bR,b,c]     =
FCRN_function_fit_rmse(fTs2R,bRGuess,MPB1_R_meas(iReg),[],MPB1_ts(iReg));
 deviance_combined= n * (log(c.SSE) - log(n))
 R_analysis;

 n1=length(find(siteData(1).iReg(:,1) >0));
  n2=length(find(siteData(1).iReg(:,2) >0));
   n3=length(find(siteData(1).iReg(:,3) >0));
    n4=length(find(siteData(1).iReg(:,4) >0));
```

```
deviance_separate =n1 *(log(siteData(1).SSE(1)) - log(n1) ) + n2
*(log(siteData(1).SSE(2)) - log(n2) ) + n3 *(log(siteData(1).SSE(3)) -
log(n3))... + n4 *(log(siteData(1).SSE(4)) - log(n4))

lr=deviance_combined-deviance_separate
1-chi2cdf(lr,12)
%%
% 2007 and 2008
MPB_NEP_annual;
MPB1_ts =[siteDataMPB1_2007.ts;siteDataMPB1_2008.ts];
MPB1_R_meas =[siteDataMPB1_2007.erm; siteDataMPB1_2008.erm];

% FCRN R Model
    fTs2R               = inline(['b(1)./(1+exp(b(2)*(b(3)-Ts)))'],'b','Ts');
    bRGuess             = [20 0.10 20];
    iReg                    = find(~isnan(MPB1_R_meas+MPB1_ts));

    nReg                    = length(iReg);

   [bR,b,c]     =
FCRN_function_fit_rmse(fTs2R,bRGuess,MPB1_R_meas(iReg),[],MPB1_ts(iReg));
 deviance_combined= n * (log(c.SSE) - log(n))
R_analysis;
 n1=length(find(siteData(1).iReg(:,1) >0));
  n2=length(find(siteData(1).iReg(:,2) >0));
   n3=length(find(siteData(1).iReg(:,3) >0));
    n4=length(find(siteData(1).iReg(:,4) >0));

%compare 2007 with 2008
lr= deviance_combined - (n1 *(log(siteData(1).SSE(1)) - log(n1) ) + n2
*(log(siteData(1).SSE(2)) - log(n2) ))
1-chi2cdf(lr,4)
```

Appendix 7: Eddy covariance data logger program and flux calculations

The program for the EC data logger (CSI CR1000) was obtained from Laval University and, modifications were made by Joe Kidston, Zoran Nesic, Dominic Lessard and Mathew Brown. It calculated half-hourly means, variances and covariances of CO_2 and H_2O densities, u, v, w, T_a (from sonic anemometer and fine-wire thermocouple) and IRGA and sonic anemometer diagnostics. These half-hourly data were transmitted to UBC daily and used to assess EC system performance.

Variances and covariances calculated by the data logger program were:

```
'Public cov_out(21)
Public cov_out(15)
Alias cov_out(1) = CO2_CO2
Alias cov_out(2) = CO2_H2O
Alias cov_out(3) = CO2_u
Alias cov_out(4) = CO2_v
Alias cov_out(5) = CO2_w
Alias cov_out(6) = H2O_H2O
Alias cov_out(7) = H2O_u
Alias cov_out(8) = H2O_v
Alias cov_out(9) = H2O_w
Alias cov_out(10) = u_u
Alias cov_out(11) = u_v
Alias cov_out(12) = u_w
Alias cov_out(13) = v_v
Alias cov_out(14) = v_w
Alias cov_out(15) = w_w
Alias cov_3_out(1) = Ts_Ts
Alias cov_3_out(2) = Ts_u
Alias cov_3_out(3) = Ts_v
Alias cov_3_out(4) = Ts_w
Alias cov_4_out(1) = Tc_Temp_Tc_Temp
Alias cov_4_out(2) = Tc_Temp_u
Alias cov_4_out(3) = Tc_Temp_v
Alias cov_4_out(4) = Tc_Temp_w
```

The EC program:

```
'=============================================================
```

```
'  Program starts here
'=============================================================
BeginProg
  'Calculate fluxes and save raw data on compile
  'Set all csat3 and irga variables to NaN
  For j = 1 To 5
     csat_in(j) = NaN
  Next j
  For j = 1 To 11
    irga_in(j) = NaN
  Next j

' Measure CSAT and LI-7500 data
  SDMSpeed (sdm_par)
  Scan (scan_interval,mSec,15,0)
  CSAT3 (csat_in(1),1,CSAT_SDM,CSAT_CMD,csat_opt)
  CS7500 (irga_in(1),1,IRGA_SDM,IRGA_CMD)

    'Measure fine wire thermocouple
    PanelTemp (ref_temp,250)
    'TCDiff (tc_temp(),3,mV2_5,1,TypeE,ref_temp,True,200,250,1.0,0)
     TCDiff (tc_temp(),2,mV2_5,1,TypeE,ref_temp,True,200,250,1.0,0)

     'syncronization for Carmen's experiment
     VoltDiff (tc_temp(3),1,mV5000,3,True ,0,250,1.0,0)

    RealTime (real_time)
    Hours_Tmp=Hours*100
    Hours_Mins=Hours_Tmp+Minutes
    rmsec=real_time(7)/1000000
    rsec=real_time(6)+rmsec

    'Load  tables containing raw high and low frequency data and system diagnostics
     CallTable RawHF
            CurrentRecord = RawHF.record
            HHourRecords = CurrentRecord - OldRecord

   'Set file marks to break up high and low frequency data into 30 min files
    If (real_time( 5) = 29  AND real_time(6) = 59 AND real_time(7) >= 900000)
       FileMark(RawHF)
       OldRecord = CurrentRecord
    EndIf
    If (real_time(5) =59 AND real_time(6) = 59 AND real_time(7) >= 900000)
      FileMark(RawHF)
      OldRecord = CurrentRecord
    EndIf
```

```
        ' Load array used to calculate covariances

        cov_in(1) = CO2
        cov_in(2) = H2O
        cov_in(3) = u_wind
        cov_in(4) = v_wind
        cov_in(5) = w_wind
        cov_3_in(1)=Tsonic
        cov_3_in(2)=u_wind
        cov_3_in(3)=v_wind
        cov_3_in(4)=w_wind

        cov_4_in(1)=Eddy_Tc
        cov_4_in(2)=u_wind
        cov_4_in(3)=v_wind
        cov_4_in(4)=w_wind
'=====================================
'Sample low frequency sensors
'=====================================
  'Get info from status table
   Battery(batt_volt)                                                                    '
PCcard_free=Status.CardBytesFree(1,1)
   memory=Status.MemoryFree(1,1)
   watchdog=Status.WatchdogErrors(1,1)

  '*****************Calculate Fluxes*****************************************
  CallTable comp_cov
  GetRecord(cov_out(1),comp_cov,1)
  CallTable Tscov
  GetRecord(cov_3_out(1),Tscov,1)
  CallTable Tc_cov
  GetRecord(cov_4_out(1),Tc_cov,1)
  CallTable flux_30m
  CallTable diag30m
  'Add file marks to divide flux table into daily files
  If (real_time(4) = 23 AND real_time( 5) = 59  AND real_time(6) = 59 AND real_time(7) >=
900000)
     FileMark(flux_30m)
 EndIf
  NextScan
EndProg
```

Below is the Matlab code used to calculate coordinate rotations, convert CO_2 and H_2O densities to mixing ratios, and calculate fluxes (reported in this thesis) from high frequency data. This

code comes from sub-functions of new_calc_and_save.m in the Biometeorology and Soil Physics Matlab library.

Coordinate rotation:

```
function [Eddy_HF_data_rot] = fr_rotatn_hf(Eddy_HF_data,angles)
%   [Eddy_HF_data] = fr_plot_raw(Eddy_HF_data,angles)
%
% Rotates the high frequency data assuming that the first the column in
Eddy_HF_data
% contain u v w

% Do the rotation
if isnan(angles(3))
   ce = cos(pi/180*angles(1));
   se = sin(pi/180*angles(1));
   ct = cos(pi/180*angles(2));
   st = sin(pi/180*angles(2));

   Eddy_HF_data_rot      = Eddy_HF_data;

   Eddy_HF_data_rot(:,1) = Eddy_HF_data(:,1)*ct*ce + Eddy_HF_data(:,2)*ct*se
+ Eddy_HF_data(:,3)*st;
   Eddy_HF_data_rot(:,2) = Eddy_HF_data(:,2)*ce - Eddy_HF_data(:,1)*se;
   Eddy_HF_data_rot(:,3) = Eddy_HF_data(:,3)*ct - Eddy_HF_data(:,1)*st*ce -
Eddy_HF_data(:,2)*st*se;

else
   ce = cos(pi/180*angles(1));
   se = sin(pi/180*angles(1));
   ct = cos(pi/180*angles(2));
   st = sin(pi/180*angles(2));
   cb = cos(pi/180*angles(3));
   sb = sin(pi/180*angles(3));

   means2(:,1) = Eddy_HF_data(:,1)*ct*ce + Eddy_HF_data(:,2)*ct*se +
Eddy_HF_data(:,3)*st;
   means2(:,2) = Eddy_HF_data(:,2)*ce - Eddy_HF_data(:,1)*se;
   means2(:,3) = Eddy_HF_data(:,3)*ct - Eddy_HF_data(:,1)*st*ce -
Eddy_HF_data(:,2)*st*se;

   Eddy_HF_data_rot      = Eddy_HF_data;
   Eddy_HF_data_rot(:,1) = means2(:,1);
   Eddy_HF_data_rot(:,2) = means2(:,2)*cb + means2(:,3)*sb;
   Eddy_HF_data_rot(:,3) = means2(:,3)*cb - means2(:,2)*sb;
End
```

Mole fractions to mixing ratios:

```
if
strcmp(configIn.Instrument(configIn.System(systemNum).Instrument(2)).Type,'70
00')
   chi = EngUnits(:,6);
   EngUnits(:,5) = EngUnits(:,5)./(1-chi/1000);
   EngUnits(:,6) = EngUnits(:,6)./(1-chi/1000);
   configIn.System(systemNum).ChanUnits(5:6) = {'\mumol/mol dry
air','mmol/mol dry air'};
```

```
end
```

Flux calculations:

```
% Sensible heat calculations
        %
        Cp_moist = spe_heat(h2o_bar); %specific heat of moist air
        SensibleSonic  = wT * rho_moist_air * Cp_moist;             %
Sensible heat (Sonic)
        Eddy_results = setfield(Eddy_results,{1},char(rotation),...
            char(detrendType),'Fluxes','Hs',SensibleSonic);
        SensibleTc1    = wTc1 * rho_moist_air * Cp_moist;       % Sensible
heat (Tc1)
        Eddy_results = setfield(Eddy_results,{1},char(rotation),...
            char(detrendType),'Fluxes','Htc1',SensibleTc1);
        SensibleTc2    = wTc2 * rho_moist_air * Cp_moist;       % Sensible
heat (Tc2)
        Eddy_results = setfield(Eddy_results,{1},char(rotation),...
            char(detrendType),'Fluxes','Htc2',SensibleTc2);

        % CO2 flux calculations
        %
        convC = mol_density_dry_air;             % convert umol co2/mol dry
air -> umol co2/m3 dry air (refer to Pv = nRT)
        Fc    = wc * convC;                      % CO2 flux (umol m-2 s-1)
        Eddy_results = setfield(Eddy_results,{1},char(rotation),...
            char(detrendType),'Fluxes','Fc',Fc);

        %
        % P energy calculation
        %
        Penergy = -10.47 * wc;                                      % Penergy

        Eddy_results = setfield(Eddy_results,{1},char(rotation),...
            char(detrendType),'Fluxes','MiscVariables','Penergy',Penergy);

        % Latent heat calculations
        %
        convH    = mol_density_dry_air.*Mw./1000;               % convert
mmol h2o/mol dry air -> g h2o/m3 (refer to Pv = nRT)

        wh_g     = wh * convH;                                  % convert
m/s(mmol/mol) -> m/s(g/m^3)
        LELicor  = wh_g * L_v;                                  % LE LICOR

        Eddy_results = setfield(Eddy_results,{1},char(rotation),...
            char(detrendType),'Fluxes','LE_L',LELicor);
```